Functional Characterization of PICH, a DNA-dependent ATPase Required for Faithful Chromosome Segregation during Mitosis

Inauguraldissertation

zur

Erlangung der Würde eines Doktors der Philosophie

vorgelegt der

Philosophisch-Naturwissenschaftlichen Fakultät

der Universität Basel

von

Manuel Kaulich

aus Berlin, Deutschland

Basel, 2010

creative commons

Namensnennung-Keine kommerzielle Nutzung-Keine Bearbeitung 2.5 Schweiz

---

Sie dürfen:

das Werk vervielfältigen, verbreiten und öffentlich zugänglich machen

Zu den folgenden Bedingungen:

Namensnennung. Sie müssen den Namen des Autors/Rechteinhabers in der von ihm festgelegten Weise nennen (wodurch aber nicht der Eindruck entstehen darf, Sie oder die Nutzung des Werkes durch Sie würden entlohnt).

Keine kommerzielle Nutzung. Dieses Werk darf nicht für kommerzielle Zwecke verwendet werden.

Keine Bearbeitung. Dieses Werk darf nicht bearbeitet oder in anderer Weise verändert werden.

- Im Falle einer Verbreitung müssen Sie anderen die Lizenzbedingungen, unter welche dieses Werk fällt, mitteilen. Am Einfachsten ist es, einen Link auf diese Seite einzubinden.
- Jede der vorgenannten Bedingungen kann aufgehoben werden, sofern Sie die Einwilligung des Rechteinhabers dazu erhalten.
- Diese Lizenz lässt die Urheberpersönlichkeitsrechte unberührt.

Die gesetzlichen Schranken des Urheberrechts bleiben hiervon unberührt.

Die Commons Deed ist eine Zusammenfassung des Lizenzvertrags in allgemeinverständlicher Sprache: http://creativecommons.org/licenses/by-nc-nd/2.5/ch/legalcode.de

Genehmigt von der Philosophisch-Naturwissenschaftlichen Fakultät

auf Antrag von

Prof. Erich A. Nigg, Prof. Markus Affolter, Prof. Josef Jiricny
(Mitglieder des Dissertationskomitees)

Basel, den 14.12.2010

Prof. Martin Spiess
- Dekan -

This thesis has been prepared from September 2006 to December 2010 in the laboratory of Professor Erich A. Nigg in the department of cell biology at the Max-Planck Institute of Biochemistry and at the Biozentrum (Growth & Development), University of Basel.

Parts of this thesis have been published:

Hübner, N.C., Wang, L.H.-C., Kaulich, M., Descombes, P., Poser, I., and Nigg, E.A. (2010) Re-examination of siRNA specificity questions role of PICH and Tao1 in the spindle checkpoint and identifies Mad2 as a sensitive target for small RNAs. Chromosoma *119*, 149-165.

Fava, L.L., Kaulich, M., Nigg, E.A., Santamaria A. A Closed-Mad2 monoclonal antibody highlights the Mad1:C-Mad2 template action in vivo. Molecular Cell. (in review process, 2010)

Kaulich, M., and Nigg E.A. Exploring the localization and function of PICH. (manuscript in progress)

TABLE OF CONTENTS

1. SUMMARY

PICH (Plk1-interacting checkpoint helicase), a DNA-dependent ATPase, was identified as a binding partner and substrate of Plk1. During mitosis, PICH localizes to the centromere/KTs of condensed mitotic chromosomes and to ultra-fine DNA bridges (UFBs) during anaphase. Upon depletion or chemical inhibition of Plk1, PICH localizes to the chromosome arms, suggesting that the kinase activity of Plk1 regulates the dynamic localization of PICH. In addition, PICH (bound to Plk1) has been proposed to function in prometaphase chromosome arm architecture and cohesion. Here, two questions were asked: how is the dynamic localization of PICH regulated and what is the mitotic function of PICH?

In the first part of this thesis, we identify the ATPase activity of PICH as being essential for its correct subcellular localization and show that ATPase-dead mutants of PICH localize to the chromosome arms. Rescue experiments with a mutant of PICH that is unable to interact with Plk1 imply that the kinase activity of Plk1 is only indirectly required to delocalize PICH from the chromosome arms. This suggests that an unknown Plk1 substrate regulates the localization of PICH. PICH-immunoprecipitation and mass spectrometry identified the uncharacterized protein BEND3 as a binding partner. BEND3 localizes to mitotic chromosomes and its depletion results in the loss of PICH and Plk1 from the centromere/KTs. BEND3 depleted cells are unable to align their chromosomes at the metaphase plate and undergo apoptosis within a short time, suggesting that BEND3 regulates not only the localization of PICH and Plk1 but has additional functions.

In the second part of this thesis, we demonstrate that PICH does not function in the spindle assembly checkpoint. Instead, we show that neutralization or depletion of PICH results in chromatin bridges during anaphase. We identify the ATPase activity of PICH as indispensable to prevent the formation of these bridges and show that they most likely arise from non-centromeric chromatin. PICH was previously shown to interact with the BTR complex (composed of BLM, TOP3A and RMI1) that has been linked to the faithful separation of chromosomes during mitosis. It is of great interest, therefore, that we discovered an association of PICH with Rif1, which has recently been shown to provide a DNA-binding interface for the BTR complex. In contrast to the colocalization of PICH and the BTR complex to non-centromeric UFBs, Rif1 localizes to

centromeric UFBs in a PICH-dependent manner. Thus, we speculate that PICH, Rif1 and the BTR complex act together to prevent chromatin bridges during mitosis.

2. INTRODUCTION

2.1 The cell cycle

The reproduction of cells is fundamental to the development of all life. In single-celled organisms, one cell division leads to two new organisms. In the development of multi-cellular organisms, countless cell divisions convert a single cell into the diverse communities of cells that make up tissues and organs. Apart from that, cell division is important to replace dead cells in the adult organism. Cell division is divided into a series of distinct, highly regulated and coordinated processes, called the cell cycle. The cell cycle ensures that a cell duplicates its contents before dividing into two daughter cells.

Division and duplication of cellular components has to be achieved with great precision and reliability over many generations. This is in particular true for the genetic information stored in the DNA of the chromosomes which duplicate once and only once per cell cycle. In eukaryotes, DNA is replicated during S (synthesis) phase into identical sister chromatids, which then must equally segregate into the daughter cells during M (mitotic) phase (Figure 1).

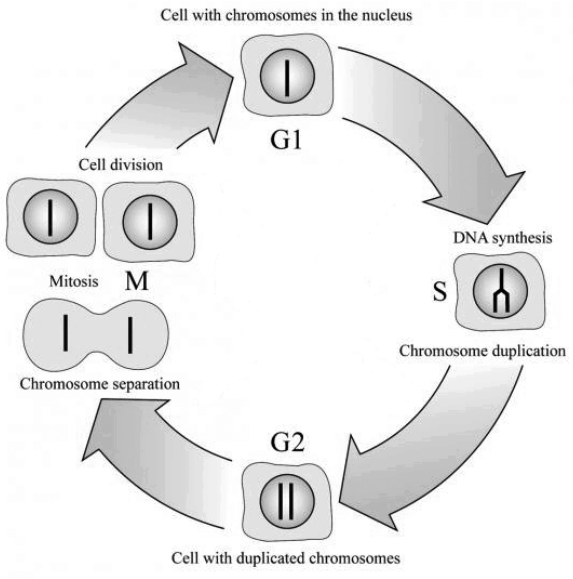

Figure 1: The eukaryotic cell cycle. Interphase consists of G1, S and G2 phase. M phase is composed of nuclear division (mitosis) and cell division (cytokinesis). Illustration adapted from "Physiology or Medicine for 2001 - Press Release", Nobelprize.org.

The accuracy of cell reproduction depends on regulatory feedback mechanisms to make sure that cell cycle events occur in the correct order and errors are not propagated. In line with this, transition into M phase depends on the completion of DNA replication, ensuring that sister chromatid separation occurs after S phase. Mitosis and S phase are separated be gap-phases (G1 and G2) that provide additional time to prepare the following cell cycle stage. G1 is particular important as cells determine to either continue cell division or exit from the cell cycle. In the presence of negative growth conditions or inhibitory signals, cells arrest in G1 or enter a nondividing state (G0) until positive growth conditions are present again.

2.2 The events of mitosis

In 1882, Walther Flemming became the first cytologist to describe the segregation of chromosomes during cell division, a process he called mitosis (Flemming, 1882). More than 100 years later, in 2001, Leland H. Hartwell, Tim Hunt and Sir Paul M. Nurse received the Nobel Prize in Physiology and Medicine for the discovery of key components of the molecular mechanisms behind Flemming's initial observations.

Mitosis or nuclear division is part of the cell cycle that encompasses the time in which sister chromatids are segregated equally to the two daughter cells. This time can be divided into five morphological distinct phases (Figure 2).

Prophase: The first mitotic phase in which the interphase chromatin condenses. The centrosomes (cellular organelle that serves as the main microtubule organizing center (MTOC)), which have been duplicated during S phase, separate and move to opposite poles. There, by nucleating microtubules (MTs) the initiation of spindle assembly occurs.

Prometaphase: The second mitotic phase, characterized by nuclear envelope breakdown (NEBD). A specialized structure at both sister chromatids, called kinetochore (KT), assembles on the centromeric region. During a highly dynamic and stochastic process KTs are captured by MTs and sister chromatids congress to the central region (metaphase or equatorial plate).

Metaphase: The third mitotic phase, in which sister chromatids are bipolar attached and aligned at the metaphase plate. Cells await the signal to separate. MTs form the typical bipolar spindle with their minus-ends proximal to the poles and their plus ends attached to the KTs.

Anaphase: The fourth and most "dramatic" phase of mitosis. Once all chromosomes are aligned, sister chromatid cohesin is lost and sister chromatids are pulled to opposite poles of the spindle (anaphase A). The spindle elongates and the poles move further apart from each other (anaphase B).

Telophase: The fifth and final phase of mitosis in which chromosomes and nuclear components are repacked into the daughter nuclei. The spindle disassembles and the nuclear envelope reforms around decondensing chromatids.

At the end of mitosis, the genetic material has been separated and cell division (cytokinesis) occurs. The central spindle compresses to form the midbody and contraction of an actin-myosin II-based ring-like structure leads to furrow ingression. Cytokinesis is terminated by abscission, resulting in two new genetically identical daughter nuclei.

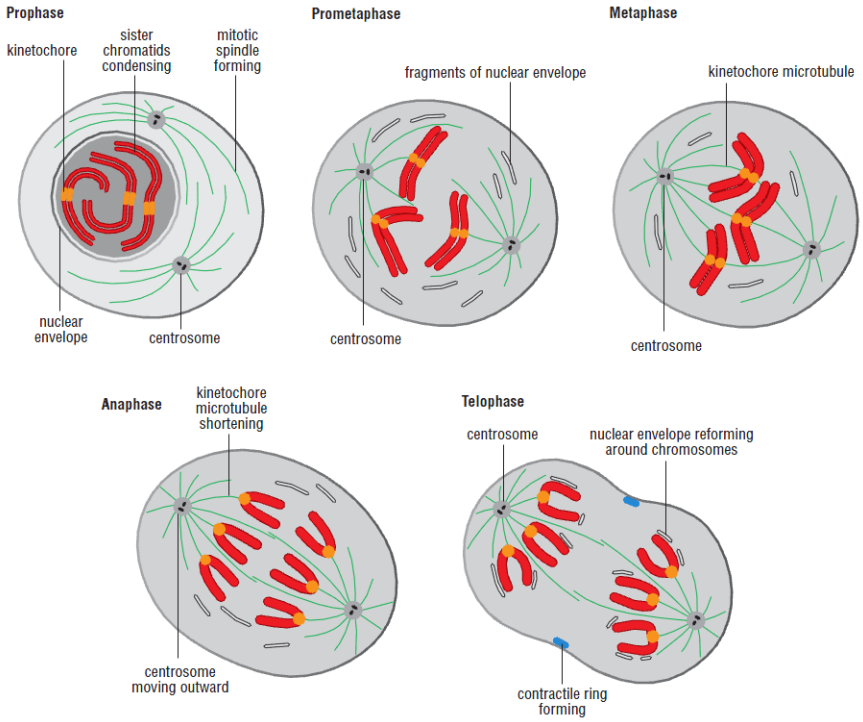

Figure 2: The events of mitosis. The five phases of mitosis: Prophase, Prometaphase, Metaphase, Anaphase and Telophase are characterized by distinct morphological characteristics. Illustration adapted from (Morgan, 2007).

2.3 Mitotic kinases

Post-translational modification of proteins is a key regulatory mechanism to control different stages of mitotic progression. Phosphorylation of proteins, mediated by protein kinases, is an optimal reversible modification to control mitotic processes such as KT-MT capturing. The two mitotic kinases cyclin-dependent kinase 1 (Cdk1) and polo-like kinase 1 (Plk1) will be introduced in the following sections.

2.3.1 The family, activation and function of Cdk1 in mitosis

A hallmark of the cell cycle is the unique and irreversible sequence of events which is controlled by a series of biochemical switches. Important components of the cell cycle are cyclin-dependent kinases (Cdks) that transiently associate with regulatory subunits called cyclins. Cdks are constantly expressed throughout the cell cycle and their enzymatic activity oscillates depending on the level of cyclins, phosphorylation and the binding to Cdk inhibitor proteins (CKIs). Cyclins are divided into 4 classes, based on their time of expression and function (Table 1).

Table 1: Cyclin classes in cell cycle. Cyclins are the main determinants of Cdk activity and are classified in four groups depending on their time of expression and function. Table adapted from (Morgan, 2007).

Species	Cyclin class (with Cdk partner)			
	G1	**G1/S**	**S**	**M**
S. cerevisiae	Cln3 (Cdk1)	Cln1,2 (Cdk1)	Clb5,6 (Cdk1)	Clb1,2,3,4 (Cdk1)
S. pombe	Puc1? (Cdk1)	Puc1, Cig1? (Cdk1)	Cig2, Cig1? (Cdk1)	Cdc13 (Cdk1)
D. melanogaster	cyclin D (Cdk4)	cyclin E (Cdk2)	cyclin E,A (Cdk2,1)	cyclin A,B,B3 (Cdk1)
X. laevis		cyclin E (Cdk2)	cyclin E,A (Cdk2,1)	cyclin A,B (Cdk1)
H. sapiens	cyclin D1,2,3 (Cdk4,6)	cyclin E (Cdk2)	cyclin A (Cdk2,1)	cyclin B (Cdk1)

At the onset of mitosis, M phase cyclins associate with and stimulate the activity of Cdk1. In addition to M phase cyclins, genetic studies in yeast have identified a network of genes that control mitotic entry. The key protein identified was the *Saccharomyces cerevisiae* Cdc28p and the *Schizosaccharomyces pombe* Cdc2p (renamed Cdk1) protein kinase activated by Cdc25p and

inhibited by the Wee1p protein kinase (Hartwell and Smith, 1985; Nurse, 1990; Nurse and Thuriaux, 1980; Russell and Nurse, 1986; Russell and Nurse, 1987). In the meantime, several studies have elucidated the regulation of Cdk1 activity and its functions during mitosis (Figure 3) (Doree and Hunt, 2002; Ferrari, 2006). Before mitosis, Cdk1 is kept inactive by phosphorylation of its ATP-binding site at threonine 14 and tyrosine 15 by the protein kinases Wee1 and Myt1 (Nigg, 2001). At the G2/M transition, the dual-specific phosphatase Cdc25C dephosphorylates these two residues and thereby stimulates the activity of Cdk1 (Izumi and Maller, 1993; Krek and Nigg, 1991). In addition, multiple feedback loops enhance the activity of Cdk1 at the onset of mitosis. Cdk1 phosphorylates and thus stimulates its own activator Cdc25C (Hoffmann et al., 1993) and phosphorylates its inhibitor Wee1 which leads to its beta-TrCP mediated proteasome-dependent degradation (Watanabe et al., 2005; Watanabe et al., 2004). Wee1 and Myt1 are components of a network which detects the completion of DNA synthesis and repair (Ferrari, 2006). Therefore, the phosphatase activity of Cdc25C exceeds the kinase activity of Wee1 at the onset of mitosis (Nigg, 2001). In addition to Cdc25C and Wee1, Cdk1 may stimulate the activity of Plk1 which phosphorylates Cdc25C and thereby further enhances the activity of Cdk1 (Barr et al., 2004; Kumagai and Dunphy, 1996; Strausfeld et al., 1994). Furthermore, activity of Cdk1 also requires phosphorylation of a threonine close to the active site catalyzed by a Cdk-activating kinase (CAK) (Obaya and Sedivy, 2002).

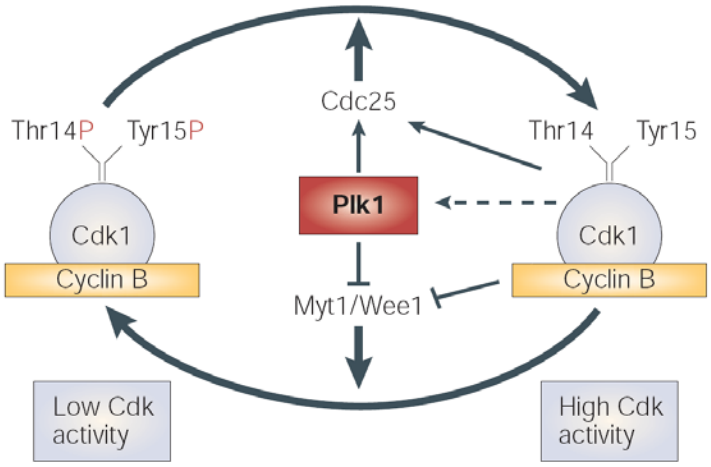

Figure 3: Cdk1 activation and positive feedback loops at G2/M transition. Before G2/M transition, Cdk1-cyclin B is kept inactive by Wee1 and Myt1 mediated phosphorylation. When the activity of Cdc25 exceeds the activity of Wee1 and Myt1, Cdk1-cyclin B gets dephosphorylated and activated. Cdk1 induced phosphorylation of Cdc25 and Wee1/Myt1 triggers a positive feedback loop which further enhances the activity of Cdk1-cyclin B. Cdk1 may also contributes to Plk1 activation, which influences the activity of Cdc25 and Wee1/Myt1. Illustration adapted from (Barr et al., 2004).

Once Cdk1 is active, it phosphorylates various substrates and fulfills different functions during mitosis. For instance, Cdk1 drives chromosome condensation by phosphorylation of condensins (Kimura et al., 1998) and nuclear envelope breakdown by phosphorylation of lamins (Peter et al., 1991). Furthermore, Cdk1 contributes to centrosome separation and assembly of the mitotic spindle by phosphorylation of microtubule-associated proteins and the kinesin-related motor protein Eg5 (Blangy et al., 1995). In addition, Cdk1 is involved in the regulation of the anaphase-promoting complex/cyclosome (APC/C), a multisubunit E3 ubiquitin ligase (Sudakin et al., 1995; Zachariae et al., 1998). The APC/C catalyzes the covalent attachment of ubiquitin chains to mitotic regulators such as cyclin B or securin which promotes their proteolysis by the 26S proteasome (Hagting et al., 2002; Peters, 2002). Upon cyclin B degradation, Cdk1 is inactivated and mitotic exit induced.

2.3.2 Polo-like kinase 1

Kinases like Cdks are the main regulators of the cell cycle, but still they don't act alone. In recent years, several other protein kinases have been identified to control the diverse events of mitosis, among them are members of the Polo family (Nigg, 2001). The first member of the Polo-family was identified in *Drosophila melanogaster* (Sunkel and Glover, 1988), followed by the discovery of the four human Plk (polo-like kinase) family members (Plk1, 2, 3, and 4) (Barr et al., 2004; Glover et al., 1998) (Table 2).

Table 2: Polo-like protein kinases. Plk members of the most frequent studied model organisms including their proposed functions. This table is not meant to be complete. Table adapted from (Barr et al., 2004; Morgan, 2007).

Species	Name (synonymes)	proposed functions
S. cerevisiae	Cdc5	Regulation of meiosis, mitosis and mitotic exit
S. pombe	Plo1p	Regulatino of mitosis and cytokinesis
D. melanogaster	Polo	Regulatino of mitosis and cytokinesis
C. elegans	Plc1, Plc2, Plc3	Required for nuclear-envelope breakdown
X. laevis	Plx1	Involved in mitotic entry and mitotic exit
	Plx2	no function determined
	Plx3	no function determined
Mammals	Plk1	Regulation of mitosis and cytokinesis
	Plk2 (Snk)	DNA-damage response, G1/S function
	Plk3 (Fnk, Prk)	DNA-damage response, G2/M function
	Plk4 (Sak)	Centrosome duplication, mitotic exit

To date, Plk1 is the best studied member of the human Plk family. The amino-terminal half contains a catalytic kinase domain and the carboxy-terminal half composes two structurally homologous polo-boxes, called Polo-box domain (PBD, Figure 4A) (Elia et al., 2003b; Leung et al., 2002). The PBD of Plk1 has diverse functions, for instance, it acts as an autoinhibitory domain towards the amino-terminal kinase domain (Mundt et al., 1997). Phosphorylation of threonine 210 by Aurora A relieves the autoinhibitory function of the PBD and increases the kinase activity of Plk1 before entry into mitosis (Archambault and Glover, 2009; Jang et al., 2002; Macurek et al., 2008; Seki et al., 2008). In addition, Plk's substrate targeting and subcellular localization is controlled by the PBD (Hanisch et al., 2006; Reynolds and Ohkura, 2003). These two later functions are mediated by high affinity of the PBD for proteins that have been phosphorylated at serine or threonine residues within a specific sequence motif (S-pS/pTP/X) (Elia et al., 2003a). PBD-binding to phosphorylated docking proteins further relieves the autoinhibited state and increases the kinase activity of Plk1, leading to the phosphorylation of the docking protein and/or other downstream substrates of Plk1 (Baumann et al., 2007; Elia et al., 2003a; Elia et al., 2003b; Lowery et al., 2005). The PBD docking site is generated by a serine/threonine kinase (priming-kinase) like Cdk1, MAP kinase or Calmodulin-dependent kinase II (CaMKII) (Elia et al., 2003a; Elia et al., 2003b; Fabbro et al., 2005; Rauh et al., 2005). However, during anaphase Plk1 can self-prime its docking sites on proteins involved in cytokinesis (Neef et al., 2007; Neef et al., 2003). In addition, the PBD of Plk1 recruits Plk1 to several mitotic structures, including the centrosomes, spindle poles, the KTs, the central spindle and to the midbody (Figure 4B).

Like its dynamic localization, Plk1 has various functions throughout mitosis (Figure 4C). As mentioned above, during G2/M transition, Plk1 has been implicated in the activation of Cdk1-cyclin B1 (Toyoshima-Morimoto et al., 2002; Toyoshima-Morimoto et al., 2001; Watanabe et al., 2004), centrosome maturation and bipolar spindle formation (Lane and Nigg, 1996; Sumara et al., 2004; van Vugt and Medema, 2004). During early mitosis, Plk1 recruits components of the spindle assembly checkpoint to the kinetochore (Ahonen et al., 2005; Kang et al., 2006; Wong and Fang, 2006), and has been shown to phosphorylate INCENP, Bub1, BubR1 and the DNA-dependent ATPase PICH (Baumann et al., 2007; Elowe et al., 2007; Goto et al., 2006; Qi et al., 2006). At the same time, Plk1 phosphorylates the cohesin subunit SA2 which contributes to the removal of sister chromatid arm cohesion (Hauf et al., 2005; Sumara et al., 2002). Interestingly,

the separation of sister chromatids seems to be independent of Plk1 function as Plk1 deficient cells still separate their chromatids when forced to enter anaphase (Gimenez-Abian et al., 2004). Besides its contribution to early mitosis, Plk1 is involved in late mitotic events, for instance targeting Mklp2 or PRC1 to the central spindle (Carmena et al., 1998; D'Avino et al., 2007). Furthermore, Plk1 activity promotes the recruitment of Ect2 to the central spindle, triggering the initiation of cytokinesis and contributing to the specification of the cleavage plane (Brennan et al., 2007; Burkard et al., 2007; Petronczki et al., 2007). Together, Plk1 has numerous mitotic functions but more await their elucidation.

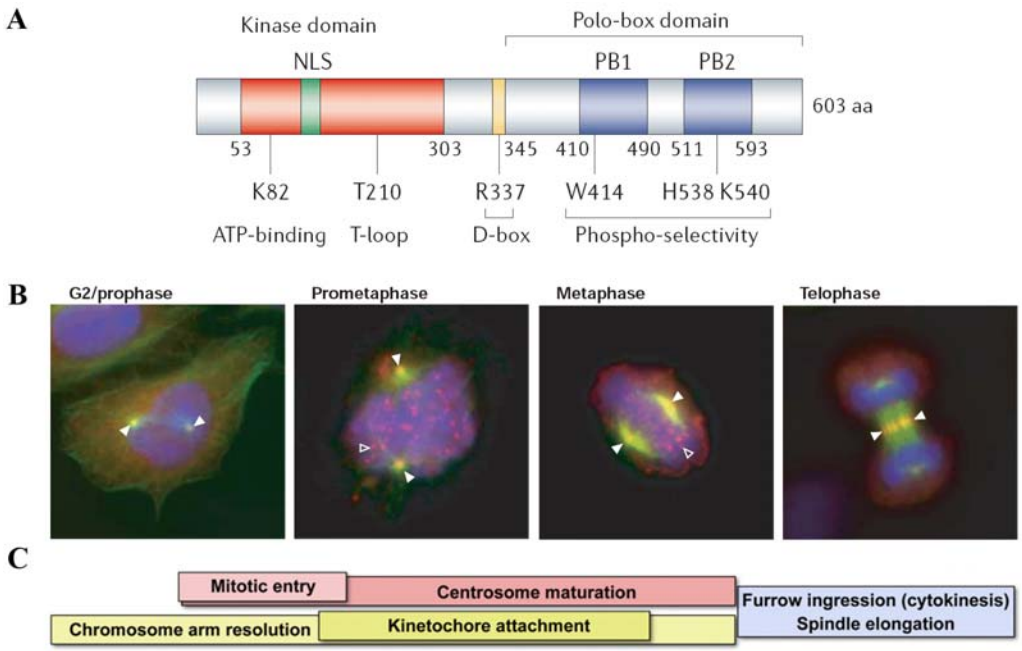

Figure 4: Structure, localization and functions of Plk1 during mitosis. A) Schematic representation of human Plk1, illustrating the open-reading frame in length, indicated by amino-acid number. Depicted are the position of the kinase domain, PBD, nuclear localization sequence (NLS) and the destruction-box (D-box). Residues essential for ATP binding, kinase activity and phospho-selectivity within the PBD are highlighted. B) Immunofluorescence images illustrating the dynamic localization of human Plk1 throughout mitosis. C) Mitotic functions of human Plk1 below the indicated mitotic stage. Illustration adapted from (Barr et al., 2004; Petronczki et al., 2008; Strebhardt and Ullrich, 2006).

2.4 The spindle assembly checkpoint

In 1991, two parallel screens performed in yeast identified genes, which, when mutated, bypassed the ability to induce a mitotic arrest in response to spindle poisons (Hoyt et al., 1991; Li and Murray, 1991). Genes identified in these screens include the *MAD* (mitotic-arrest

deficient) and the *BUB* (budding uninhibited by benimidazole) genes that act in a highly sensitive surveillance mechanism called the spindle assembly checkpoint (SAC). The SAC, conserved in all eukaryotes, senses the correct bipolar (amphitelic, from both poles) attachment of KTs to MTs to ensure that replicated sister chromatids are equally distributed to daughter cells (Cleveland et al., 2003; Li and Murray, 1991; Musacchio and Hardwick, 2002; Pinsky and Biggins, 2005; Stern and Murray, 2001). Thus, anaphase-onset is delayed until all chromosomes are properly attached and aligned at the metaphase plate and cell-biological studies have shown that a single unattached kinetochore is sufficient to inhibit the onset of anaphase (Rieder et al., 1995). During early mitosis, SAC proteins are recruited to unattached kinetochores and create a "wait anaphase signal" (Chen et al., 1996; Taylor and McKeon, 1997). How this "wait anaphase signal" is generated is currently discussed, but the phosphorylation state of SAC proteins seems to contribute to SAC activity (Ahonen et al., 2005; Elowe et al., 2007; Nicklas et al., 1995). However, the molecular source of the inhibitory signal remains elusive.

The SAC should only be silenced once all sister KTs are bipolar attached, to ensure equal segregation of chromatids during anaphase (Figure 5). In contrast, monotelic attachments are characterized by the attachment of only one sister KT to MTs, a normal condition during prometaphase. Furthermore, MTs from only one pole might attach to both sister KTs (syntelic attachment) or a single KT is captured by MTs from opposite poles (merotelic attachment). Several lines of evidence indicate that the SAC senses tension across sister KTs upon MT attachment. Therefore, the SAC is activated by syntelic attachments (low tension) and the KT-MT attachment is destabilized, but satisfied by high tension between amphitelic-attached sister KTs (Nicklas et al., 1995; Nicklas et al., 2001; Rieder et al., 1995; Rieder et al., 1994). Merotelic attachments are not sensed by the SAC due to their ability to produce sufficient tension. Still, merotelic and syntelic attachments are destabilized by the action of the protein kinase Aurora B, member of the chromosomal passenger complex (CPC), probably by regulating the microtubule depolymerase MCAK (Andrews et al., 2004; Biggins and Murray, 2001; Ditchfield et al., 2003; Giet et al., 2005; Hauf et al., 2003; Tanaka et al., 2002). Uncorrected KT-MT attachments can result in lagging chromatids and chromosome missegregation during anaphase which highlights the importance of their correction; but to which extent a lack of MT attachment or tension contributes to SAC inactivation and where and how tension is sensed remain elusive (Musacchio and Hardwick, 2002; Pinsky and Biggins, 2005).

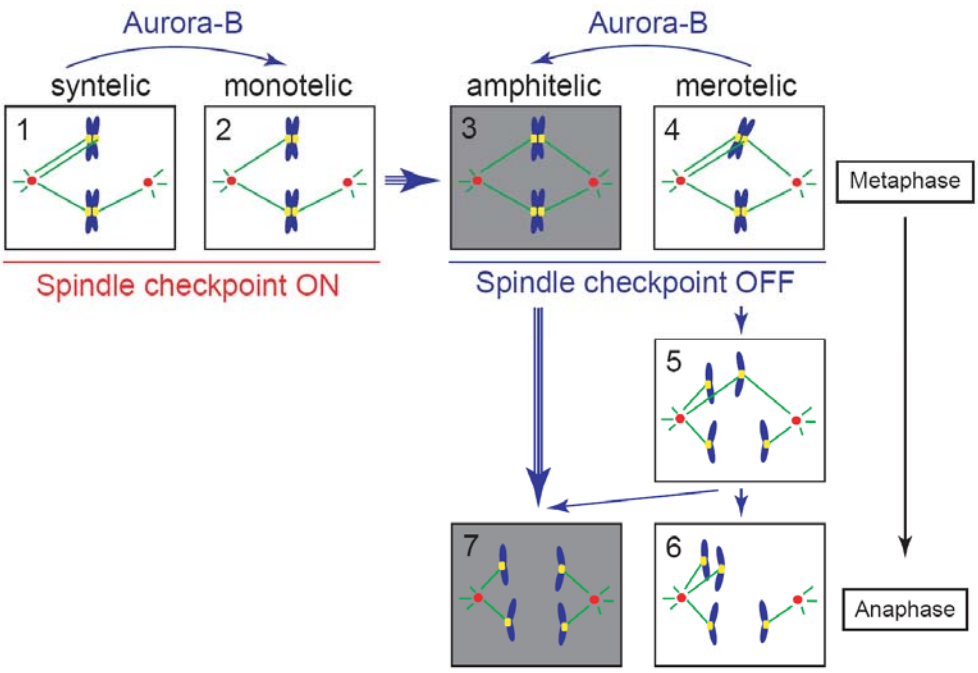

Figure 5: KT-MT attachments. Amphitelic attachments (3) of sister KTs promote anaphase onset (7). Syntelic (1) or monotelic (2) attachments prevent SAC silencing and anaphase onset. Merotelic (4) attachments are not sensed by the SAC. Incorrect KT-MT attachments, if not corrected by Aurora B, can result in lagging chromatids and chromosome missegregation during anaphase (5 and 6). Illustration adapted from (Giet et al., 2005).

Genetical and biochemical studies identified various proteins involved in SAC signaling, notably Mad1, Mad2, Bub3 and the protein kinases Bub1, BubR1 and Mps1. Mad2 is a major effector of the SAC and can adopt two conformational states, the inactive "open" and the active "closed" conformation (Mapelli et al., 2007; Musacchio and Salmon, 2007; Yu, 2006). The conformational transition of Mad2 is probably catalyzed by a Mad1:Mad2 interaction at the kinetochore. The Mad1:Mad2 complex thereby acts as a template to generate the "closed" conformation of Mad2 by a mechanism know as conformational dimerization. "Closed" Mad2 is a potent binding partner of Cdc20, a KT-bound cofactor of the E3 ubiquitin ligase APC/C (Peters, 2006; Yu, 2007). In addition, a mitotic checkpoint complex (MCC), composed of Bub3, BubR1, "closed" Mad2 and Cdc20, has been identified to efficiently inhibit the APC/C (Hardwick et al., 2000; Morrow et al., 2005; Sudakin et al., 2001). Still, how the MCC assembles and inhibits the APC/C is currently unclear (Herzog et al., 2009; Nilsson et al., 2008; Sczaniecka and Hardwick, 2008). Furthermore, the SAC components Mad1, Bub1, Mps1 and Aurora B are required to enhance the SAC signal and rate of MCC formation (Abrieu et al., 2001; Morrow et al., 2005);

but again, how these proteins act together to inhibit the APC/C remains elusive. However, as soon as sister chromatids are bipolar attached and aligned at the metaphase plate, the SAC needs to be silenced in order to induce anaphase. Among others, two prominent mechanisms contribute to SAC silencing. First, p31/comet, a protein that binds with high affinity to "closed" Mad2 and thereby inhibits the conformational dimerization of Mad2 (Musacchio and Salmon, 2007). The second mechanism centers on the dynein dependent "stripping" of Mad1, Mad2 and other checkpoint components from the KT to the spindle poles along MTs (Howell et al., 2001; Maiato et al., 2004; Wojcik et al., 2001). Once the SAC is satisfied and turned "off", activated APC/C ubiquitinylates and thus promotes the proteolysis of two key substrates, cyclin B1 and securin (Figure 6) (Bharadwaj and Yu, 2004; Pines, 2006). Securin is an inhibitory binding partner of separase, a cystein protease that cleaves sister chromatid cohesin. Therefore, anaphase onset is initiated by the activation of separase and inactivation of Cdk1.

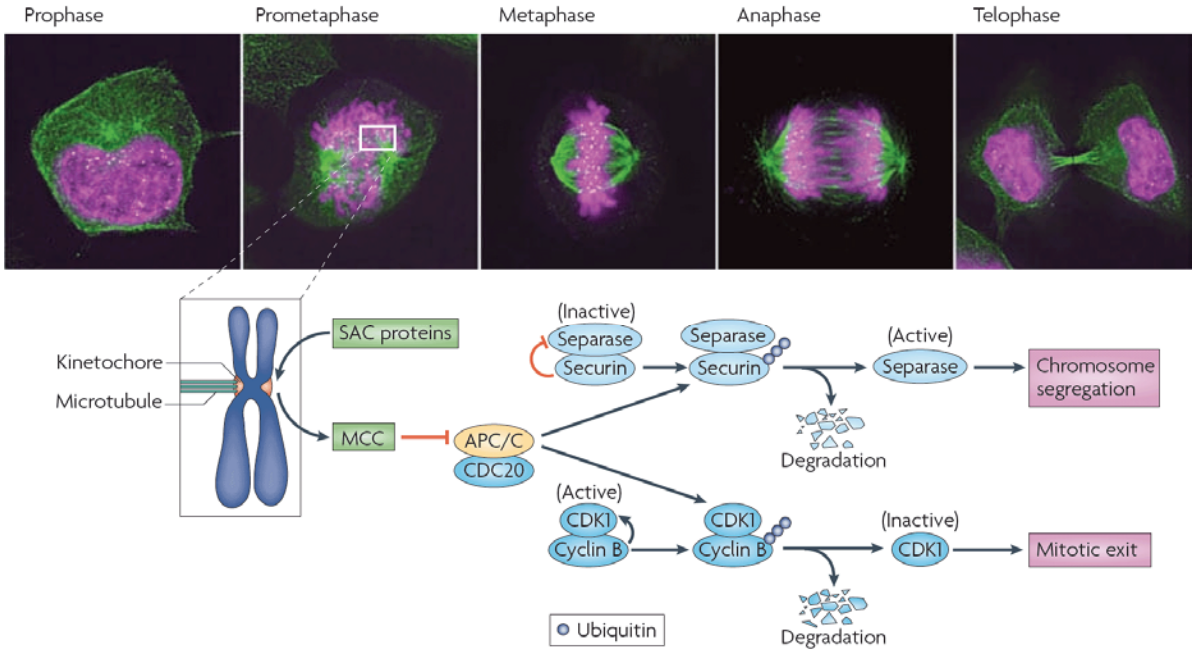

Figure 6: Simplified model for SAC signaling in mitosis. Immunofluorescence images: DNA and MTs are marked in purple and green, respectively. To enter mitosis, cells require the activity of Cdk1-cyclin B. Prior to anaphase, the activity of the protease separase is restricted by binding to securin. Unattached KTs (red hemi-circles) contribute to MCC formation, which blocks the ability of Cdc20 to activate the APC/C. Bipolar attachment of sister KTs (shown as white dots) promotes SAC silence and release of Cdc20 that activates the APC/C. The APC/C mediates the ubiquinylation and thereby the degradation of cyclin B and securin. Once activated, separase cleaves the cohesin ring complex that holds sister chromatids together, promoting sister chromatid separation. Degradation of cyclin B inactivates Cdk1 and initiates mitotic exit. Illustration adapted from (Yanagida, 2009).

2.5 Snf2 type helicases

DNA and RNA play central roles in diverse cellular processes such as transcription, recombination, genome replication, repair, expression and epigenetics. Therefore, DNA and RNA structure, compaction and accessibility are controlled by many proteins, including enzymes to spatially and temporally modulate DNA and RNA depending on the requirements of the cell.

In 1976, the enzymatic unwinding of DNA was described in bacteria (*Escherichia coli*) (Abdel-Monem et al., 1976; Abdel-Monem and Hoffmann-Berling, 1976). Since then, proteins that enzymatically unwind DNA or RNA (helicases) were identified in all organisms. In 1988, a large group of proteins was identified, members of which share a series of short ordered motifs, named helicase motifs (Gorbalenya and Koonin, 1988; Gorbalenya et al., 1988a; Gorbalenya et al., 1988b). The motifs are sequentially labeled I, Ia, II, III, IV, V and VI and comprise the classical Walker A (phosphate-binding loop) and Walker B ($Mg2^{+}$-binding aspartic acid) motifs (Gorbalenya and Koonin, 1993). This group of proteins is subdivided, based on their similarity, into so-called superfamilies (SF) 1, 2 and 3 (SF1, SF2 and SF3, respectively) (Subramanya et al., 1996). Structural characterization revealed that SF1 and SF2 are related to each other by a common core of two recA-like domains (Subramanya et al., 1996), whereas SF3 type helicases share only three conserved motifs. The Snf2 class of helicases is a subclass of the SF2 superfamily, which members share a helicase-like region similar to the *Saccharomyces cerevisiae* protein Snf2p. Based on sequence alignments, the Snf2 class family is further subdivided into subfamilies like Snf2-like, Iswi-like, Chd1-like, SSO1653-like and Rad54-like (Figure 7) (Eisen et al., 1995; Flaus et al., 2006).

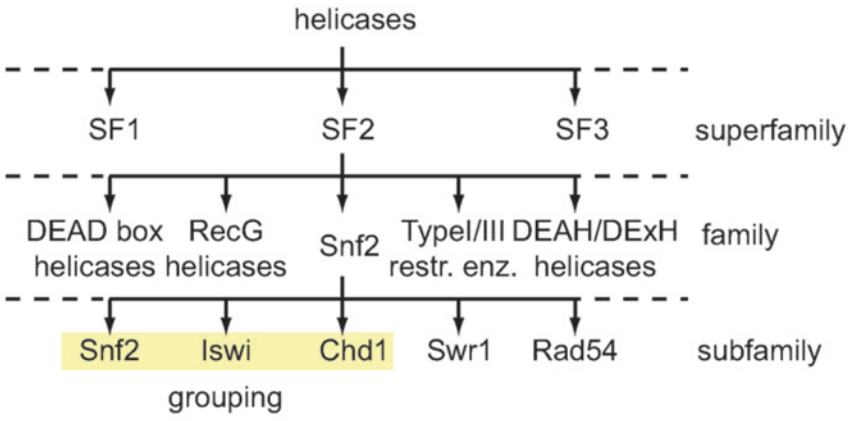

Figure 7: Snf2 family-tree. Schematic diagram illustrating the hierarchical classification of superfamily, family and subfamily. Illustration adapted from (Flaus et al., 2006).

Initially identified in screens for genes involved in the yeast phenotypes mating-type switching (SWI) and sucrose non-fermenting (SNF) (Carlson and Laurent, 1994; Nasmyth and Shore, 1987; Neigeborn and Carlson, 1987; Stern et al., 1984), the Snf2 protein was shown to function as the catalytic subunit of the multi-subunit SWI/SNF chromatin remodeling complex (Becker and Horz, 2002). SWI/SNF proteins are rare in yeast, but 5-7% of the yeast genes require the activity of the SWI/SNF chromatin remodeling complex for their expression, highlighting its importance for various pathways (Monahan et al., 2008; Zraly et al., 2006).

Many Snf2 related proteins have been identified, often as parts of multi-subunit protein complexes, for instance the SWI/SNF, RSC, Swr1, Tra1 or the INO80 complex (Cote et al., 1994; Liu et al., 2001; Saha et al., 2002; van Attikum and Gasser, 2005). In contrast to classical processive helicases, Snf2 related helicases metabolize ATP to regulate processes like replication, transcription, recombination, translocation along double stranded DNA (dsDNA), DNA repair, chromatin remodeling or to generate superhelical torsion (Becker and Horz, 2002; Beerens et al., 2005; Durr et al., 2006; Havas et al., 2001; Lia et al., 2006; Saha et al., 2002; Svejstrup, 2003). Together, Snf2 family helicases are often part of large multi-subunit protein complexes that regulate chromatin structure. Still, it remains elusive how ATP hydrolysis can change the structure of DNA in detail and how domains, polypeptides and motifs within Snf2 family complexes act together.

2.6 Plk1-interacting checkpoint helicase (PICH)

The DNA-dependent ATPase PICH (Plk1-interacting checkpoint helicase) was first identified in a Plk1-PBD Far Western ligand binding assay as a strong binding partner and substrate of Plk1 (Baumann et al., 2007). Sequence analysis characterized PICH as a Snf2 family related helicase harboring an amino-terminal Snf2-like helicase domain (including Walker A and B motifs for ATP metabolization) upstream of an extended HELICc domain (Figure 8). In addition, two TPR (tetratricopeptide repeat) motifs known to mediate protein-protein interactions were identified at the very amino- and carboxy-terminal end of PICH (Lamb et al., 1995). The HELICc extension shares high homology with the human Snf2 family members CSB/ERCC6 and the Rad54 protein. Therefore, PICH was suggested to be a member of the Rad54-like helicases or the Snf2 family of helicases SF2 subfamilies (Baumann et al., 2007; Eisen et al., 1995; Flaus et al., 2006). Within

the PICH sequence, a new motif located carboxy-terminally to the HELICc domain was identified and called PICH-family domain (PFD) (Baumann et al., 2007). Sequence alignments, using the PFD sequence revealed PICH orthologs in vertebrates, plants, non-vertebrates, *Dictyostelium* and in the single-cell eukaryotic parasite *Entamoeba*. Interestingly, no PICH orthologs were found in yeast or the classical model organisms *Drosophila melanogaster* or *Caenorhabditis elegans* (Baumann et al., 2007).

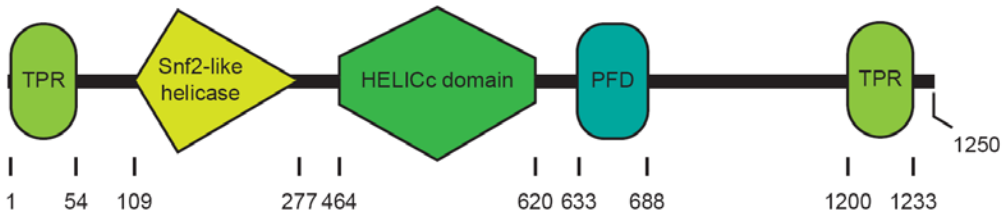

Figure 8: Structure of PICH. Illustration depicting the Snf2-like helicase and extended HELICs (C-term) domains. The PICH-family domain (PFD), a new motif to identify PICH orthologs. PICH harbors two TPR motifs located at the very amino- and carboxy-terminal end.

During early mitosis, PICH localizes to the centromere/KT region of condensed mitotic chromosomes (Baumann et al., 2007). Human cells, depleted of PICH by siRNA duplexes failed to arrest in mitosis when treated with the MT poisons nocodazole or taxol. Interestingly, these cells were unable to recruit the essential SAC component Mad2 to KTs (Baumann et al., 2007), suggesting a role for PICH in the SAC. Moreover, PICH was shown to localize to ultra-fine DNA bridges (UFBs) composed of centromeric DNA, connecting two sister KTs from anaphase onwards (Baumann et al., 2007; Wang et al., 2008). This localization prompted the authors to hypothesize a tension-sensor function for PICH as part of the SAC. However, recent work showed that the PICH siRNA duplexes used in this early study not only affect PICH, but also lower the mRNA and protein level of Mad2 (Hübner et al., 2009), questioning the role of PICH in SAC signaling and identifying Mad2 as a sensitive target for off-target effects.

During anaphase, UFBs increase in length until they become resolved, presumably by the action of topoisomerase 2 (Baumann et al., 2007; Wang et al., 2010). Interestingly, components of the BTR complex have been shown to colocalize and associate with PICH at anaphase UFBs (Chan et al., 2007; Hutchins et al., 2010). The BTR complex, including the RecQ helicase BLM (mutated in Bloom syndrome), is essential for the suppression of chromosomal instability (Payne

and Hickson, 2009). In addition, the two Fanconi anemia (FA) proteins FANCD2 and FANCI have been shown to colocalize with PICH to anaphase UFBs. FANCD2 and FANCI associate specifically with fragile site loci and mark abnormal intertwined DNA structures, induced by replication stress (Chan et al., 2009a; Naim and Rosselli, 2009a).

Depletion of Plk1 induces a dramatic change in the localization of PICH from the centromere/KT to the chromosome arms (Baumann et al., 2007). Interestingly, the chemical inhibition of Plk1 by the small Plk1 inhibitor TAL (ZK-Thiazolidinone) changes the localization of PICH and co-targeted Plk1 to the chromosome arms (Santamaria et al., 2007). In line with this, PICH and Plk1 have recently been shown to be involved in prometaphase chromosome arm architecture and cohesion (Kurasawa and Yu-Lee, 2010; Leng et al., 2008).

However, the detailed mechanism of PICH recruitment to the centromere/KT, chromosome arms and anaphase UFBs and its function at mitotic chromatin remain elusive.

3. AIM OF THIS WORK

First, the DNA-dependent ATPase PICH shows a highly dynamic localization to different mitotic structures during mitosis. Early in mitosis, PICH localizes to the centromere/KT of condensed mitotic chromosomes and upon depletion or chemical inhibition of Plk1, PICH and co-targeted Plk1, gain localization to the chromosome arms. PICH was shown to be a binding partner and substrate of the protein kinase Plk1. (Baumann et al., 2007; Santamaria et al., 2007). From anaphase on, PICH localizes to ultra-fine DNA bridges, connecting the separating sister KTs (Baumann et al., 2007; Wang et al., 2008). The unique localization of PICH to the centromere/KT, chromosome arms and ultra-fine DNA bridges prompted us to investigate the mechanisms underlying the dynamic localization of PICH. Therefore, we asked which proteins or pathways are essential to remove PICH from the chromosome arms and which mechanisms protect it at the centromere/KT during early mitosis.

Second, the function of PICH has been studied extensively in the past. On the one hand PICH was suggested to be part of the spindle assembly checkpoint pathway, on the other hand PICH as well as Plk1 have been proposed to function in prometaphase chromosome arm architecture and cohesion (Kurasawa and Yu-Lee, 2010; Leng et al., 2008). However, we have recently shown that the siRNA duplexes used in the above studies not only affect PICH, but also reduce the mRNA and protein level of the essential SAC component Mad2 (Hübner et al., 2009), thereby making functional conclusions during early mitosis difficult. Thus, we reinvestigated the function of PICH using methods that do not affect any known proteins directly. Furthermore, we set out to identify new interactors of PICH to unravel the mechanisms underlying the function of PICH.

4. RESULTS

4.1 Generation of a PICH monoclonal antibody

To study the dynamic localization and function of PICH during mitosis, a PICH-specific monoclonal antibody was generated. A fragment of PICH (79-752aa) was expressed in *Escherichia coli*, purified and used for immunization of mice (Figure 9, A and B). Screening followed by subcloning of ELISA-positive clones resulted in 4 different hybridoma cell lines (called 142-177-2/9 and 142-26-3/15) that were tested further. Immunofluorescence of HeLaS3 cells showed that all four antibodies decorate the centromere/KT region of mitotic chromosomes (Figure 9, C to F). This staining is sensitive to PICH knockdown by siRNA, demonstrating PICH specificity. Furthermore, the antibodies recognize centromeric UFBs induced by Sgo1 depletion as has been shown before (Baumann et al., 2007), confirming the reactivity of the antibodies. In addition, antibodies 142-26-3 and 142-26-15 detect a single PICH siRNA-sensitive band of 175kDa in western blot analyzes (Figure 9, E to F), attesting to their specificities.

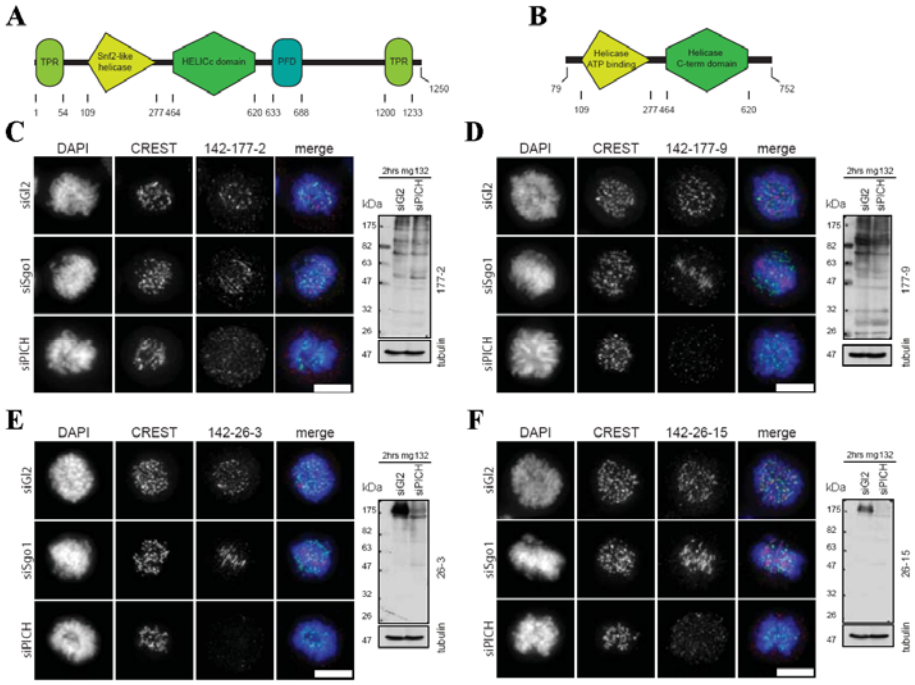

Figure 9: Characterization of 4 different hybridoma cell lines. A) ExPASy domain prediction of human PICH. B) Illustration depicting the truncated specie of PICH used for immunization of mice. C-F) Immunofluorescence and western blot analysis of individual hybridoma cell lines. DNA (DAPI) is shown in blue, CREST in green and PICH in red. Scale bars represent 10µm.

Because PICH localizes to ultra-fine DNA bridges during anaphase that increase in length before they become resolved (Baumann et al., 2007), we analyzed the ability of antibody 142-26-3 to decorate anaphase UFBs in more detail. Immunofluorescence of HeLaS3 cells showed localization of antibody 142-26-3 to anaphase UFBs that resolve during anaphase (Figure 10).

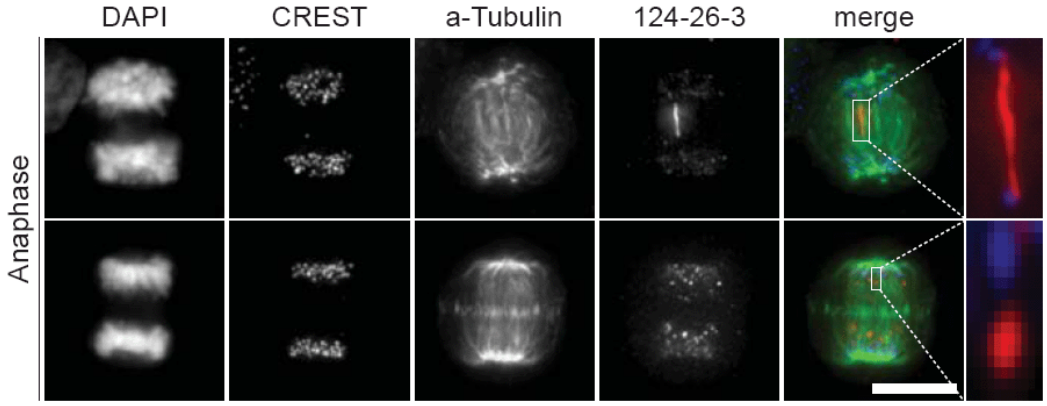

Figure 10: Antibody 142-26-3 decorates anaphase UFBs. Immunofluorescence of HeLaS3 cells stained for DNA (DAPI), CREST (blue), alpha-Tubulin (green) and PICH (142-26-3, red). Antibody 142-26-3 specifically decorates anaphase UFBs that resolve during anaphase. Scale bar represents 10µm.

To test whether antibody 142-26-3 also recognizes the native form of PICH, we performed immunoprecipitation experiments. Lysates of HeLaS3 cells that were synchronized in mitosis with nocodazole were used for immunoprecipitation. In contrast to mouse IgGs (negative control), antibody 142-26-3 precipitated a protein of approximately 175kDa that was recognized by the same antibody in western blotting. Co-precipitation of Plk1 further confirmed the reactivity of 142-26-2 with PICH (positive control) (Figure 11).

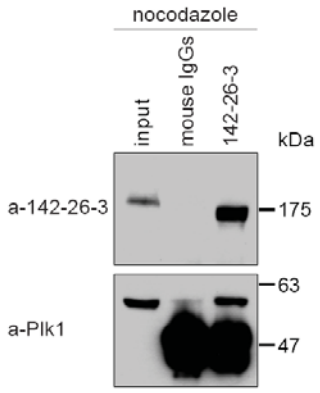

Figure 11: Antibody 142-26-3 immunoprecipitates endogenous PICH. Lysates of nocodazole synchronized HeLaS3 cells were used for immunoprecipitation. Antibody 142-26-3 precipitates a protein of 175kDa bound to Plk1.

The characteristics of the four hybridoma cell lines in immunofluorescence, western blot and immunoprecipitation are in line with previous results obtained for PICH using a polyclonal antibody (Baumann et al., 2007), attesting to their specificities. The properties of the four hybridoma cell lines are summarized in Table 3. In this study, antibody 142-26-3 was used, unless indicated otherwise.

Table 3: Characterization of 4 different hybridoma cell lines. Hybridoma cell lines were analyzed for their isotype and characteristics in IF, WB and IP. (+: positive, -: negative, n.d.: not determined)

Hybridoma	Isotype	Immuno-fluorescence (IF)	Endogenous protein (WB)	Immuno-precipitation (IP)
142-177-2	IgG1	+	-	n.d.
142-177-9	IgG1	+	-	n.d.
142-26-3	IgG1	+	+	+
142-26-15	IgG1	+	+	n.d.

4.2 Mechanisms controlling PICH localization

At the onset of mitosis, PICH localizes to the centromere/KT region of condensed chromosomes. Depletion or chemical inhibition of Plk1 causes the relocalization of PICH (and bound Plk1) to the chromosome arms, demonstrating that Plk1 regulates the localization of PICH. From early anaphase on, PICH associates with UFBs until these become resolved in late anaphase. However, the components that determine and regulate the localization of PICH have not been determined yet.

4.2.1 PICH at chromosome arms

4.2.1.1 PICH homodimerizes

PICH was characterized as a Snf2-like member of the superfamily 2 (SF2) of helicases and several proteins of this family have been shown to act as homodimers (Awad et al., 2010; Baumann et al., 2007; Boehmer et al., 1993; Gorbalenya and Koonin, 1993). To analyze a possible self-association of PICH, we performed co-immunoprecipitation of flag- and myc-tagged PICH transiently expressed in HEK293T cells. We detected an interaction between flag- and myc-tagged PICH. This was independent of the ability to bind Plk1, as the T1063A mutant of PICH, that does not bind Plk1, can still homodimerise (Figure 12A). In contrast, no interaction between PICH and the chromosomal passenger protein INCENP could be detected, confirming the specificity of PICH self-association.

Within the sequence of PICH, two TPR domains have been predicted (Figure 9A) (Baumann et al., 2007). Because TPR domains have been shown to mediate protein-protein interactions (Lamb et al., 1995), we analyzed a potential contribution of the TPR domains to the self-association of PICH by co-immunoprecipitation. Interestingly, PICH oligomerization was not abolished when the TPR domains were truncated individually (PICH-N or PICH-C, N- or C-terminal truncation) or together (PICH-NC) (Figure 12B), indicating that the homodimerisation of PICH is not mediated by its TPR domains.

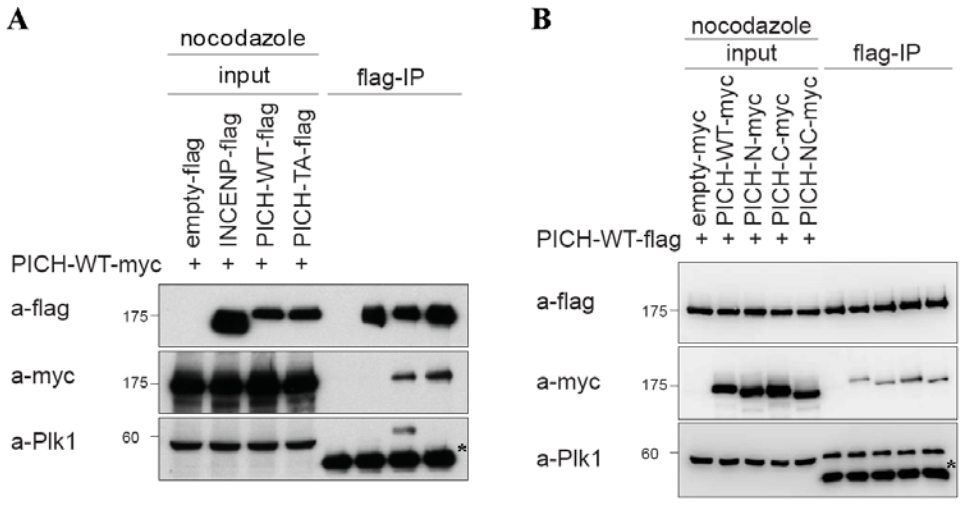

Figure 12: PICH oligomerizes independently of its TPR-domains. A) Co-immunoprecipitation of transiently transfected PICH in HEK293T cells. PICH oligomerization is independent of Plk1 binding to PICH. No interaction of PICH with INCENP confirms specificity of the PICH-PICH interaction. B) Co-immunoprecipitation of transiently transfected PICH-TPR mutants in HEK293T cells. Truncation of both TPR domains does not abolish the PICH-PICH interaction. PICH-N and PICH-C, either the N- or C-terminal TPR domain is truncated, or both (PICH-NC). A-B) Asterisk represents IgG-heavy chain.

4.2.1.2 The TPR domains of PICH are required for correct subcellular localization

During early mitosis PICH specifically localizes to the centromere/KT region of mitotic chromosomes. To ask whether the TPR domains of PICH are required for its mitotic localization we performed immunofluorescence of HeLaS3 cells, transiently transfected with the TPR-domain mutants of PICH. Truncation of either the amino- or carboxy-terminal TPR domain had no significant effect on the localization of PICH. But when both TPR domains were truncated, PICH localized to the chromosome arms in addition to its centromere/KT localization (Figure 13).

Thus, the TPR domains are required for the distinct localization of PICH during early mitosis. Furthermore, the chromosome arm localization of PICH-NC suggests that PICH may interact in a TPR domain-mediated fashion with an unknown protein that regulates the delocalization of PICH from chromosome arms.

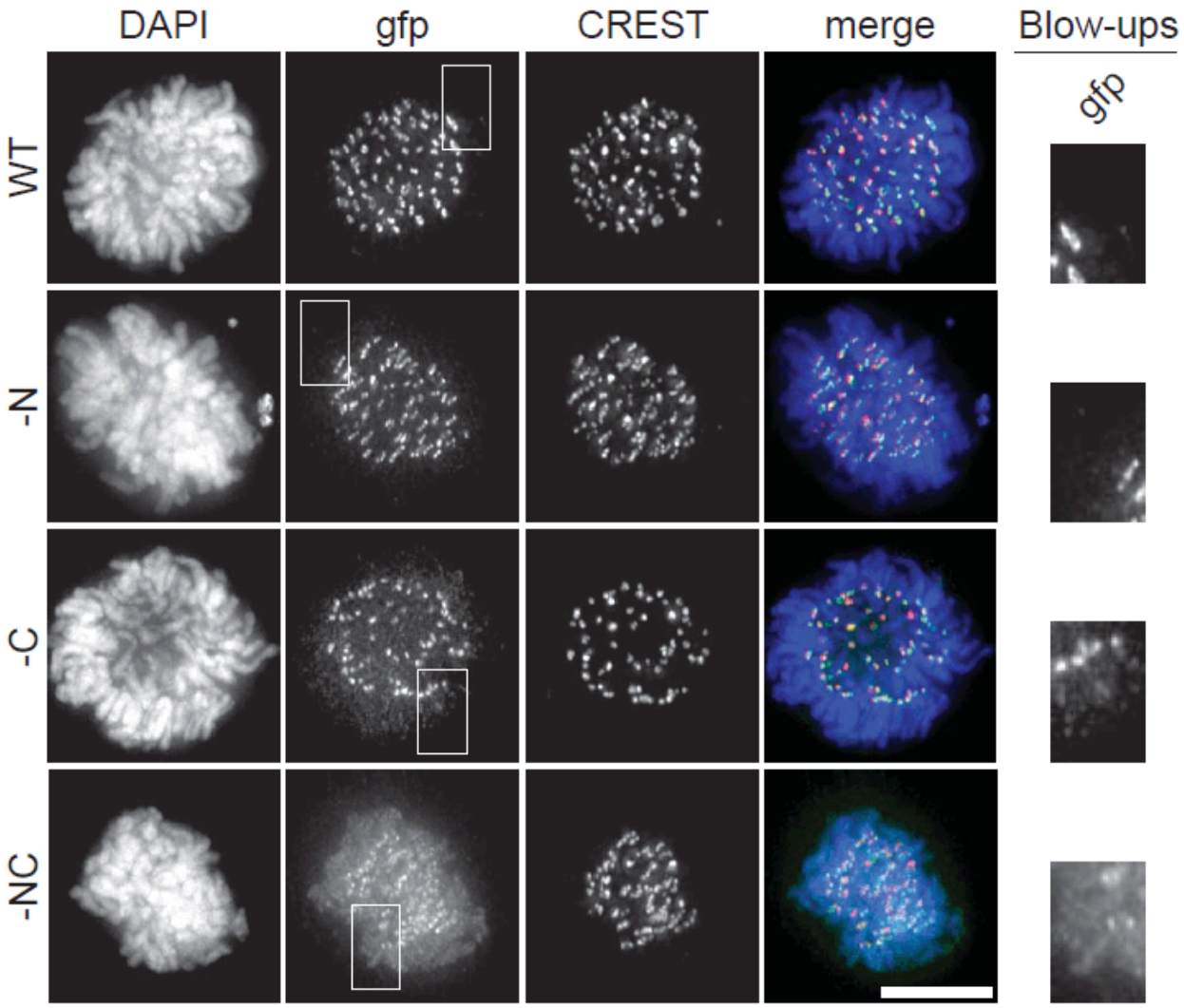

Figure 13: PICH-TPR domains are required for chromosome arm delocalization of PICH. Immunofluorescence of HeLaS3 cells transiently transfected with indicated TPR-domain mutants of PICH. Truncation of both PICH-TPR domains results in PICH localization to the chromosome arms. DNA (DAPI) shown in blue, PICH (gfp) in green and CREST in red. Scale bar represents 10µm.

4.2.1.3 The chromosome arm localization of PICH is regulated by its ATPase activity

In addition to the significance of the TPR domains for PICH localization we hypothesized that the ATPase activity of PICH might regulate its localization. To examine this possibility, we first applied low temperature to cultured cells to inhibit all enzymatic reactions that occur within living cells and subsequently performed immunofluorescence. When HeLaS3 cells were subjected to 4°C for 30 minutes, PICH localized to the chromosome arms (Figure 14A). Since the mitotic spindle has been shown to depolymerize at low temperatures (Sillje et al., 2006), we used the staining for alpha-Tubulin as control for the low temperature treatment. To further show that an enzymatic reaction is required for PICH to delocalize from the chromosome arms, we ask whether the effect of cold treatment is reversible. In HeLaS3 cells exposed to 4°C for 30 minutes and subsequently transferred to 37°C for 5 minutes PICH localized only to the centromere/KT region of mitotic chromosomes (Figure 14B), demonstrating the dynamic association of PICH to the chromosome arms.

To rule out a possible effect of MT-KT attachment in regulating the chromosome arm localization of PICH, we compared the localization of PICH in cells treated with nocodazole or exposed to low temperatures. In nocodazole treated cells, PICH did not localize to chromosome arms (Figure 14C), suggesting that the chromosome arm localization of PICH is MT independent.

PICH has been shown to be phosphorylated by Cdk1 and Plk1 during mitosis (Baumann et al., 2007). To ask whether cold treatment affects the phosphorylation of PICH we analyzed the gel electrophoretic mobility of PICH by western blot. Compared to nocodazole-arrested cells, cold treatment did not detectably change the mobility of PICH (Figure 14D). However, Plk1 has been shown to regulate the chromosome arm localization of PICH (Baumann et al., 2007; Santamaria et al., 2007). Therefore, we cannot rule out at this stage that the chromosome arm localization of PICH in low temperatures is an indirect effect of Plk1 inhibition.

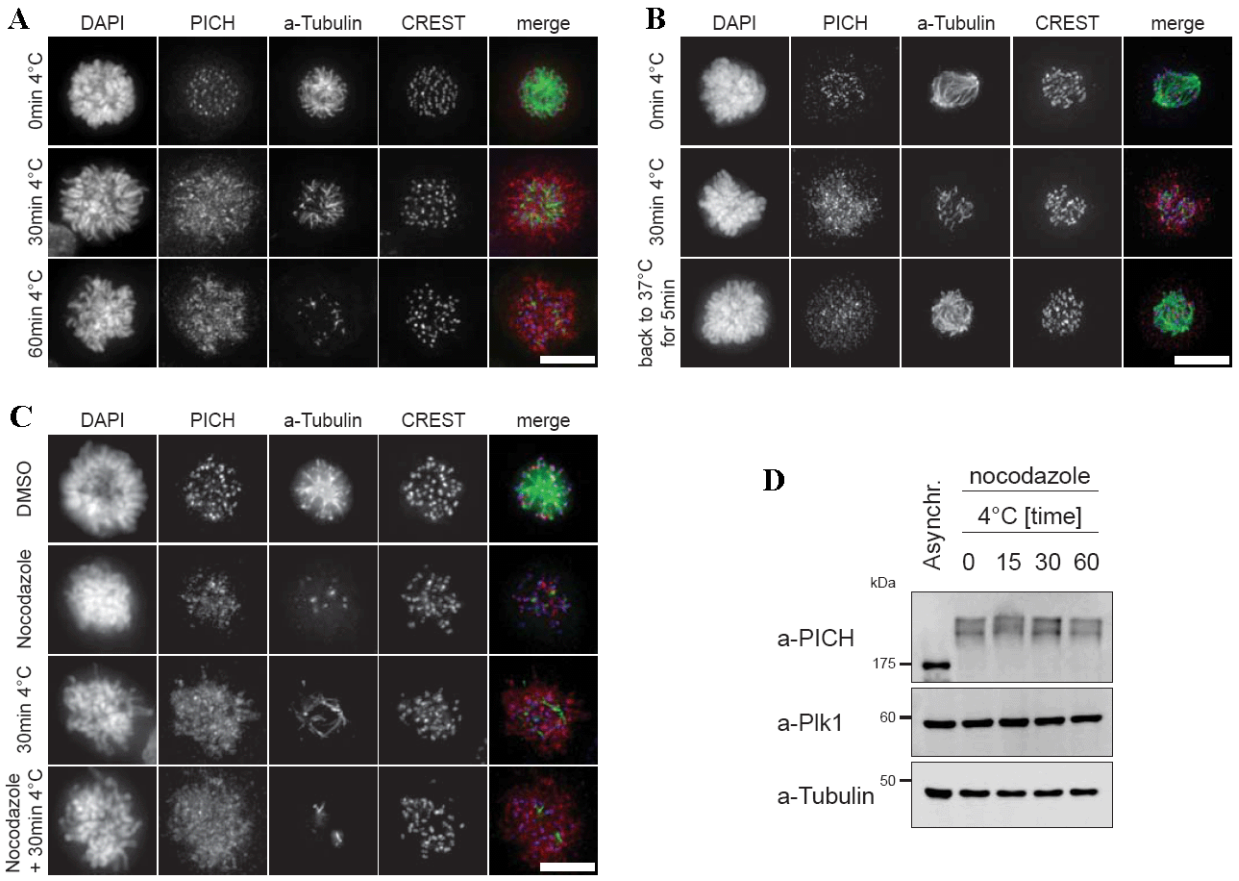

Figure 14: PICH localizes to the chromosome arms in cold treatment. A-C) Immunofluorescence of HeLaS3 cells treated as indicated. DNA was stained with DAPI, PICH is shown in red, alpha-Tubulin in green and CREST in blue. Scale bar represents 10µm. D) Western blot of HeLaS3 lysates treated as indicated. The gel-electrophoretic mobility of PICH is not affected by low temperatures.

Next, we directly wanted to test whether the ATPase activity of PICH is involved in the dynamic localization of PICH. To this end, we generated point mutations within the classical Walker A and B motifs of PICH to generate an ATPase-dead mutant (PICH-WAB). To show that this mutant is indeed ATPase dead, we performed *in vitro* ATPase assays with transiently overexpressed PICH. In contrast to wild-type PICH (PICH-WT), PICH-WAB was unable to metabolize ATP (Figure 15A). Interestingly, when we analyzed the localization of PICH-WAB in transiently transfected HeLaS3 cells, PICH-WAB and co-targeted Plk1 localized to the chromosome arms and to the centromere/KT region of mitotic chromosomes (Figure 15B). Thus, the ATPase activity of PICH is required for the chromosome arm delocalization of PICH.

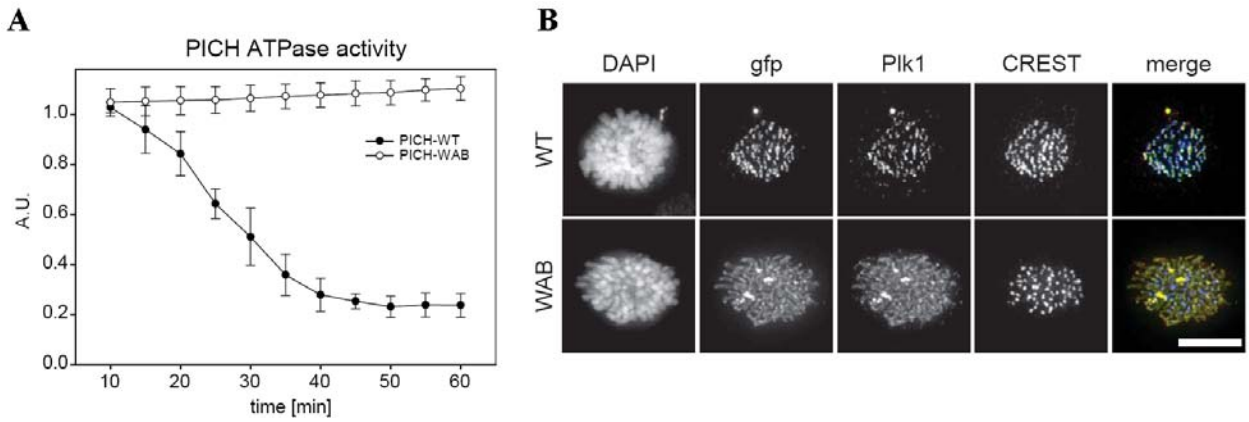

Figure 15: ATPase-dead PICH localizes to the chromosome arms. A) ATPase assay using PICH-WT and PICH-WAB. Walker A and B motifs of PICH are required for its ATPase activity. ATPase activity is shown in arbitrary units (A.U.) as a function of time (min.). Standard deviation obtained after 3 independent experiments. B) Immunofluorescence of HeLaS3 cells transiently transfected with PICH-WT and PICH-WAB. PICH-WAB localizes to the chromosome arms. DNA was stained with DAPI, PICH (gfp) is shown in green, Plk1 in red and CREST in blue. Scale bar represents 10µm.

4.2.1.4 Plk1 indirectly regulates the chromosome arm localization of PICH

In addition to the role of the TPR domains and the ATPase activity of PICH (see sections 4.2.1.2 - 3) the kinase activity of Plk1 has been shown to be required for the delocalization of PICH from the chromosome arms (Baumann et al., 2007; Santamaria et al., 2007). To analyze whether Plk1 directly regulates the chromosome arm localization of PICH by phosphorylation, we performed rescue experiments. We mutated the Plk1-binding site (threonine 1063) of PICH to alanine (PICH-TA), which completely abolished its binding to Plk1 (Figure 16A). HeLaS3 cells were transiently transfected with PICH siRNA duplexes and siRNA-refractory plasmids (Figure 16B), coding for either PICH-WT or PICH-TA. The cells were arrested in mitosis with nocodazole and analyzed by immunofluorescence. Surprisingly, the localization of PICH-TA was indistinguishable from that of PICH-WT (Figure 16C), demonstrating that phosphorylation of PICH by Plk1 does not regulate the chromosome arm delocalization of PICH. However, when Plk1 was subsequently inhibited by the small chemical compound TAL, both PICH-WT and PICH-TA localized to the chromosome arms (Figure 16C). This shows that the kinase activity of Plk1 is essential for the chromosome arm delocalization of PICH during early mitosis, but that the direct phosphorylation of PICH by Plk1 is not required. To date, the Plk1 substrate that regulates the dynamic association of PICH with chromatin remains elusive.

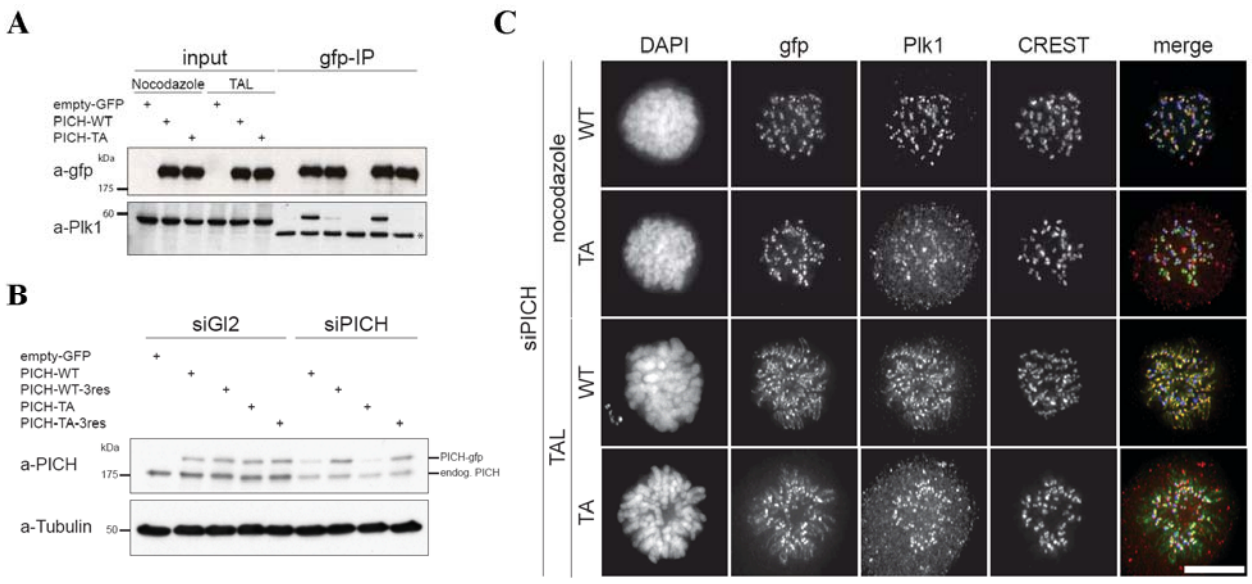

Figure 16: Plk1 indirectly regulates the chromosome arm localization of PICH. A) Immunoprecipitation of PICH and Plk1. PICH Plk1 interaction depends on PICH-T1063 and is independent of Plk1 kinase activity. Asterisk represents IgG-heavy chain. B) PICH plasmids are refractory to PICH siRNA after introduction of 7 silent point-mutations. C) Immunofluorescence of HeLaS3 cells transiently transfected with PICH siRNA and siRNA refractory plasmids. Plk1 indirectly regulates the chromosome arm delocalization of PICH. DNA stained with DAPI, PICH (gfp) shown in green, Plk1 in red and CREST in blue. Scale bar represents 10µm.

4.2.1.5 Plk1 does not regulate the ATPase activity of PICH

We have shown that ATPase-inactive PICH (and bound Plk1) localizes to the chromosome arms. In addition, PICH localizes to the chromosome arms when Plk1 is depleted or chemically inhibited. This raises the question of whether Plk1 regulates the ATPase activity of PICH. In order to answer this question we performed *in vitro* ATPase assays. First, we compared the ATPase activity of PICH-WT and PICH-TA that were overexpressed in HEK293T cells arrested in nocodazole. No detectable difference in ATPase activity between PICH-WT and PICH-TA could be observed (Figure 17A). Second, we analyzed the ATPase activity of PICH-WT in either nocodazole- or TAL-arrested cells. Interestingly, TAL treatment did not result in any decrease in the ATPase activity of PICH-WT (Figure 17B), demonstrating that Plk1 inhibition does not interfere with the ATPase activity of PICH. Finally, we asked whether the ATPase activity of PICH changes or is regulated throughout the cell cycle. To our surprise, PICH-WT from thymidine-arrested cells was as active as that from nocodazole-arrested cells (Figure 17C), suggesting that PICH is constitutively active throughout the cell cycle. Western blot analysis

using antibodies against marker proteins confirmed the synchronization at the expected cell cycle stage (Figure 17D).

Taken together, these data show that the ATPase activity of PICH is not regulated by Plk1 and does not change during the cell cycle.

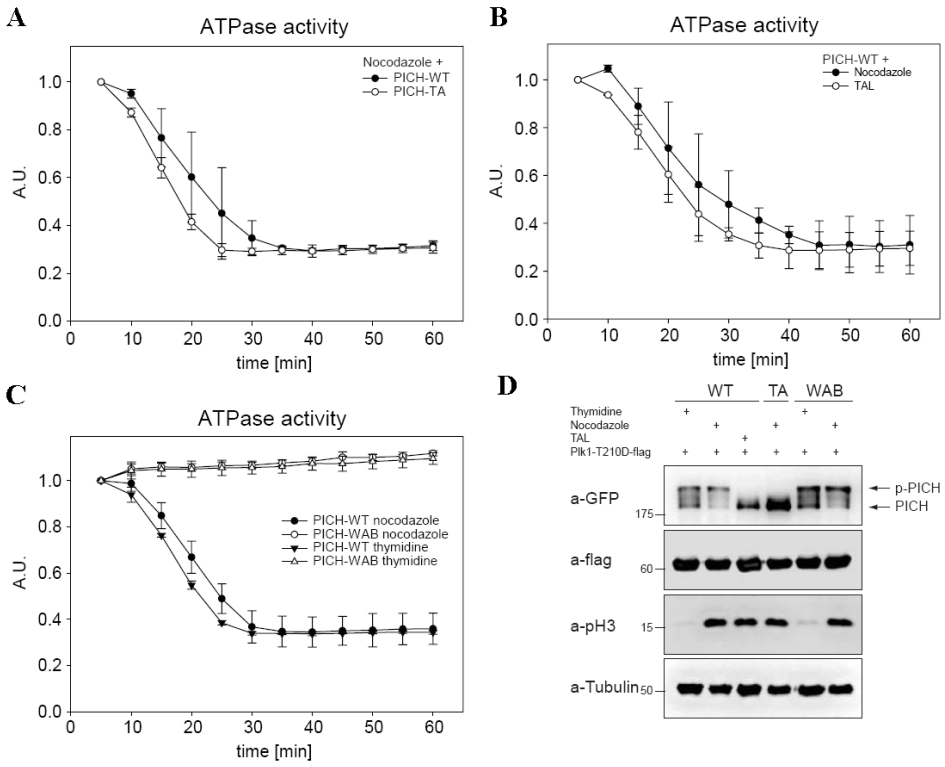

Figure 17: Plk1 does not regulate the ATPase activity of PICH. A-C) *In vitro* ATPase assay using different mutants of PICH overexpressed in HEK293T cells. ATPase activity is shown in arbitrary units (A.U.) as a function of time (min.). Standard deviation obtained after 3 independent experiments. D) Western blot of HEK293T cells treated as indicated, confirming the cell cycle stage.

4.2.1.6 PICH at chromosome arms is independent of sister chromatid arm cohesin

The above results identify the kinase activity of Plk1 as being indirectly required to remove PICH from chromosome arms. However, the direct substrate of Plk1 remains unknown. Interestingly, during prophase and prometaphase, when Plk1 acts to remove PICH from the chromosome arms, Plk1 phosphorylates the SA2 subunit of chromosome arm cohesin to promote sister chromatid arm separation (the prophase pathway) (Hauf et al., 2005; Sumara et al., 2002). Thus we asked, whether chromosome arm delocalization of PICH depends on the removal of sister chromatid arm cohesin. To this end, we used siRNA duplexes to target the 3'UTR (un-

translated region) of human SA2 (Figure 18A) and overexpressed a mutant of SA2 that cannot be phosphorylated by Plk1 (SA2-12xA; kindly provided by Olaf Stemmann). In immunoprecipitation SA2-12xA co-precipitated the cohesin subunits SMC1 and SMC3, confirming its *in vivo* functionality (Figure 18B). Interestingly, when endogenous SA2 was replaced by SA2-12xA, PICH localized to the centromere/KT and not to chromosome arms (Figure 18C). However, the subsequent inhibition of Plk1 by TAL recruited PICH to chromosome arms. Thus, the Plk1 dependent phosphorylation of SA2 does not regulate the delocalization of PICH from chromosome arms.

In addition to the phosphorylation of cohesin subunits by Plk1, a protein called Wapl was shown to regulate the dynamic association of cohesin with chromosome arms (Gandhi et al., 2006; Kueng et al., 2006). Depletion of Wapl blocks cohesin dissociation from chromosomes during the early stages of mitosis and prevents the resolution of sister chromatids (Kueng et al., 2006). Therefore, we analyzed the localization of PICH in HeLaS3 cells depleted of Wapl. Western blot analysis confirmed the efficiency of previously reported siRNA duplexes targeting Wapl (Figure 18D) (Kueng et al., 2006). However, immunofluorescence of Wapl-depleted HeLaS3 cells did not result in the recruitment of PICH to the chromosome arms (Figure 18E).

These results show that neither the phosphorylation of SA2 by Plk1 nor the removal of sister chromatid arm cohesin during early mitosis regulates the chromosome arm delocalization of PICH. Therefore, it is unlikely that sister chromatid arm cohesin is the “Plk1 substrate” that regulates the chromosome arm localization of PICH.

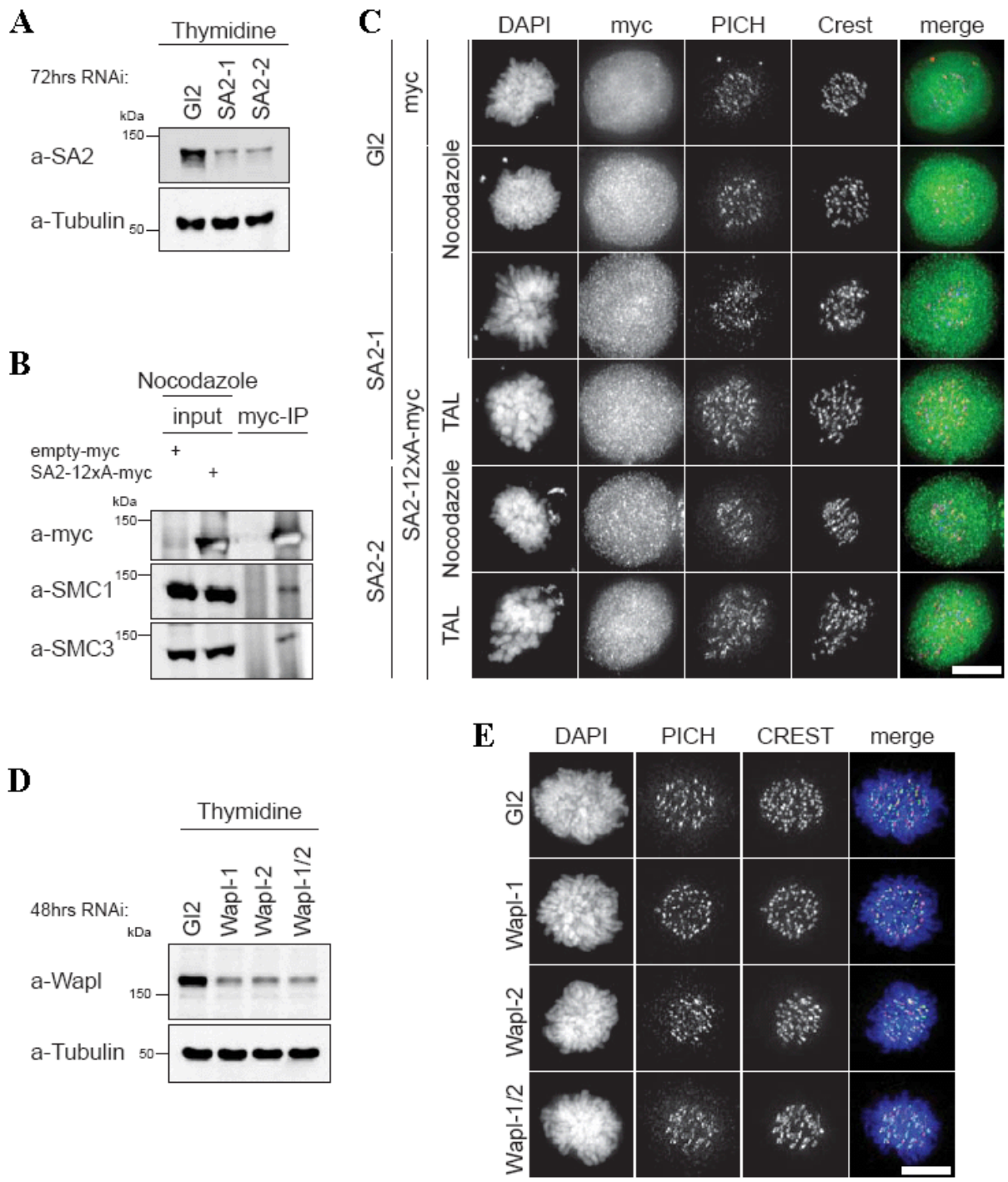

Figure 18: Dissociation of sister chromatid arm cohesin and chromosome arm delocalization of PICH are uncoupled. A) Depletion efficiency of two new SA2 siRNA duplexes analyzed by western blot. B) Immunoprecipitation of SA2-12xA transiently transfected into HEK293T cells. SA2-12xA interacts with cohesin ring complex components. C) Immunofluorescence of SA2-12xA rescue. SA2 phosphorylation does not regulate the chromosome arm localization of PICH. DNA stained with DAPI, myc expression shown in green, PICH in red and CREST in blue. Scale bar represents 10µm. D) Depletion efficiency of previously reported Wapl siRNA duplexes analyzed by western blot. E) Immunofluorescence of Wapl depleted HeLaS3 cells. Cohesin stabilization does not correlate with chromosome arm localization of PICH. DNA (DAPI) shown in blue, PICH in red and CREST in green. Scale bar represents 10µm.

4.2.2 PICH at the centromere/KT

4.2.2.1 Centromere/KT localization of PICH is independent of centromere cohesion

In contrast to the dynamic localization of PICH to the chromosome arms, PICH stably decorates the centromere/KT region of mitotic chromosomes. To date, little is known about proteins or mechanisms that regulate the localization of PICH at the centromere/KT.

To characterize this localization of PICH we hypothesized that it might depend on the presence of cohesin. In contrast to chromosome arm cohesin, centromere/KT cohesin is protected from dissociation by a protein called shugoshin 1 (Sgo1) during early mitosis (Kitajima et al., 2004). Sgo1 recruits the protein phosphatase PP2A to the centromere/KT, which has been suggested to dephosphorylate cohesin subunits, resulting in stable centromere cohesion (Kitajima et al., 2006). Moreover, Sgo2, a paralogue of *Schizosaccharomyces pombe* Sgo1, has been identified to be required for faithful segregation of mitotic chromosomes (Kitajima et al., 2004). Thus, we asked whether the centromere/KT localization of PICH depends on centromeric sister chromatid cohesion. We transfected HeLaS3 cells with previously reported siRNA duplexes targeting Sgo1 and Sgo2 and analyzed the localization of PICH. Western blot analysis confirmed the siRNA efficiency of the previously reported siRNA duplexes (Figure 19A) (Huang et al., 2007; McGuinness et al., 2005). Interestingly, PICH localization at the centromere/KT was unaffected when Sgo1, Sgo2 or both were depleted (Figure 19B).

Thus, the localization of PICH at the centromere/KT is independent of centromeric cohesin and cohesion.

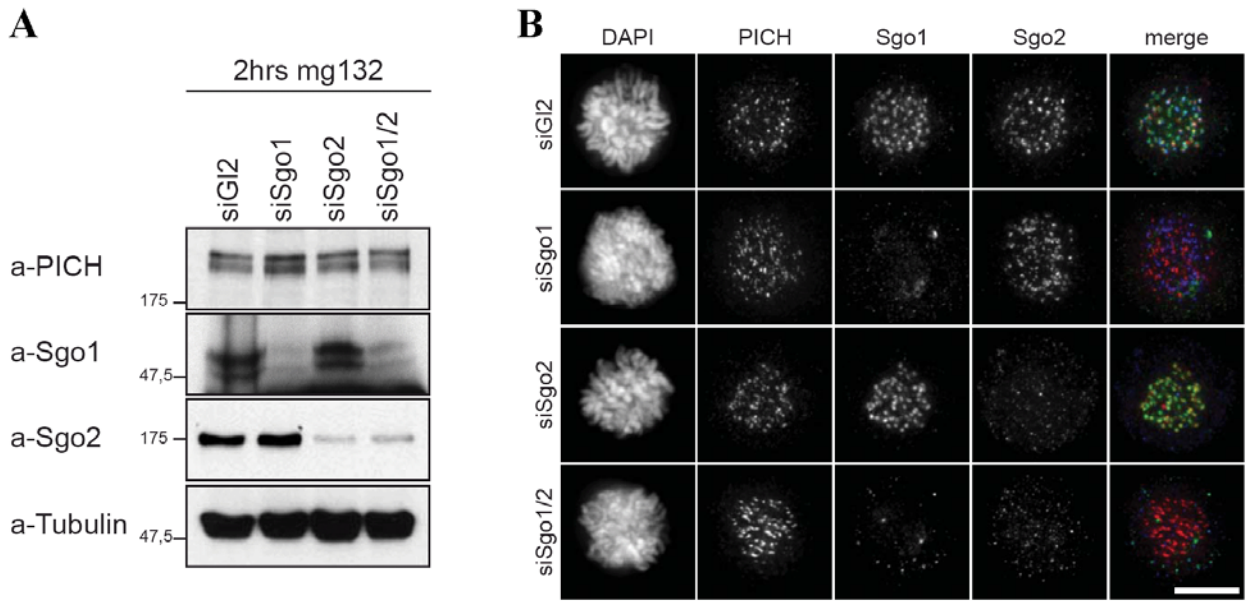

Figure 19: Centromere/KT PICH is independent of centromeric cohesion. A) Depletion efficiency of Sgo1 and Sgo2 siRNA duplexes analyzed by western blot. B) Immunofluorescence of HeLaS3 cells transfected with Sgo1, Sgo2 or both siRNA duplexes. PICH localizes to the centromere/KT in the absence of centromeric cohesion. DNA was stained with DAPI; PICH is shown in red, Sgo1 in blue and Sgo2 in green. Scale bar represents 10µm.

4.2.2.2 Centromere/KT PICH is protected from Cdk1 and Plk1

In addition to Plk1, Cdk1 has been shown to phosphorylate PICH, thereby priming PICH for Plk1 binding (Baumann et al., 2007). To ask whether Cdk1, like Plk1, contributes to the distinct mitotic localization of PICH we treated HeLaS3 cells with either TAL or roscovitine, a chemical inhibitor of Cdk1/2 (Rudolph et al., 1996), or both. As mentioned above, TAL treatment recruited PICH to the chromosome arms, but did not affect the centromere/KT localization of PICH. Interestingly, the inhibition of Cdk1/2 did not affect the localization of PICH (Figure 20), supporting the result that the direct phosphorylation of PICH by Plk1 does not influence PICH localization. Surprisingly, co-inhibition of both kinases interfered with the chromosome arm recruitment of PICH and significantly enhanced the centromere/KT intensity of PICH (Figure 20A). Western blot analysis revealed that the protein abundance of PICH was unaffected (Figure 20B). This implies that centromere/KT levels of PICH increase in the absence of Cdk1/2/Plk1 kinase activity. Conversely, it is possible that an increase in kinase activity might decrease PICH levels at centromeres/KTs. Thus, an equilibrium between the kinases Cdk1 and Plk1 and unknown phosphatases might regulate the localization of PICH at centromeres/KTs, even though this hypothesis has to be tested further.

Taken together, the kinase activities of Cdk1 and Plk1 seem to limit the localization of PICH at the centromeres/KTs.

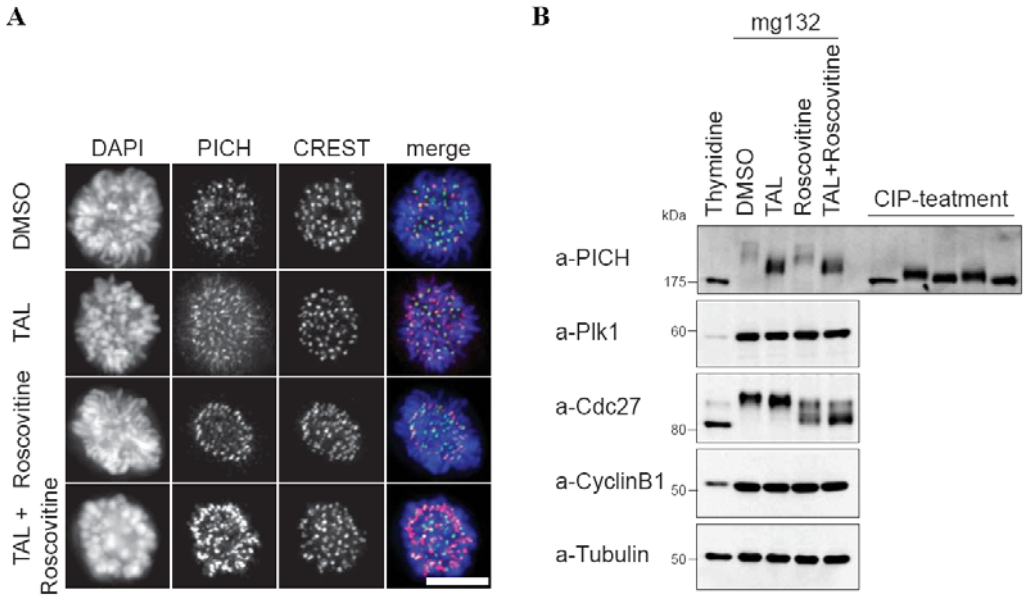

Figure 20: Dynamic localization of PICH depends on Cdk1 and Plk1. A) Immunofluorescence of HeLaS3 cells treated with TAL, roscovitine or in combination. Chromosome arm localization of PICH depends on Cdk1 and centromere/KT associated PICH is protected from Cdk1 and Plk1. Cells were synchronized with thymidine, released and directly supplemented with TAL. Roscovitine was added for 30min to mitotic cells. DNA (DAPI) is shown in blue, PICH is red and CREST in green. Scale bar represents 10µm. B) Western blot analysis of HeLaS3 cells treated as indicated. Protein abundance of PICH is unaffected in Cdk1 and Plk1 co-inhibition.

4.2.3 Summary

To understand the dynamic localization of PICH we generated mutants of PICH and performed rescue experiments. These experiments revealed that the TPR domains and the ATPase activity of PICH are important for its dissociation from chromosome arms. In addition, we identified the kinase activity of Plk1 as being indirectly required for the dynamic association of PICH with chromosome arms, but not required for the ATPase activity of PICH. Furthermore, we showed that the chromosome arm delocalization of PICH is independent of sister chromatid arm cohesin, leaving the Plk1 substrate unidentified that regulates the chromatin association of PICH.

Moreover, we addressed possible mechanisms regulating the centromere/KT localization of PICH. Like PICH arm localization, centromere/KT-associated PICH localizes independently of centromeric cohesion. However, co-inhibition of Cdk1 and Plk1 revealed a function for both kinases in regulating the localization of PICH at the centromere/KT.

4.2.4 BEND3, a potential Plk1 substrate required for mitosis

4.2.4.1 Identification of BEND3

Although several members of the Snf2-family of helicases have been shown to function as multi-subunit protein complexes (Cote et al., 1994; Ito et al., 1997; Shen et al., 2000), Plk1 is the only known binding partner of PICH so far. To identify new binding partners of PICH, we performed immunoprecipitation experiments of endogenous and overexpressed PICH. Besides Plk1 and ATP-dependent DNA and RNA helicases, members of the renal cell carcinoma (RCC) family and components of the BTR and FA complexes were identified (a complete list can be found in section 4.4 of the results). Additionally, we found the uncharacterized protein BEND3 (Figure 21A) (also known as KIAA1553 or RP11-59I9.2).

The coding sequence for BEND3 is located on chromosome 6q21 and comprises 2487 nucleotides, resulting in a predicted protein of 828 amino acids. BLAST (NCBI) and PROSITE (ExPASy) sequence analysis revealed 4 BEN domains within the BEND3 protein sequence (Figure 21B). BEN domains are modules composed of 4 alpha-helices that can be found in several animal proteins like BANP/SMAR1 or NAC1 (Abhiman et al., 2008). The BEN domain is found in one or more copies in these proteins and was named after the experimentally characterized proteins BANP, E5R and NAC1 (BEN). Interestingly, the BEN domain is predicted to mediate protein-DNA and protein-protein interactions during chromatin organization and transcription (Abhiman et al., 2008).

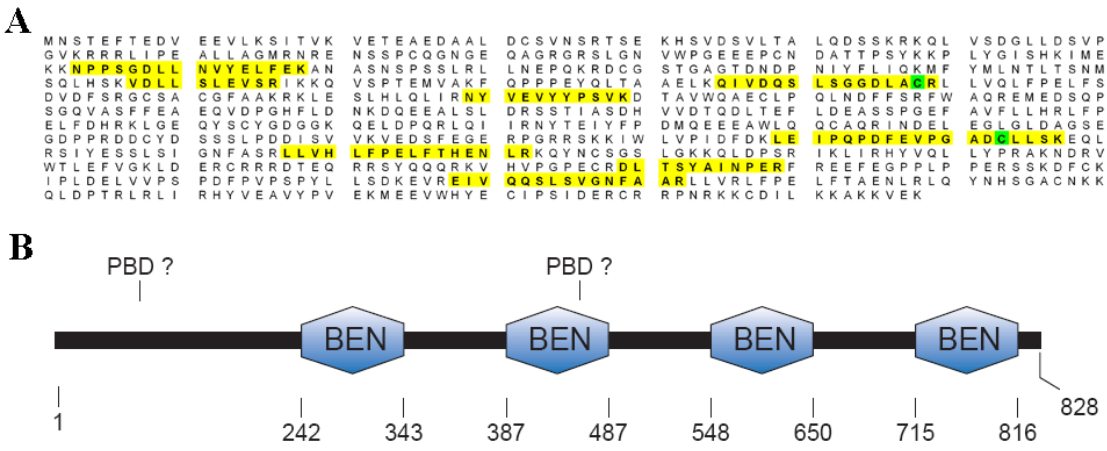

Figure 21: BEND3, a new binding partner of PICH. A) Protein sequence of human BEND3. Yellow highlighted peptides were found by mass-spectrometry after immunoprecipitation of PICH-WT and PICH-WAB. Depicted in green, cysteine residues modified with carbamidomethyl (due to sample preparation). B) ExPASy domain prediction of human BEND3. In addition, two conserved PBD binding sites were identified.

BEND3 belongs to the family of BEN domain containing proteins that differ in size and in the number of contained BEN domains (Figure 22). BEND1 (or BANP) is the only protein of the family that has been characterized to date and has been reported to function as a tumor suppressor (Birot et al., 2000; Kaul et al., 2003).

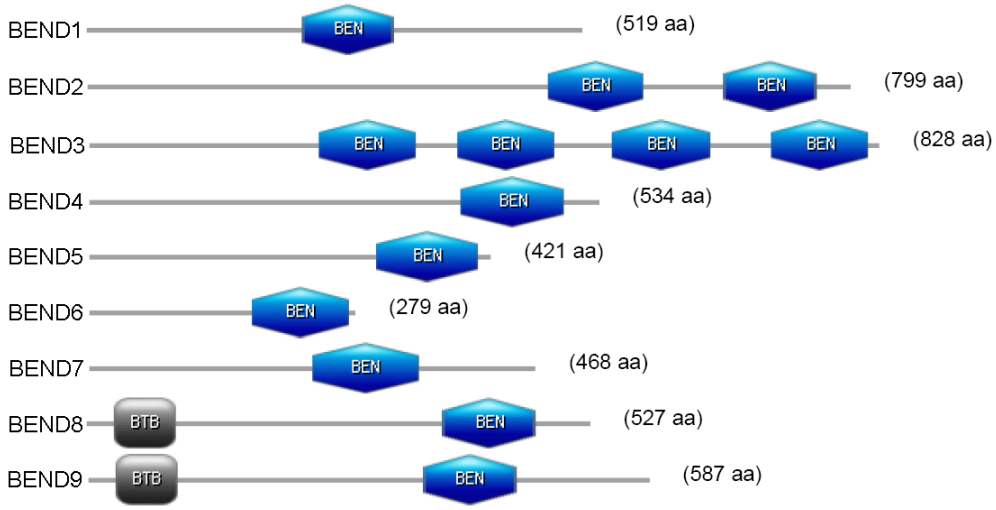

Figure 22: BEN domain containing family of proteins. The human family of BEN domain-containing proteins. BEN domains are highlighted in blue. The size of the corresponding protein is indicated by the total amino acid (aa) number. BEND8 and BEND9 contain additional BTB domains, reported to mediate homodimerization (Bardwell and Treisman, 1994).

4.2.4.2 BEND3 localizes to the chromatin during mitosis

Because BEN domains are predicted to mediate protein-DNA interactions (Abhiman et al., 2008), we analyzed the intracellular distribution of BEND3. We generated a plasmid coding for human BEND3 and transfected HeLaS3 cells with this plasmid. The cells were arrested with nocodazole and analyzed by western blotting for the expression of exogenous BEND3. A prominent band of approximately 110kDa was detectable (Figure 23A), matching the calculated molecular weight of BEND3 of 94.49kDa in addition to the myc-tag. Next, we analyzed the mitotic localization of BEND3. We transiently transfected BEND3-myc into HeLaS3 cells, synchronized them in mitosis with nocodazole and performed immunofluorescence. Interestingly, BEND3-myc localized to mitotic chromosomes (Figure 23B), confirming a recent report in which BEND3 was found in a large scale proteomic analysis to be associated with mitotic chromatin (Ohta et al., 2010).

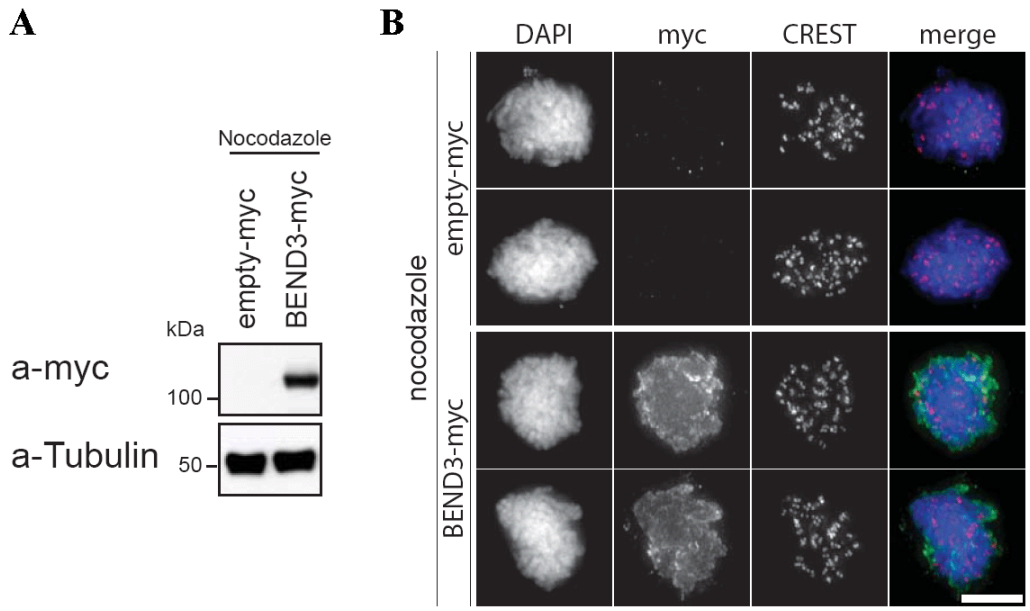

Figure 23: BEND3 localizes to mitotic chromatin. A) Western blot analysis of HeLaS3 cell-lysates, transiently transfected with BEND3-myc. B) Immunofluorescence of nocodazole treated HeLaS3 cells, transiently transfected as indicated. BEND3 localizes to mitotic chromatin. DNA (DAPI) is shown in blue, BEND3 (myc) is shown in green and CREST in red. Scale bar represents 10µm.

4.2.4.3 BEND3 deficiency leads to mitotic catastrophe

Recently, BEND3 has been identified as a protein that associates with mitotic chromatin, but no functional predictions have been made (Ohta et al., 2010). To investigate the possible function of BEND3 in mitosis, we designed two siRNA duplexes specific for human BEND3. First, we analyzed the efficiency of the two siRNA duplexes. To this end, we transiently transfected HeLaS3 cells with BEND3-myc and the BEND3 siRNA duplexes. To avoid possible cell cycle effects of BEND3 depletion, we synchronized the cells with thymidine for the last 24hrs of transfection. Both siRNA duplexes significantly reduced the expression of exogenously expressed BEND3-myc, whereby the BEND3-2 siRNA duplex lead to a slightly better depletion (Figure 24A). Next, we analyzed the phenotype of BEND3 depletion. We transfected HeLaS3 cells with the BEND3 siRNA duplexes and followed the cells by light microscopy. Interestingly, after 72hrs, BEND3 siRNA transfection resulted in a strong accumulation of dead cells (Figure 24B), suggesting that BEND3 is essential for cell viability.

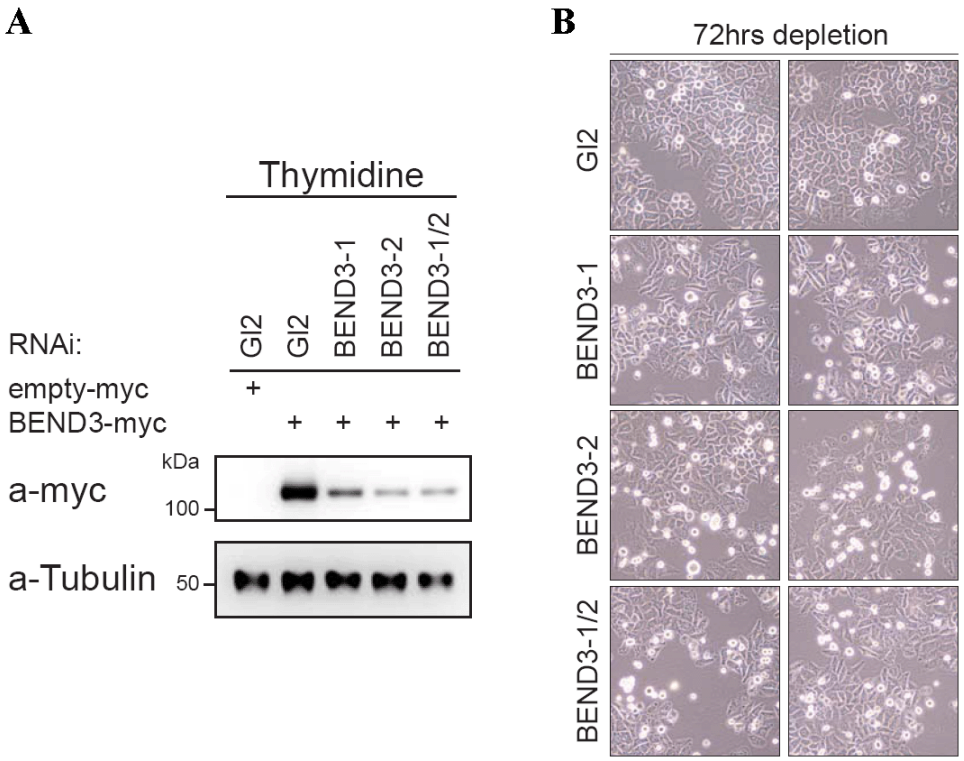

Figure 24: BEND3 siRNA duplexes are effective and BEND3 depletion induces cell death. A) Western blot analysis of HeLaS3 cell lysates, transiently transfected with BEND3-myc plasmid and the indicated BEND3 siRNA duplexes. Both BEND3 siRNA duplexes affect the protein level of exogenously expressed human BEND3. B) Light-microcopy images of HeLaS3 cells treated with the indicated siRNA duplexes. 72hrs of BEND3 depletion negatively affects cell viability.

To analyze the phenotype of BEND3 depletion in more detail, we transfected HeLaS3 cells, stably expressing histone 2B-GFP, with a pool of both BEND3 siRNA duplexes and followed their cell cycle progression by time-lapse microscopy. Control cells entered mitosis, formed a metaphase plate and separated their chromatids properly. However, cells transfected with BEND3 siRNA duplexes entered mitosis, but were unable to align their chromosomes at the metaphase plate (Figure 25A). Furthermore, within a time period of 1.5hrs, approximately 60% of the cells underwent chromatin condensation and cell fragmentation, resulting in apoptosis and mitotic catastrophe (Figure 25B). This identifies BEND3 as an important protein for mitotic progression.

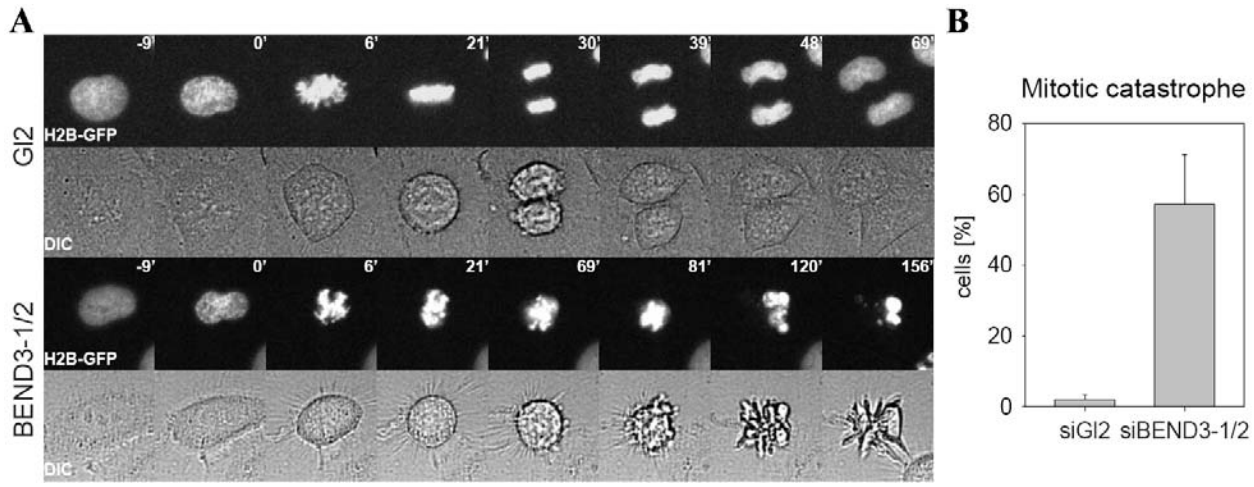

Figure 25: BEND3 is required for mitosis. A) Stills of representative HeLaS3 cells transfected with either Gl2 or BEND3 siRNA duplexes. Time represents progression through mitosis, starting with NEBD. Histone 2B-GFP shows chromatin and DIC the optical density. B) Bar graph showing the quantification of cells in A. 60% of BEND3-depleted cells are unable to progress through mitosis and undergo mitotic catastrophe. Error represents standard error from three individual experiments.

4.2.4.4 BEND3 is a binding partner and potential substrate of Plk1

In order to analyze a possible connection between PICH, Plk1 and BEND3, we asked whether BEND3 is a Plk1 substrate during mitosis. First, we analyzed whether BEND3 associates with Plk1 during mitosis. Interestingly, exogenously expressed BEND3-myc co-precipitated endogenous Plk1 (Figure 26A), suggesting an association of both proteins during mitosis. By analyzing the amino acid sequence of BEND3, we identified two potential binding sites for polo-box binding domains (two SSP motifs, comprising residues 92-94 and 405-407). Future experiments will be needed to test whether these motives are required for the interaction with Plk1. Second, we asked whether BEND3 is a potential substrate of Plk1. To this end, we overexpressed BEND3-myc together with the hyperactive form of Plk1 (Plk1-T210D) and arrested the cells in mitosis. Interestingly, BEND3 showed a slower migrating form in SDS gels when Plk1-T210D was present (Figure 26B). The appearance of this form was due to the kinase activity of Plk1, as it was absent when cells were treated with the Plk1 inhibitor TAL. Furthermore, we bioinformatically identified 32 putative Plk1 phosphorylation sites within the sequence of BEND3 (Figure 26C). However, whether Plk1 indeed phosphorylates BEND3 directly and whether this phosphorylation affects the chromatin localization of PICH remains to be tested.

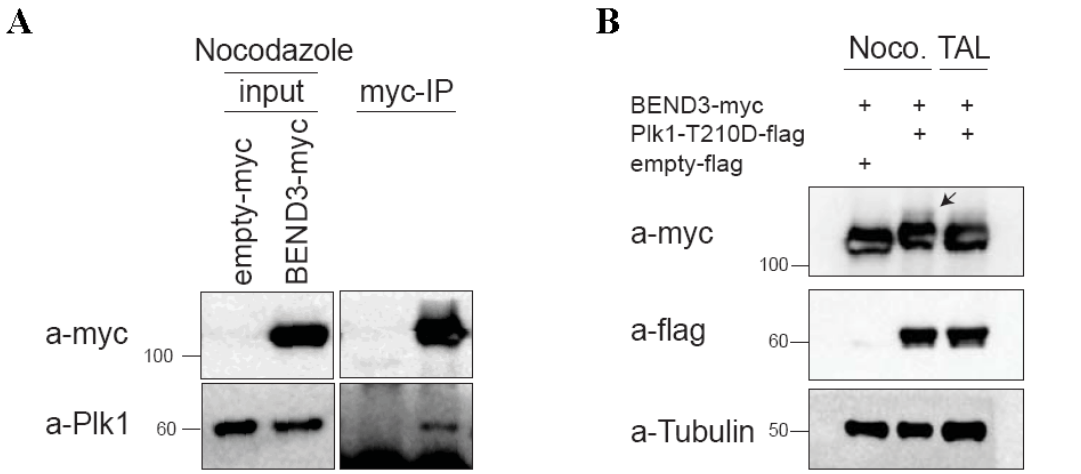

C

MNSTEFTEDVEEVLKSITVKVETEAEDAALDCSVNSRTSEKHSVDSVLTALQDSSKRKQLVSDGLLDSVPGVKRRRL
IPEALLAGMRNRENSSPCQGNGEQAGRGRSLGNVWPGEEEPCNDATTPSYKKPLYGISHKIMEKKNPPSGDLLNVYE
LFEKANASNSPSSLRLLNEPQKRDCGSTGAGTDNDPNIYFLIQKMFYMLNTLTSNMSQLHSKVDLLSLEVSRIKKQV
SPTEMVAKFQPPPEYQLTAAELKQIVDQSLSGGDLACRLLVQLFPELFSDVDFSRGCSACGFAAKRKLESLHLQLIR
NYVEVYYPSVKDTAVWQAECLPQLNDFFSRFWAQREMEDSQPSGQVASFFEAEQVDPGHFLDNKDQEEALSLDRSST
IASDHVVDTQDLTEFLDEASSPGEFAVFLLHRLFPELFDHRKLGEQYSCYGDGGKQELDPQRLQIIRNYTEIYFPDM
QEEEAWLQQCAQRINDELEGLGLDAGSEGDPPRDDCYDSSSLPDDISVVKVEDSFEGERPGRRSKKIWLVPIDFDKL
EIPQPDFEVPGADCLLSKEQLRSIYESSLSIGNFASRLLVHLFPELFTHENLRKQYNCSGSLGKKQLDPSRIKLIRH
YVQLLYPRAKNDRVWTLEFVGKLDERCRRRDTEQRRSYQQQRKVHVPGPECRDLTSYAINPERFREEFEGPPLPPER
SSKDFCKIPLDELVVPSPDFPVPSPYLLSDKEVREIVQQSLSVGNFAARLLVRLFPELFTAENLRLQYNHSGACNKK
QLDPTRLRLIRHYVEAVYPVEKMEEVWHYECIPSIDERCRRPNRKKCDILKKAKKVEK

Figure 26: BEND3, a new binding partner and potential substrate of Plk1. A) Western blot analysis after immunoprecipitation of exogenously expressed BEND3-myc. BEND3 interacts with Plk1. B) Western blot analysis of HEK293T cell-lysates transfected with indicated plasmids. Co-expression of hyperactive Plk1 induces a slower migrating band of BEND3 that is absent when Plk1 is inhibited by TAL. C) Amino acid sequence of BEND3. Highlighted in red and bold letters are putative Plk1 phosphorylation sites. Letters corresponding to the two polo-box binding domains are underlined and shown in italic.

4.2.4.5 The localization of PICH and Plk1 depends on BEND3

Next, we analyzed whether the absence of BEND3 would affect the localization of PICH during mitosis. We transfected HeLaS3 cells with BEND3 siRNA duplexes and synchronized the cells by thymidine, followed by a 10hrs release prior to PTEMF fixation. Interestingly, in cells that had strong defects in aligning their chromosomes at the metaphase plate, PICH and Plk1 were undetectable at the centromere/KT (Figure 27A), suggesting a functional relationship between BEND3, PICH and Plk1. Western blot analysis of BEND3 siRNA-transfected HeLaS3 cell lysates revealed that the protein abundance of PICH and Plk1 was unaffected (Figure 27B), implying that PICH and Plk1 are delocalized rather than degraded in BEND3-depleted cells. To rule out that the architecture of the KT and the mitotic spindle is affected by BEND3 depletion, we analyzed the localization of Hec1 or alpha-Tubulin in BEND3 depleted cells, respectively.

We observed that Hec1 localization to the KT was not affected and that the mitotic spindles were bipolar (Figure 27C). Thus, BEND3 is required for the localization of PICH and Plk1 at the centromere/KT and that their requirement does not reflect a general defect in spindle architecture and KT structure.

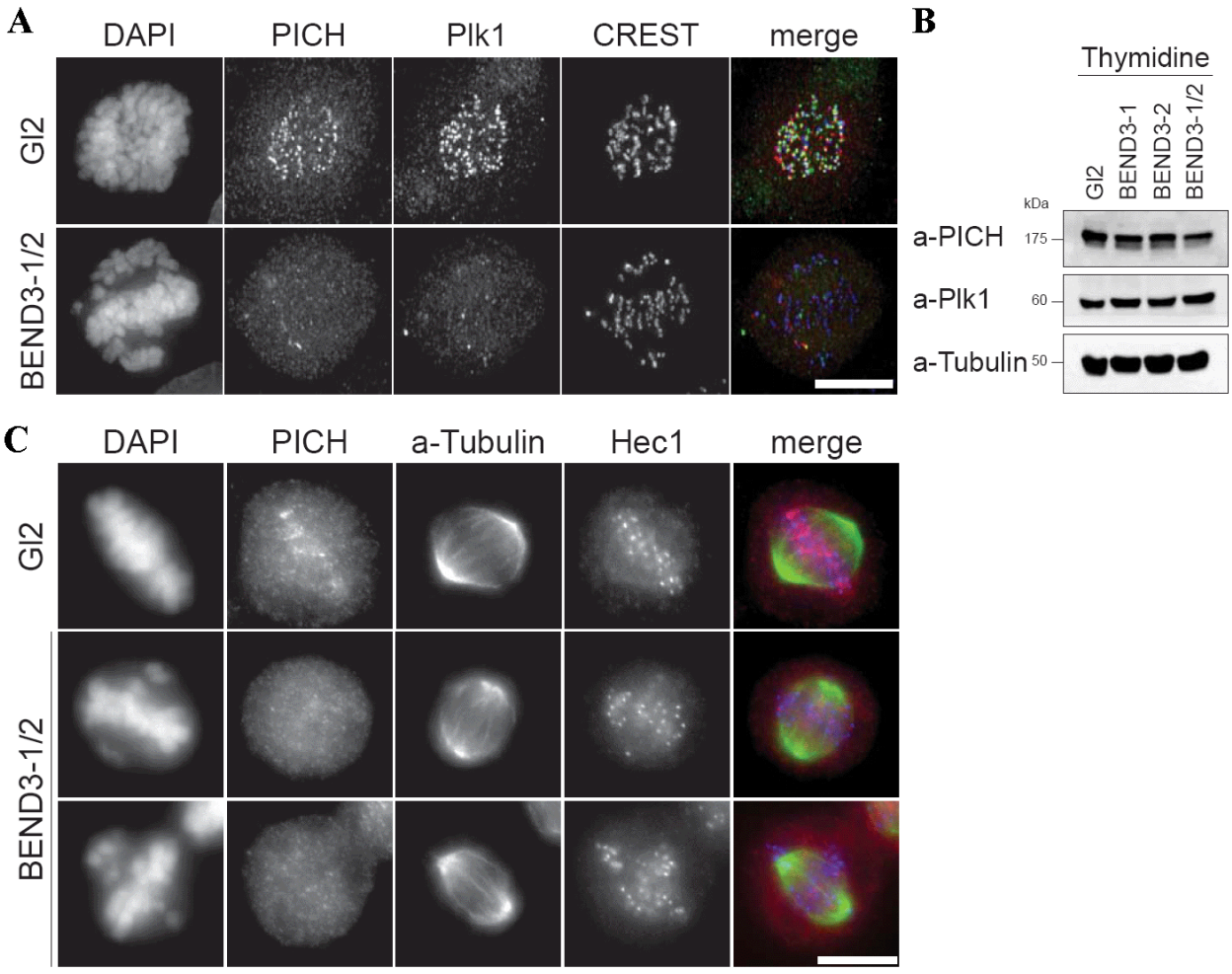

Figure 27: Centromere/KT PICH and Plk1 localization depends on BEND3 A) Immunofluorescence of HeLaS3 cells transfected with either Gl2 or BEND3 siRNA duplexes. PICH and Plk1 delocalize from the centromere/KT upon BEND3 depletion. DNA was stained with DAPI; PICH is shown in red, Plk1 in green and CREST in blue. Scale represents 10µm. B) Western blot analysis of HeLaS3 cell lysates treated as indicated. The protein level of PICH and Plk1 are not affected by BEND3 depletion. C) Immunofluorescence of HeLaS3 cells transfected with either Gl2 or BEND3 siRNA duplexes. Hec1 and alpha-Tubulin localization is unaffected when BEND3 is absent. DNA was stained with DAPI; PICH is shown in red, alpha-Tubulin in green and Hec1 in blue. Scale represents 10µm.

4.2.4.6 Summary

To understand the association of PICH with mitotic chromatin in more detail, we performed immunoprecipitation of PICH followed by mass spectrometry. We identified the protein BEND3 as a binding partner of PICH and characterized BEND3 as a member of the BEN domain containing family of proteins. Interestingly, BEND3 localizes to mitotic chromatin during mitosis and its depletion affects the alignment of chromosomes at the metaphase plate and subsequently results in apoptosis. Furthermore, we show that BEND3 is a binding partner and potential substrate of Plk1 during mitosis. Interestingly, BEND3 depletion leads to the delocalization of PICH and Plk1, but does not affect the structure of the mitotic spindle or the localization of Hec1 to KTs. We therefore hypothesize that Plk1 might phosphorylate BEND3 to regulated the localization of PICH during mitosis.

4.3 Functional characterization of PICH

4.3.1 PICH is not required for the SAC

Depletion of PICH with two independent siRNA duplexes had originally been shown to abolish a SAC-dependent mitotic arrest (Baumann et al., 2007). In addition, the essential SAC component Mad2 had been reported to delocalize from the KT upon PICH depletion (Baumann et al., 2007), implying that PICH has a function in the SAC. However, in a recent study these results had to be revised, as we could show that the originally used PICH siRNA duplexes also reduce the mRNA and protein levels of Mad2 (Hübner et al., 2009). Furthermore, several siRNA duplexes have subsequently been identified that effectively deplete PICH but do not affect Mad2 protein abundance or localization, thereby questioning the role of PICH in SAC signaling (Hübner et al., 2009). To confirm that PICH does not function in SAC signaling and to explore the "real" function of PICH, we performed single-cell microinjection with antibodies that detect the native form of PICH; a monoclonal PICH antibody (mAB, characterized above, section 4.1) and a polyclonal antibody (pAB) specific for PICH (Baumann et al., 2007).

Initially, we wanted to confirm that the SAC override by PICH depletion was only due to an off-target effect on Mad2 mRNA. Thus, HeLaS3 cells were treated with nocodazole for 5hrs, microinjected and kept in culture for additional 3hrs prior to immunofluorescence. As expected, the injection of cells with antibodies targeting PICH or myc (negative control) did not lead to a mitotic exit in the presence of nocodazole (Figure 28, A and B), demonstrating the PICH independency of the SAC. In contrast, injection of a previously reported monoclonal Mad2 antibody (positive control) completely abolished the mitotic arrest and lead to mitotic exit of injected cells (Chan et al., 2009b), confirming the importance of Mad2 for SAC signaling.

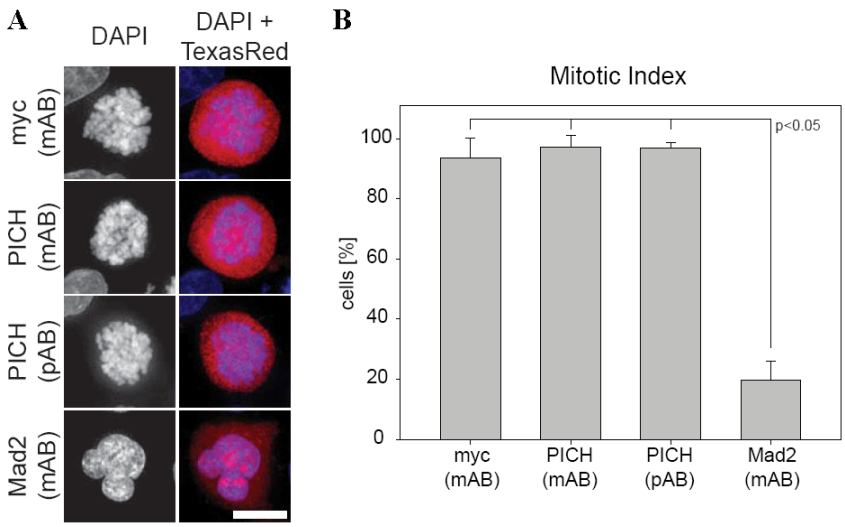

Figure 28: PICH does not function in the SAC. A) Immunofluorescence of antibody-microinjected HeLaS3 cells treated with nocodazole. PICH-antibody injection does not abolish a SAC-dependent arrest. B) Bar graph illustrating the quantification of A. Mad2 antibody injection significantly abolishes a nocodazole-induced SAC-dependent arrest in mitosis. Error bars represent standard error from three individual experiments.

4.3.2 PICH deficiency results in chromatin bridges during anaphase

Next, we set out to identify the potential role of PICH in mitotic progression. Recently, PICH has been shown to function in prometaphase chromosome arm architecture and cohesion (Kurasawa and Yu-Lee, 2010; Leng et al., 2008). However, the siRNA duplexes used in those studies have been shown to induce an off-target effect on Mad2 mRNA and protein levels (Hübner et al., 2009). To circumvent this problem and elucidate the function of PICH at prometaphase chromosome arms we analyzed living cells microinjected with PICH antibodies by time-lapse microscopy. HeLaS3 cells stably expressing histone 2B-GFP were presynchronized in interphase with thymidine for 24hrs, released for 7hrs, then microinjected with different antibodies and subsequently monitored by time-lapse microscopy. The time between NEBD and the onset of anaphase slightly increased in all tested conditions (Figure 29B), most likely representing cellular stress due to the procedure of microinjection. However, PICH antibody injection did not affect the timing of anaphase-onset, compared to the control antibody, confirming that the SAC is independent of PICH (Figure 29, A and B). Most interestingly, PICH antibody-injected cells showed a significant increase in chromatin bridges during anaphase (control AB: 3-5%, PICH AB: 18-19%) (Figure 29, A and C), which implies a role for PICH in faithful sister chromatid segregation.

To confirm that PICH deficiency leads to chromatin bridges during anaphase, we also depleted PICH with specific siRNA duplexes and analyzed the cells by time-lapse microscopy. For these experiments we used siRNA duplexes that have recently been shown to efficiently deplete PICH without affecting SAC signaling (Hübner et al., 2009). HeLaS3 cells stably expressing histone 2B-mCherry were transfected with PICH siRNA duplexes for 48hrs, synchronized with thymidine for 24hrs, released for 7hrs and analyzed by time-lapse microscopy. Similar to the result obtained by antibody injection, PICH knockdown did not accelerate the time required from NEBD to anaphase onset (Figure 30, A and B). However, PICH depletion resulted in a significant increase in chromatin bridges during anaphase compared to control cells (27% and 5%, respectively) (Figure 30, A and C), confirming that PICH functions in the faithful segregation of chromosomes during mitosis.

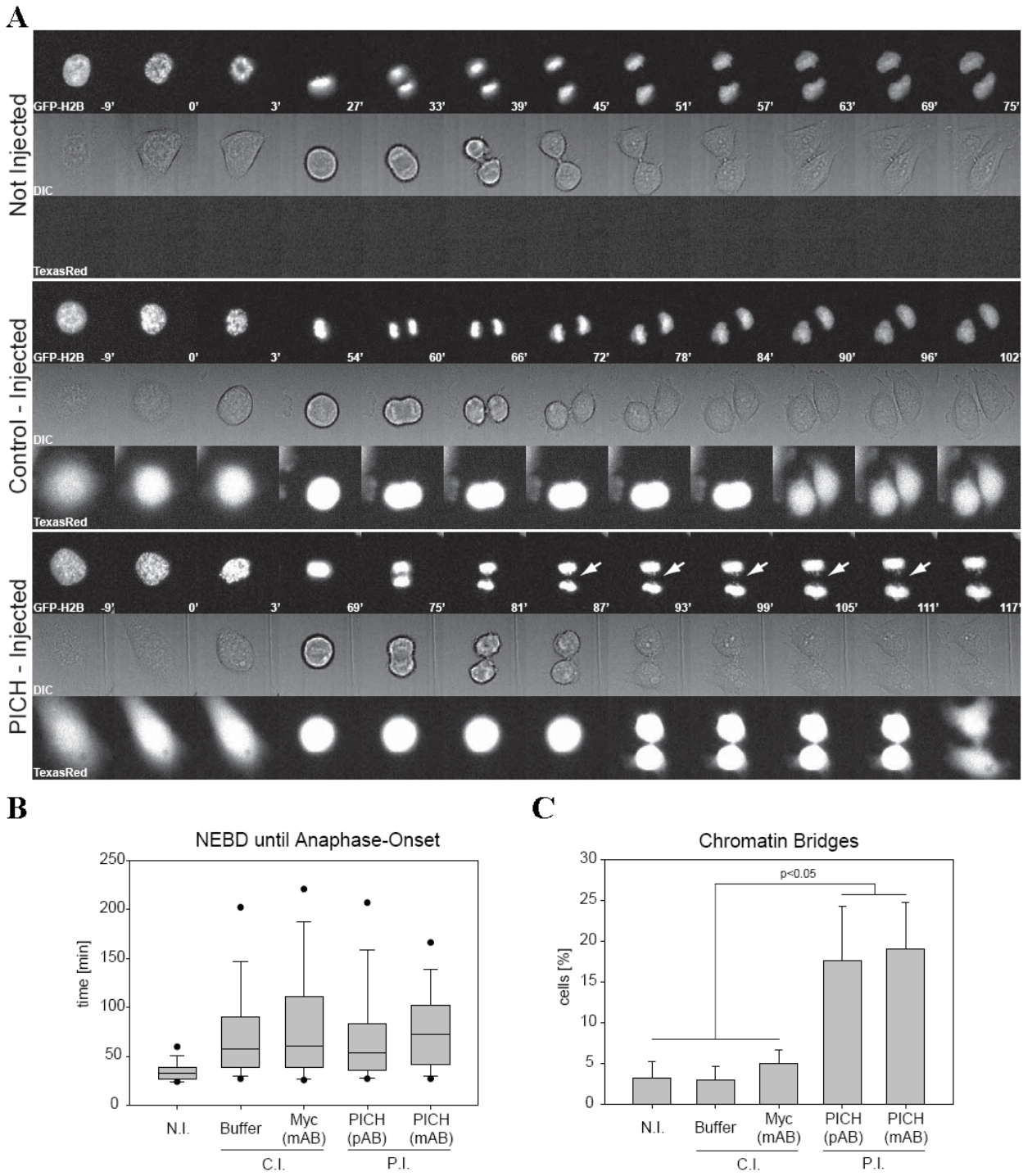

Figure 29: PICH antibody injection leads to chromatin bridges during anaphase. A) Stills of representative HeLaS3 cells microinjected with indicated antibodies. Time represents progression through mitosis, starting with NEBD. Histone 2B-GFP shows chromatin, DIC shows optical density and Texas-Red indicates positive injection. Arrows highlight chromatin bridges during anaphase. B) Box-and-whisker plot illustrating the quantification of mitotic progression of A. PICH neutralization does not accelerate mitotic progression. (N.I.: not injected, C.I.: control injected, P.I.: PICH injected) C) Bar graph showing the quantification of chromatin bridges of A. PICH antibody injection results in chromatin bridges during mitosis. Error bars represent standard error from three individual experiments.

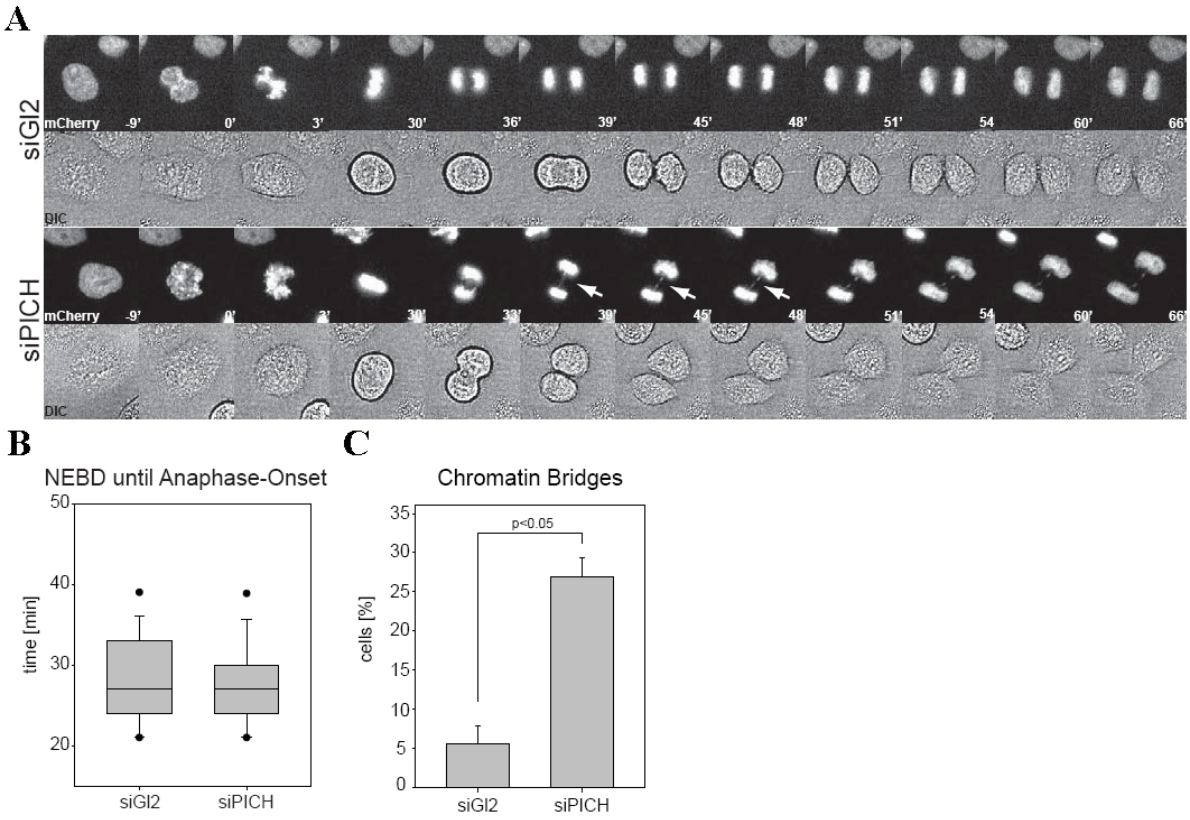

Figure 30: PICH knockdown results in chromatin bridges during anaphase. A) Stills of representative HeLaS3 cells transfected with either Gl2 or PICH siRNA duplexes. Time represents progression through mitosis, starting with NEBD. Histone 2B-mCherry shows chromatin and DIC the optical density. Arrows indicate chromatin bridges during anaphase. B) Box-and-whisker plot showing the quantification of mitotic progression of A. PICH knockdown does not accelerate mitotic progression. C) Bar graph showing the quantification of chromatin bridges of A. PICH knockdown results in chromatin bridges during mitosis. Error bars represent standard error from three individual experiments.

To visualize the segregation defect of mitotic chromosomes upon PICH knockdown in more detail, we analyzed anaphase cells of fixed PICH-depleted HeLaS3 cells. The analyzed cells revealed a broad heterogeneity in the number of chromatin bridges, from one single to multiple chromatin bridges per cell (Figure 31).

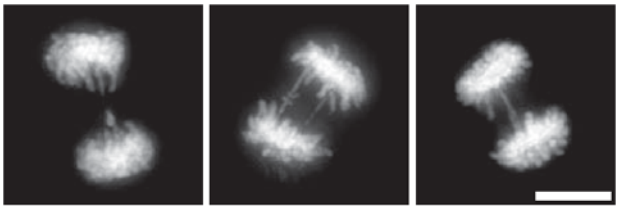

Figure 31: Heterogeneity of PICH depletion-induced chromatin bridges. Representative images of HeLaS3 anaphase cells depleted of PICH for 48hrs. PICH deficiency can lead to multiple chromatin bridges during anaphase. Chromatin stained with DAPI. Scale bar represents 10µm.

4.3.3 PICH depletion results in the formation of micronuclei

We have shown that PICH deficiency can lead to the formation of chromatin bridges during anaphase. Previously, chromatin bridges have been shown to break into multiple fragments at the end of mitosis, promoting the formation of micronuclei (MN) (Hoffelder et al., 2004; Naim and Rosselli, 2009a; Rosin and German, 1985; Utani et al., 2010). Therefore, we analyzed the frequency of MN in asynchronously growing PICH-depleted HeLaS3 cells. In contrast to Gl2 transfection, PICH depletion resulted in a significant increase of MN (0.92% to 4.19%, respectively) (Figure 32, A and B). This strongly suggests that PICH-deficiency induced chromatin bridges break into fragments and form MN.

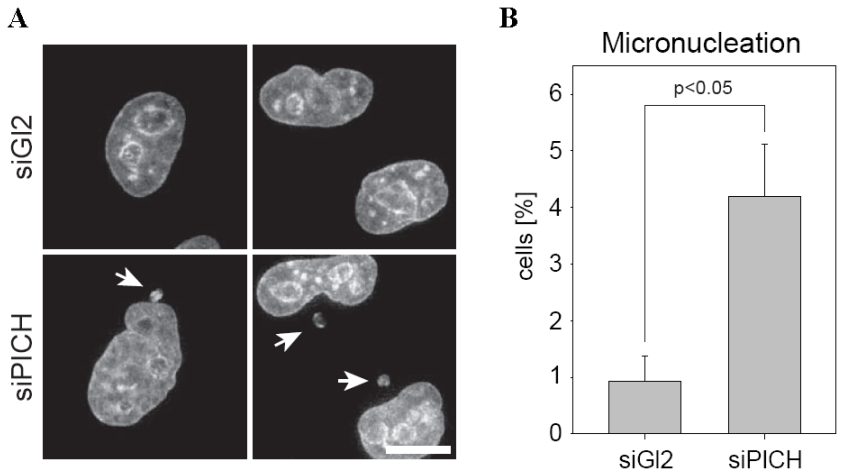

Figure 32: PICH depletion-induced chromatin bridges promote MN formation. A) Representative images of HeLaS3 interphase cells depleted of PICH for 48hrs. Chromatin was stained with DAPI. Arrows indicate MN. B) Bar graph illustrating the quantification of A. PICH deficiency promotes MN formation. Error bars represent standard error from three individual experiments.

4.3.4 The ATPase activity of PICH is indispensable to prevent the formation of chromatin bridges

We have shown that PICH exhibits ATPase activity *in vitro* that depends on the classical Walker A and Walker B motives (section 4.2.1.3). Furthermore, neutralization or knockdown of PICH results in the formation of chromatin bridges (section 4.3.2-3). To ask whether the ATPase activity of PICH is required for chromatin bridge resolution, we performed rescue experiments coupled to time-lapse microscopy. Interestingly, the transient expression of wild-type but not ATPase-dead PICH prevented the formation of chromatin bridges during anaphase (2% and 32%,

respectively) (Figure 33, A and B). Thus, the ATPase activity of PICH is indispensable to prevent the formation of chromatin bridges during anaphase.

Recently, it has been shown that PICH localization to chromosome arms (and bound Plk1) contribute to prometaphase chromosome arm architecture (Kurasawa and Yu-Lee, 2010). As impaired chromosome arm architecture can result in chromatin bridges, we asked whether the PICH-Plk1 interaction is required to prevent the formation of chromatin bridges. We mutated the Plk1 docking site of PICH and performed time-lapse microscopy of cells expressing mutant PICH protein in a siRNA background. To mimic the phosphorylation at threonine 1063 and promote a stable interaction between PICH and Plk1, we mutated threonine 1063 to aspartic (TE) and glutamic acid (TD). Unfortunately, neither PICH-TE nor PICH-TD interacted with Plk1 (Figure 34, A and B), making rescue experiments with these constructs impossible. In contrast, PICH-TA prevented the formation of chromatin bridges (Figure 33, A and B), in spite of its inability to bind Plk1 (Figure 34B). The chromatin-bridge rescue exerted by PICH-TA still required the ATPase activity of PICH, as PICH-WAB-TA (ATPase inactive and unable to bind Plk1) was unable to prevent the formation of chromatin bridges during anaphase (Figure 33, A and B). These data demonstrate that the interaction between PICH and Plk1 is not required to prevent chromatin bridges during anaphase, but they do not exclude the possibility that the disruption of this interaction is required.

The above experiment also revealed that, towards the end of mitosis, the dissociation of ATPase-dead PICH from the chromatin was significantly prolonged compared to PICH-WT (90 min to 26 min, respectively) (Figure 33, A and C). Therefore, we asked whether ATPase-dead PICH affects the exit of mitosis. To answer this question, we analyzed the reformation of the nuclear envelope in cells expressing ATPase-dead PICH. In contrast to wild-type PICH, ATPase-dead PICH colocalized with the chromatin even after the nuclear envelope had reformed (Figure 34C), demonstrating that mitotic exit had occurred, even though PICH still associated with chromatin. Interestingly, in this experimental set-up, chromatin bridges were induced by overexpression of ATPase-dead PICH despite the presence of endogenous PICH. This demonstrates that ATPase-dead PICH acts antagonistically to endogenous PICH like a dominant negative mutant of PICH.

Thus, the ATPase activity of PICH is essential for the resolution of chromatin bridges during anaphase, but this activity is independent of the interaction between PICH and Plk1.

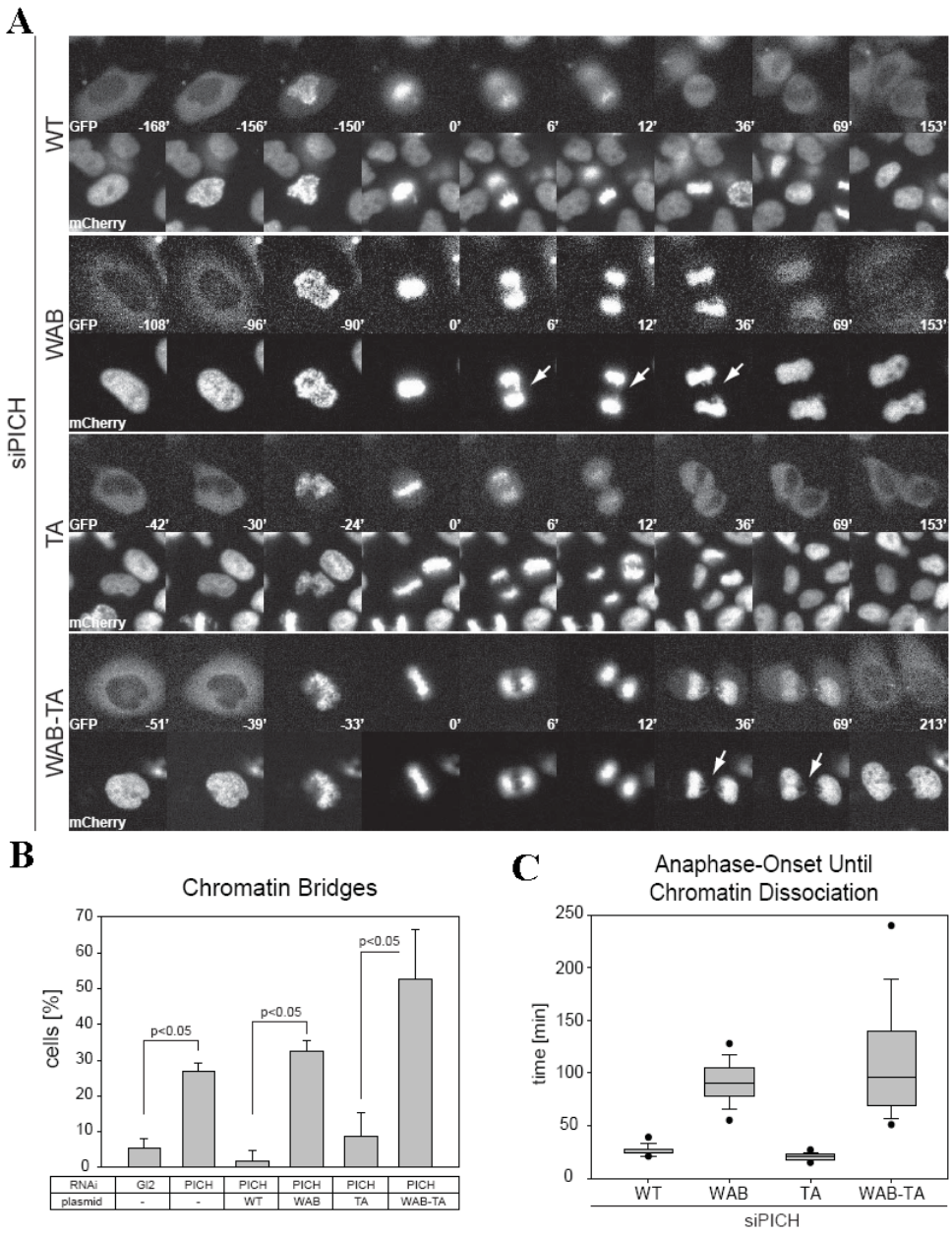

Figure 33: The ATPase activity of PICH is indispensable to prevent chromatin bridges during anaphase. A) Stills of representative HeLaS3 cells transfected with PICH siRNA duplexes and siRNA refractory PICH plasmids. Time represents progression through mitosis, starting with anaphase onset. Histone 2B-mCherry shows chromatin and DIC the optical density. Arrows indicate chromatin bridges during anaphase. B) Bar graph illustrating the occurrence of chromatin bridges of cells in A. Error bars represent standard error from three individual experiments. C) Box-and-whisker plot showing the quantification of the time required from anaphase onset until the chromatin dissociation of indicated PICH species.

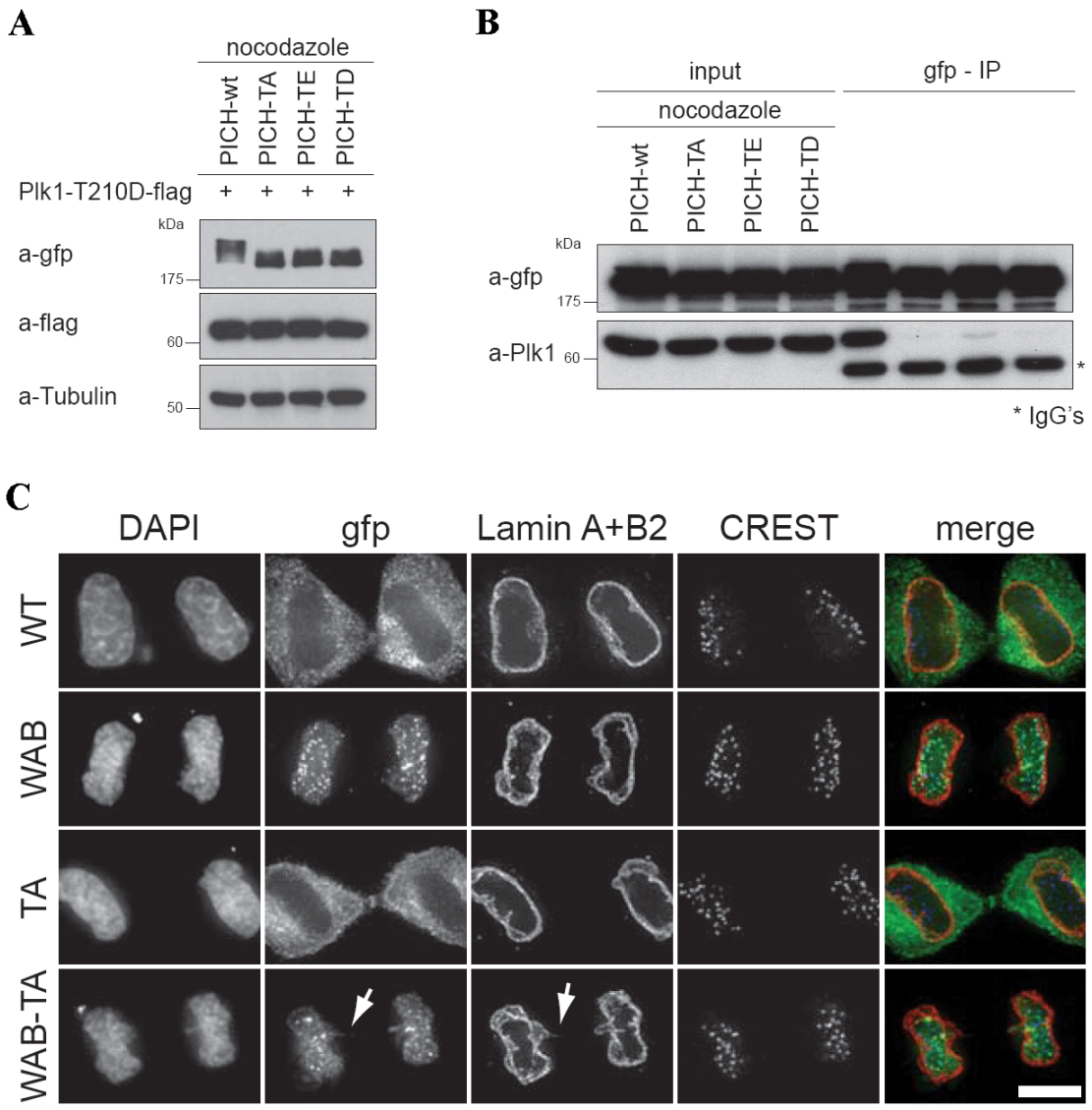

Figure 34: ATPase-dead PICH does not interfere with mitotic exit. A) Western blot analysis of HEK293T cell lysates, treated as indicated. PICH mutants generated to mimic phosphorylation at threonine 1063 are no substrate for Plk1 during mitosis. B) Western blot analysis of immunoprecipitated PICH species. PICH mimic mutants are unable to bind Plk1. C) Immunofluorescence of HeLaS3 cells transiently transfected with indicated PICH constructs. ATPase-dead PICH stays associated with the chromatin even after the nuclear envelop has reformed. Arrow indicates chromatin bridges. DNA stained with DAPI, gfp is shown green, Lamin A+B2 in red and CREST in blue. Scale bar represents 10µm.

4.3.5 Sequestration of Plk1 by PICH and consequences for mitotic progression

We have shown that the ATPase activity of PICH is required to prevent the formation of chromatin bridges during mitosis (section 4.3.4). We also observed a striking increase in the time from NEBD until anaphase onset (by 3 fold; from 30min to 95min) (Figure 35B) when constructs of PICH were expressed that bind Plk1 (PICH-WT and PICH-WAB) compared to

those that do not bind Plk1 (PICH-TA and PICH-WAB-TA) (Figure 35A). In addition, only 58-60% of those cells exited mitosis, while the others remained arrested at prometaphase until the end of filming or died (Figure 35C). Interestingly, the fate of a single transfected cell correlated with the level of overexpressed protein, as analyzed by GFP signal intensity, during prometaphase. Strong expression of PICH-WT correlated with a mitotic arrest, whereas low expression correlated with mitotic exit (Figure 35D).

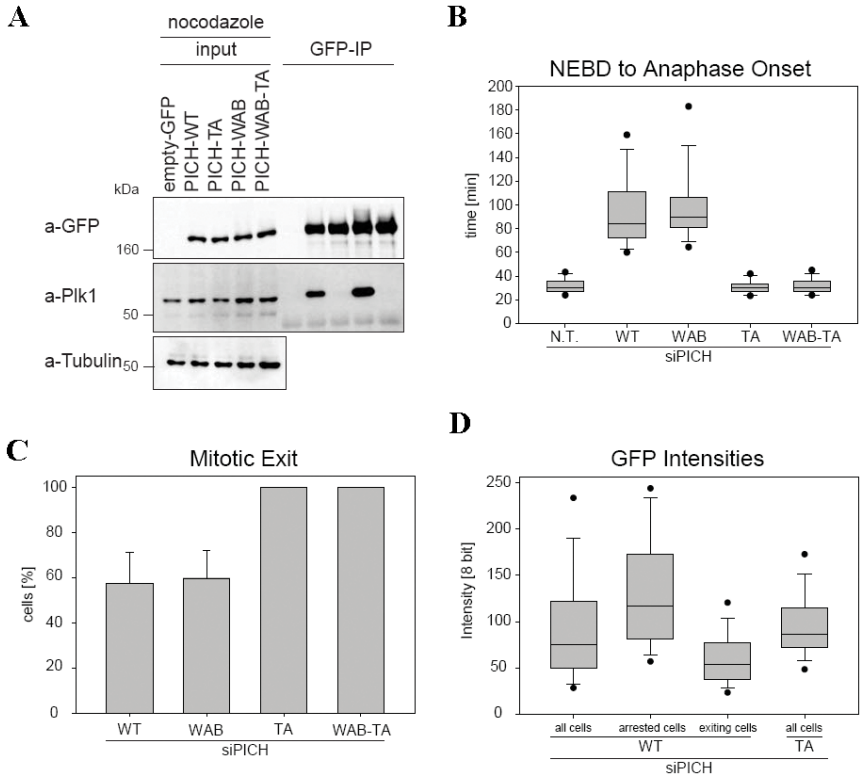

Figure 35: Expression level of PICH determines the fate of a mitotic cell. A) Western blot analysis of immunoprecipitated PICH species overexpressed in HEK293T cells. Mutation of threonine 1063 abolishes binding to Plk1. B) Box-and-whisker plot illustrating the time required from NEBD until anaphase onset for individual PICH species. PICH-WT and PICH-WAB prolong mitotic progression. C) Bar graph showing the percentage of cells that is able to exit from mitosis when different PICH species are expressed. Error bars represent standard error from three individual experiments. D) Box-and-whisker plot illustrating the GFP intensities of PICH-WT and PICH-TA expressing cells with respect to their fate in mitosis. The expression level of PICH determines the fate of a mitotic cell.

The delay in mitotic progression induced by PICH overexpression is very similar to the phenotype of Plk1 depletion or inhibition (Santamaria et al., 2007; Sumara et al., 2004). We thus hypothesize that PICH sequesters Plk1, thereby promoting the delay in mitotic progression. During early mitosis, PICH and Plk1 colocalize to the centromere/KT of condensed mitotic

chromosomes, making this stage unfeasible to analyze a potential sequestration of Plk1 by PICH. However, during anaphase, Plk1 localizes to the central spindle, whereas PICH localizes to the centromere/KT and UFBs. Therefore, we analyzed whether the transient overexpression of PICH-WT or PICH-TA affects the localization of Plk1 during anaphase. In contrast to PICH-TA, PICH-WT recruited Plk1 to the centromere/KT of separating chromatids during anaphase (Figure 36A, upper panel). However, during telophase, Plk1 localized exclusively to the midbody even in cells overexpressing PICH (Figure 36A, lower panel), arguing that the interaction of PICH and Plk1 was abolished at that stage. Immunoprecipitation of endogenous PICH revealed that the disassembly of PICH-Plk1 correlates with the degradation of cyclin B1 and interference with anaphase-onset (mg132 treatment) stabilizes this interaction (Figure 36B). Thus, these data demonstrate that the transient overexpression of PICH affects the localization of Plk1 during anaphase, implying a sequestration of Plk1 by PICH during mitosis.

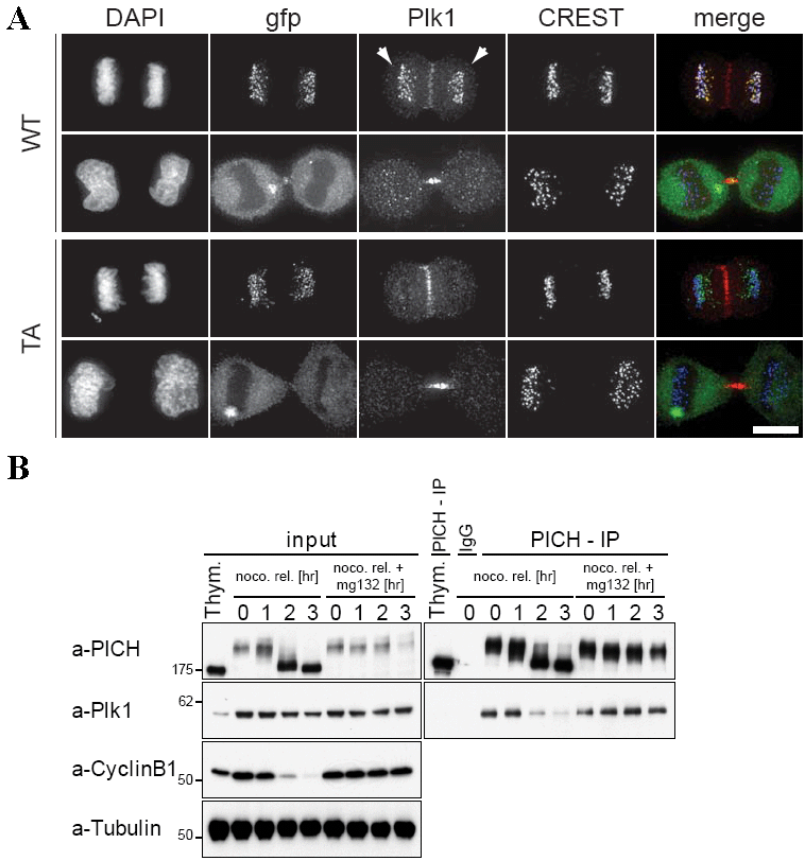

Figure 36: Overexpressed PICH sequesters Plk1. A) Immunofluorescence of HeLaS3 cells transiently transfected with PICH-WT and PICH-TA. PICH-WT recruits Plk1 to the centromere/KT of separating chromatids. DNA stained with DAPI, PICH (gfp) is shown in green, Plk1 in red and CREST in blue. Scale bar represents 10µm. B) Western blot of immunoprecipitated PICH after nocodazole release. PICH Plk1 disassembly correlates with cyclin B1 degradation and anaphase onset.

4.3.6 PICH-induced chromatin bridges arise at non-centromeric loci

During anaphase, PICH localizes to UFBs connecting the separating centromere/KTs of chromatids (Baumann et al., 2007). These PICH-positive UFBs have been shown to consist of centromeric DNA (Wang et al., 2008), therefore we will refer to them as centromeric UFBs. Interestingly, the resolution of centromeric UFBs during anaphase requires the activity of a type 2 topoisomerase (Baumann et al., 2007), arguing that centromeric UFBs most likely represent fully replicated but still catenated DNA strands (for review see Wang, 2002). Recently, PICH positive non-centromeric UFBs have been identified by colocalization of PICH with FA-family members (FANCD2 and FANCI) and the BTR complex (Chan et al., 2007; Chan et al., 2009a; Hutchins et al., 2010; Naim and Rosselli, 2009a). Both, FA-family members and the BTR complex have been shown to contribute to DNA repair and act most likely synergistically (Knipscheer et al., 2009; Meetei et al., 2003; Pichierri et al., 2004; Wu and Hickson, 2003). Therefore, we asked whether the chromatin bridges that we observed when PICH was depleted originate from centromeric or non-centromeric loci. We performed rescue experiments and analyzed the existence of centromeric UFBs in early and late anaphase cells by costaining the cells with CREST to visualize the centromere for immunofluorescence. In early anaphase, PICH-WT and PICH-WAB localized to centromeric UFBs that were flanked by CREST (Figure 37A). In late anaphase, however, these centromeric UFBs were absent in both PICH-WT and PICH-WAB-expressing cells (Figure 37, A and B). This suggests that centromeric UFBs are resolved independently of the PICH ATPase activity during anaphase.

In contrast to wild-type, PICH-WAB localized to non-centromeric UFBs, determined by the lack of CREST signal (Figure 37A). In line with this, late anaphase cells that expressed PICH-WAB developed chromatin bridges (Figure 37, A and C). Thus, non-centromeric loci are probably the source of the chromatin bridges in late anaphase. In an unperturbed anaphase, spindle forces pull the sister chromatids to the poles in a fashion that the centromere/KTs are separated in an aligned conformation. The PICH-WAB induced chromatin bridges strongly affected this aligned conformation, as the centromere/KTs were often detected within or at the ends of the chromatin bridges (Figure 37A), also implying that non-centromeric loci lead to chromatin bridges. Furthermore, the depletion of Sgo1 has been shown to induce premature sister chromatid separation and to increase the number of PICH-positive centromeric UFBs (Baumann et al., 2007; McGuinness et al., 2005). Interestingly, when Sgo1 is depleted, PICH-positive centromeric

UFBs can reach lengths of several µm without inducing chromatin bridges (Figure 37D). Together these data demonstrate that chromatin bridges induced by PICH depletion do not result from centromeric loci, but most likely result from non-centromeric loci.

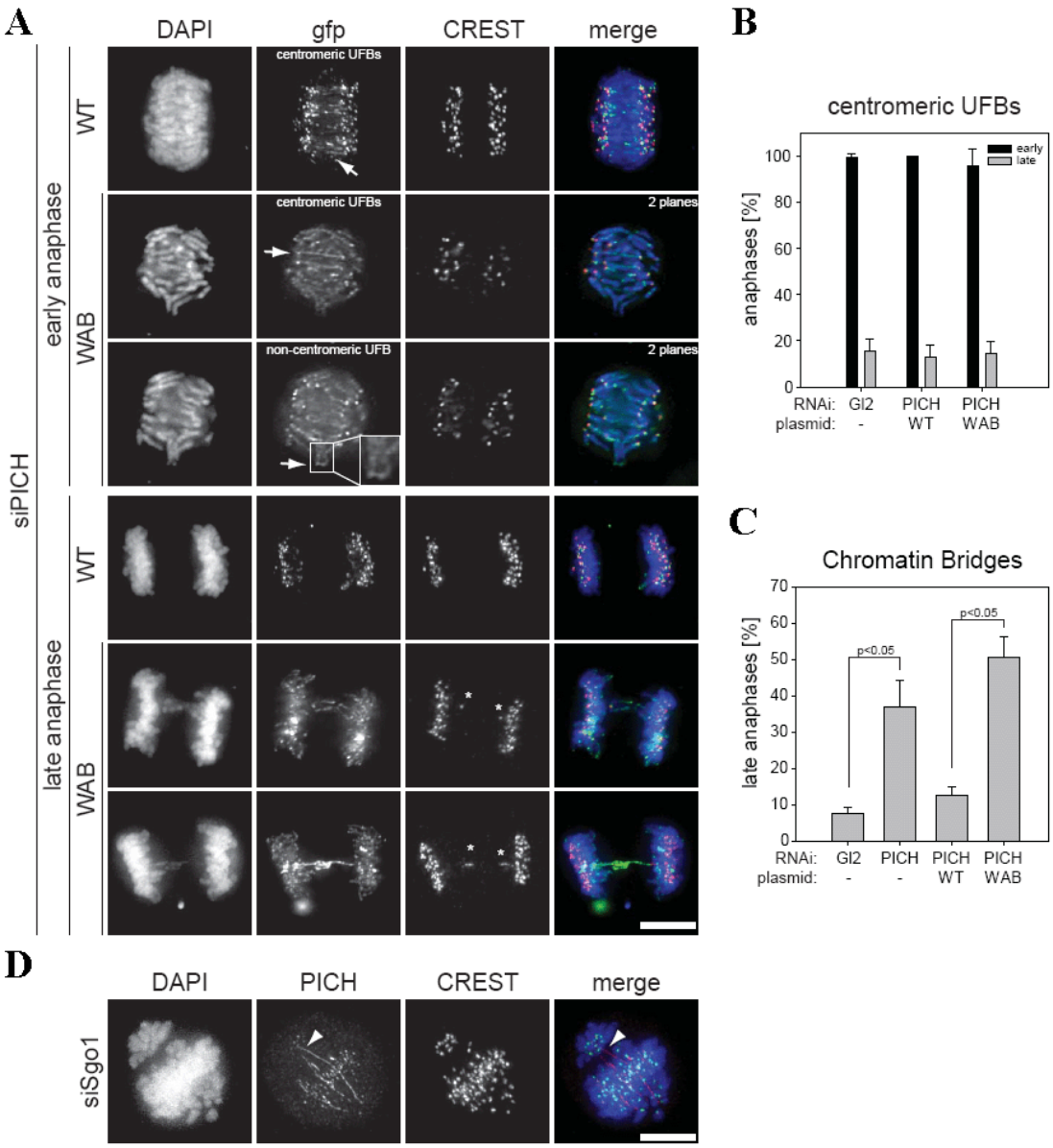

Figure 37: PICH deficiency-induced chromatin bridges arise from non-centromeric loci. A) Immunofluorescence of HeLaS3 cells transiently transfected with PICH siRNA and siRNA-refractory plasmids coding for PICH-WT and PICH-WAB. PICH-WT and PICH-WAB localize to centromeric UFBs in early but not late anaphase. PICH-WAB localizes to non-centromeric bridges connecting chromatids. Centromere/KTs are often detected within chromatin bridges (asterisks). DNA stained with DAPI (blue), PICH (gfp) is shown in green and CREST in red. Scale bar represents 10µm. B-C) Bar graphs illustrating the decrease in centromeric UFBs throughout anaphase and the induction of chromatin bridges by PICH-WAB in late anaphase cells. Error bars represent standard error from three individual experiments. D) Immunofluorescence of Sgo1 depleted HeLaS3 cells. PICH-positive centromeric UFBs can reach lengths of several µm without inducing chromatin bridging. DNA stained with DAPI (blue), PICH is shown in red and CREST in green. Scale bar represents 10µm.

4.3.7 PICH interacts with and regulates the localization of the BTR complex

In a systematic approach performed to identify protein complexes that form during mitosis, PICH was identified as a binding partner of the BTR complex (Hutchins et al., 2010). In that study, PICH, but not Plk1, was shown to interact with the BTR complex, suggesting that PICH interacts in a mutually exclusive manner with either Plk1 or the BTR complex. Furthermore, PICH was reported to colocalize with the BTR complex to non-centromeric UFBs that are flanked by the FA-family member FANCD2 (Chan et al., 2007; Chan et al., 2009a; Naim and Rosselli, 2009a). FANCD2 associates specifically with fragile site loci and presumably marks abnormally intertwined DNA structures induced by replication stress (Chan et al., 2009a; Naim and Rosselli, 2009a). Interestingly, the number of FANCD2-flanked PICH-BLM-positive UFBs is significantly increased, when cells are exposed to aphidicolin prior to mitosis (Chan et al., 2009a; Naim and Rosselli, 2009a), suggesting a common function for PICH and BLM after DNA damage. In addition, in an *in vitro* assay PICH is able move stalled replication folks (Dr. Lily Wang, personal communication), that form in the presence of aphidicolin.

To better understand the relationship between PICH and the BTR complex/FA family, we initially performed immunoprecipitation experiments, isolating overexpressed PICH-WT and PICH-WAB from nocodazole-arrested HEK293T cells. Surprisingly, only PICH-WAB was able to co-precipitate the BTR complex and the FA-family member FANCG (Table 4 and Figure 38). This suggests that the ATPase activity of PICH negatively regulates the association with the BTR complex. The BTR component BLM localizes to the cytoplasm during early mitosis and to a subset of UFBs upon anaphase onset. Because PICH-WAB interacts with the BTR complex prior to anaphase, we asked whether exogenous PICH-WAB would affect the sub-cellular localization of BLM during early mitosis. We transiently transfected HeLaS3 cells with PICH-WT or PICH-WAB and arrested the cells at prometaphase with nocodazole. In contrast to PICH-WT, PICH-WAB recruited endogenous BLM to distinct loci that did not colocalize with CREST (Figure 39, blow-ups), further demonstrating that the ATPase activity of PICH regulates the association with the BTR complex and that ATPase-inactive PICH is able to recruit BLM.

Figure 38: PICH interacts with the BTR complex; peptides identified by mass spectrometry. Protein sequence of the human BLM helicase. Yellow highlighted peptides were found by mass-spectrometry after immunoprecipitation of PICH-WAB. Depicted in green, cysteine residues modified with carbamidomethyl (due to sample preparation).

Table 4: ATPase-dead PICH interacts with the BTR complex. ATPase-dead PICH, but not ATPase-active PICH, interacts with the BTR complex and members of FA-family prior to anaphase. (n.d.: not determined)

IP of	Plk1	BTR complex			FA-member
		BLM	TOP3A	RMI1	
PICH-WT	+	n.d.	n.d.	n.d.	n.d.
PICH-WAB	+	+	+	n.d.	+

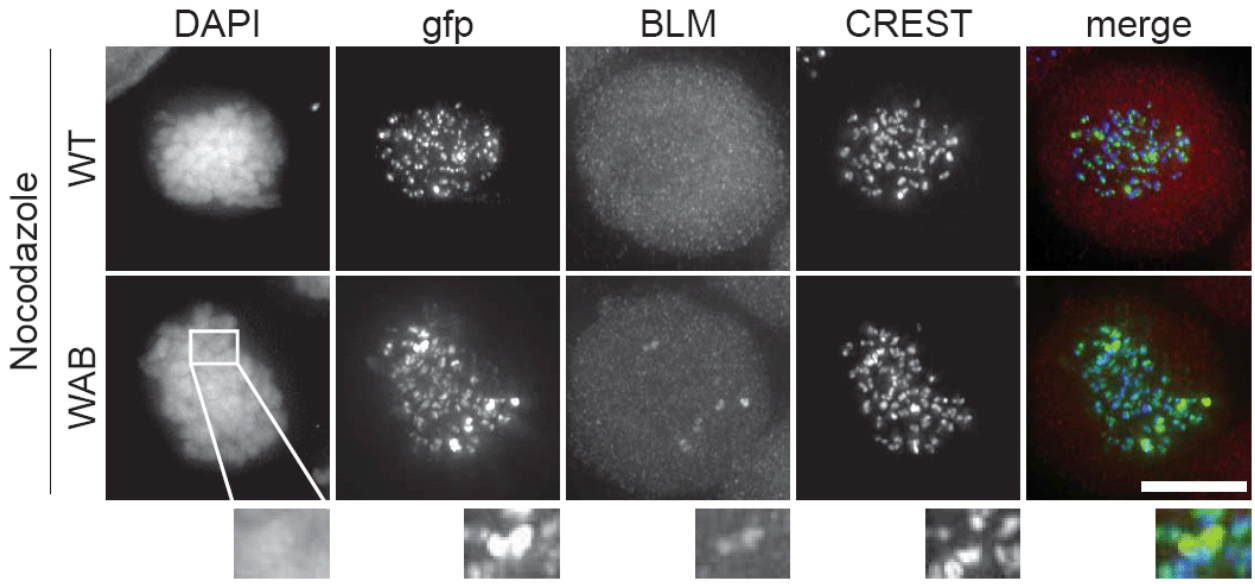

Figure 39: ATPase-dead PICH recruits BLM prior to anaphase. Immunofluorescence of HeLaS3 cells, transiently transfected with PICH-WT or PICH-WAB and arrested in prometaphase by nocodazole. ATPase-dead PICH recruits BLM to loci of high PICH localization during prometaphase. Blow-ups highlight the recruitment of BLM by PICH-WAB to sites distinct from CREST positive centromeres. DNA was stained with DAPI, PICH (gfp) is shown in green, BLM in red and CREST in blue. Scale bar represents 10µm.

Given that, ATPase-dead PICH is able to recruit BLM during prophase we asked whether BLM would colocalize to chromatin bridges that are induced by PICH-WAB during anaphase. Although BLM could not be detected on bridges themselves, it often localized to the ends of PICH positive chromatin bridges (Figure 40), suggesting a recruitment of BLM to the termini of PICH-WAB induced chromatin bridges.

Cells derived from Bloom-syndrome patients (BLM inactive) or depleted of endogenous BLM have been shown to develop chromatin bridges during anaphase (Chan et al., 2007), demonstrating that BLM is required for the faithful segregation of chromatids during mitosis. Thus, PICH and the BTR complex may act synergistically to prevent chromatin bridges during mitosis.

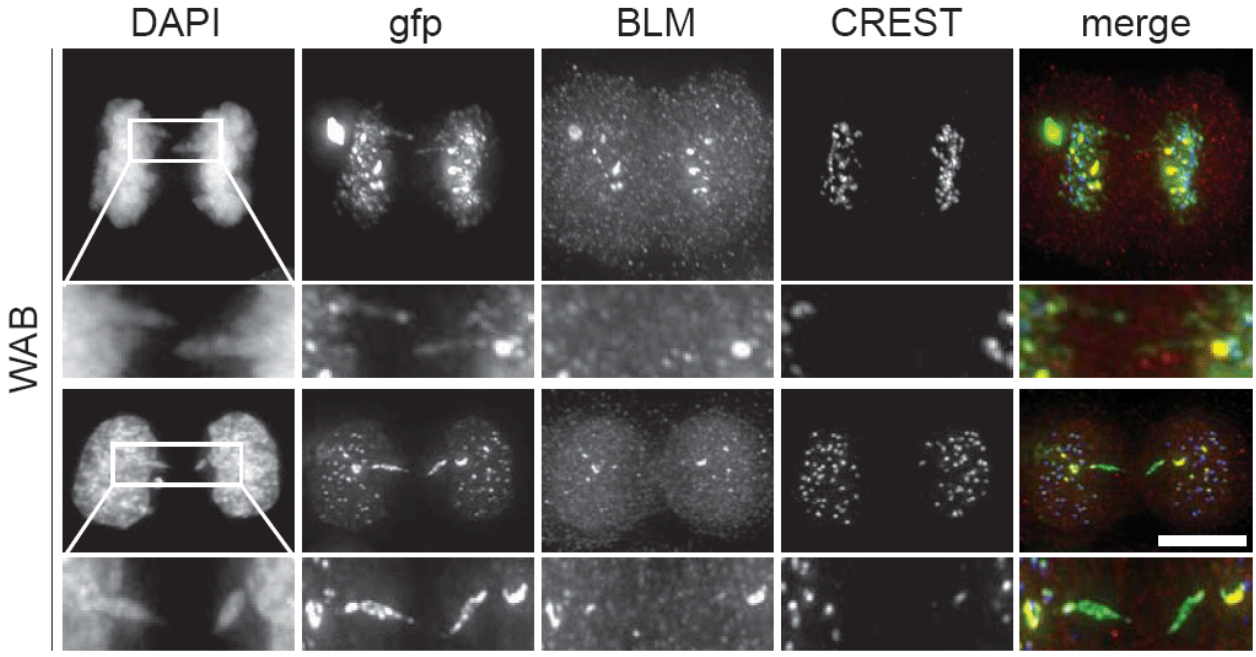

Figure 40: BLM localizes to chromatin bridges. Immunofluorescence of HeLaS3 cells transiently transfected with PICH-WAB. BLM colocalizes with PICH to chromatin bridges. Blow-ups highlight the colocalization of BLM to PICH-WAB induced chromatin bridges. DNA was stained with DAPI, PICH (gfp) is shown in green, BLM in red and CREST in blue. Scale bar represents 10µm. Asterisks point to a frequently observed PICH-gfp aggregate, to which BLM is recruited.

4.3.8 Rif1, a new binding partner of PICH

In addition to the BTR complex we found that both PICH-WT and PICH-WAB associated with Rif1 during mitosis. The RAP1-interacting factor, Rif1, was first identified in budding and

fission yeast for regulating the length of telomeres (Hardy et al., 1992). In contrast to the yeast ortholog, however, human Rif1 does not regulate the length of telomeres (Xu and Blackburn, 2004). Instead, human Rif1 was shown to function downstream of ATM and 53BP1 in the S-phase checkpoint after DNA-damage (Silverman et al., 2004), contributing to cell survival after replication stress and to homology-directed DNA-damage repair (Buonomo et al., 2009). Interestingly, immunofluorescence of human Rif1 revealed its localization along fiber-like structures during anaphase that diminish as anaphase progresses (Xu and Blackburn, 2004). Moreover, human Rif1 interacts with and provides a DNA-binding interface for the BTR complex to restart stalled replication forks to allow normal replication (Xu et al., 2010).

Considering that human Rif1 interacts with the BTR complex and localizes to structures reminiscent of PICH-positive UFBs during anaphase, it is intriguingly that we identified human Rif1 as a new interaction partner of PICH. Mass spectrometry in fact identified 13 unique peptides (7.1% sequence coverage) of Rif1 in PICH immunoprecipitates.

Next, we asked whether Rif1 colocalizes with PICH during the cell cycle. To this end, we performed immunofluorescence of HeLaS3 cells and stained for PICH and Rif1 (antibody kindly provided by Dr. Weidong Wang, (Xu et al., 2010)). Even though the localization of Rif1 during the cell cycle had been studied previously, a potential co-localization with PICH had never been analyzed (Silverman et al., 2004; Xu and Blackburn, 2004). During interphase, Rif1 localized to the nuclear envelope and the nucleoplasm (Figure 42). In early mitosis, Rif1 then localized weakly to the centromere/KT. From early anaphase on Rif1 was prominent at fiber-like structures that colocalized with PICH. This localization diminished during anaphase until Rif1 became reassociated with the nuclear envelope and the chromatin during late mitosis (Figure 42).

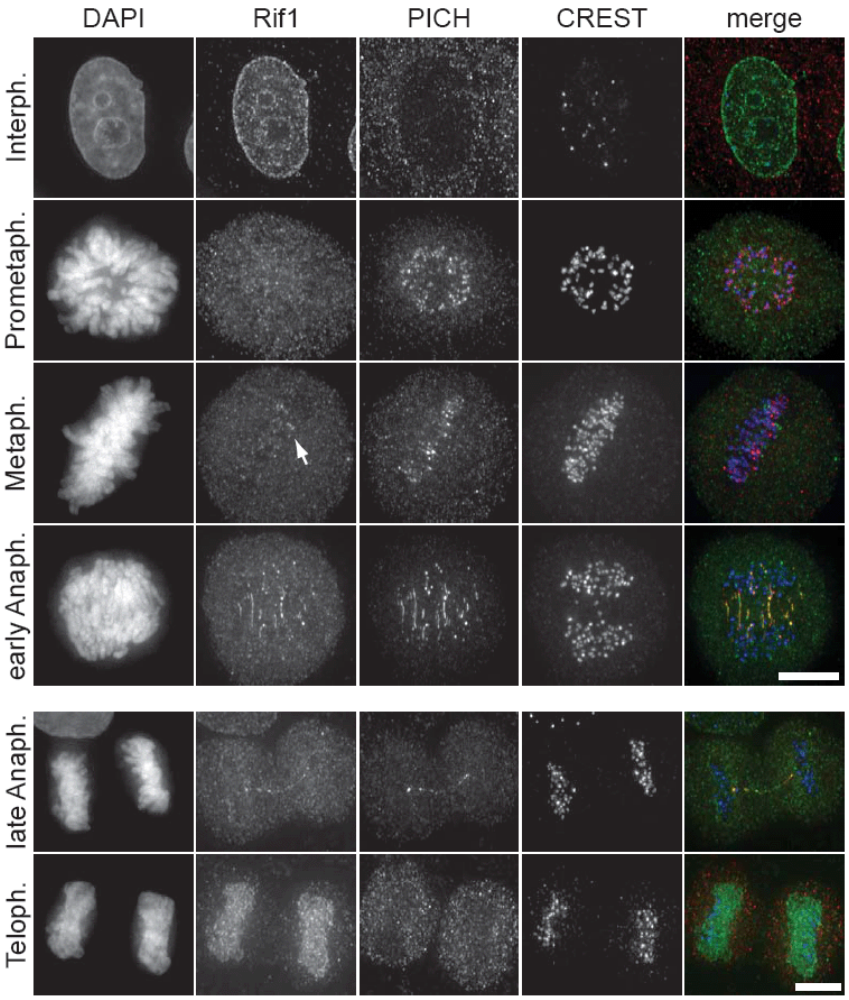

Figure 42: Mitotic localization of Rif1. Immunofluorescence of HeLaS3 cells. Rif1 localizes to the nuclear envelope during interphase. During early mitosis, Rif1 localizes weakly to the centromere/KT (arrow) until it localizes at fiber-like structures that colocalize with PICH during anaphase. In late mitosis, Rif1 localizes to the nuclear envelope and the chromatin. DNA stained with DAPI, Rif1 is shown in green, PICH in red and CREST in blue. Scale bars represent 10µm.

Furthermore, we depleted Sgo1 in HeLaS3 cells to increase the amount the centromeric UFBs and subsequently performed immunofluorescence for Rif1 and PICH. We observed that Rif1 completely colocalized with PICH to centromeric UFBs (Figure 43). These results demonstrate that the Rif1 fiber-like structures are not microtubule-associated structures, as had been hypothesized earlier (Xu and Blackburn, 2004), but are PICH-positive centromeric UFBs.

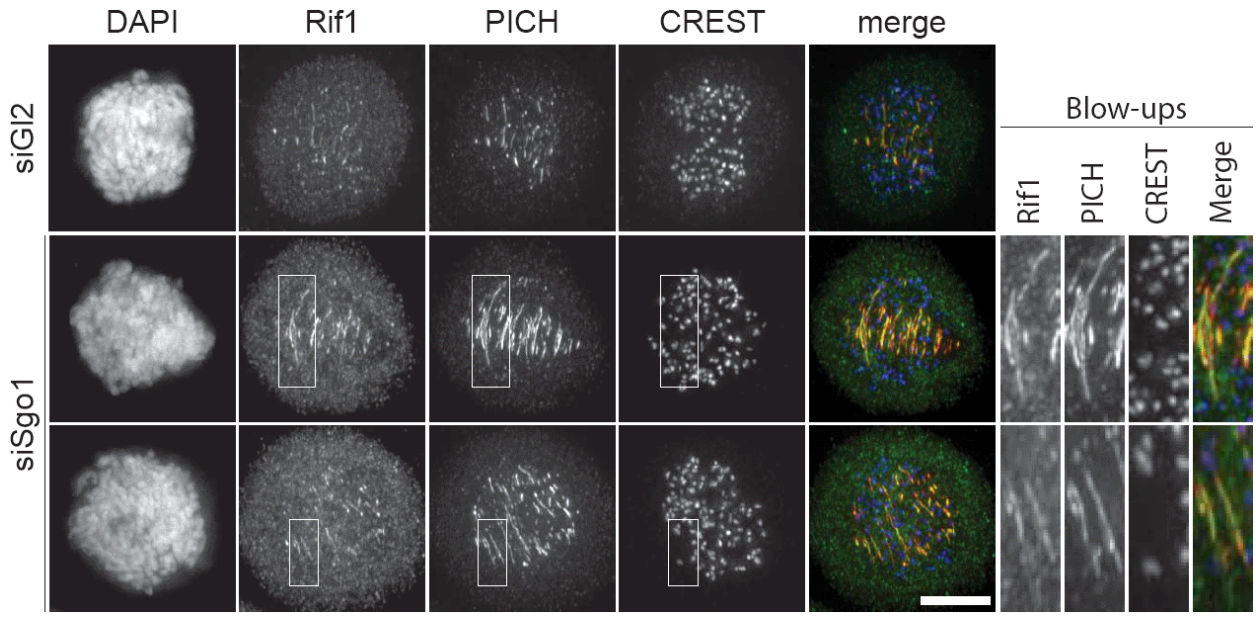

Figure 43: Rif1 localizes to PICH-positive centromeric UFBs. Immunofluorescence of HeLaS3 cells transfected with either Gl2 or Sgo1 siRNA duplexes. Rif1 colocalizes with PICH to centromeric UFBs during early anaphase. Blow-ups represent a 2.5 fold magnification of the white marked area. Note the exact colocalization of Rif1 with PICH. DNA stained with DAPI, Rif1 is shown in green, PICH in red and CREST in blue. Scale bar represents 10µm.

Recently, Rif1 has been shown to be a new component of the BTR complex whose function is required for faithful DNA replication (Xu et al., 2010). In particular, Rif1 provides a new DNA-binding interface for the BTR complex to promote the recovery of stalled replication forks (Xu et al., 2010). As PICH interacts with and regulates the localization of the BTR complex (see section 4.3.7 of this work and a previous study (Hutchins et al., 2010)), we hypothesize that PICH regulates the localization of the BTR complex via the interaction with Rif1. To address this, we depleted PICH from HeLaS3 cells and analyzed the localization of Rif1 in anaphase cells. In contrast to control-treated cells, Rif1 did not localize to UFBs in anaphase when PICH was depleted (Figure 44A), suggesting that PICH is essential for the anaphase UFB localization of Rif1. In addition, when PICH was depleted, Rif1 stayed associated with the centromere/KT during anaphase until it localizes to the nuclear envelope and the chromatin in late mitosis (Figure 44B). Thus, PICH regulates the localization of Rif1 to centromeric UFBs.

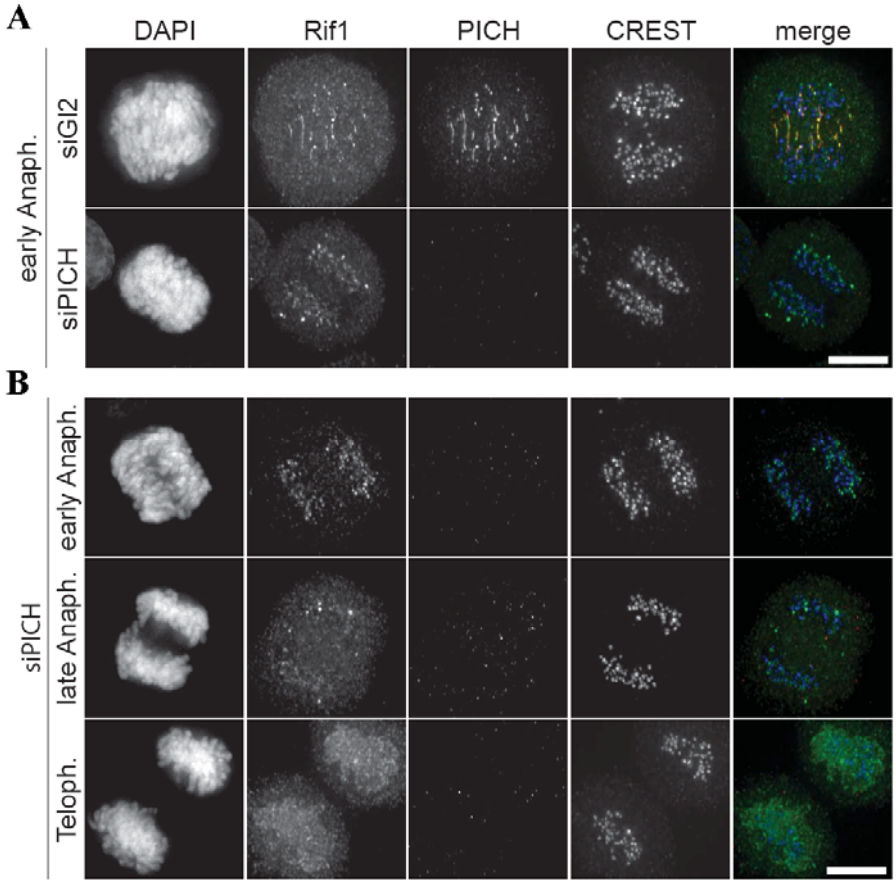

Figure 44: PICH regulates the centromeric UFB localization of Rif1. A) Immunofluorescence of HeLaS3 cells transfected with either Gl2 or PICH siRNA duplexes. Centromeric UFB localization of Rif1 is regulated by PICH. B) Immunofluorescence of HeLaS3 cells transfected with PICH siRNA duplexes. Rif1 stays associated with the centromere/KT during anaphase when PICH is depleted. A+B) DNA stained with DAPI, Rif1 is shown in green, PICH in red and CREST in blue. Scale bars represent 10µm.

During interphase Rif1 and the BTR complex are recruited to foci of DNA damage in an ATM kinase- and 53BP1-dependent manner (Silverman et al., 2004; Xu et al., 2010; Xu and Blackburn, 2004). As we have shown that PICH interacts with both Rif1 and the BTR complex during mitosis, we asked whether PICH is recruited to these interphase foci of DNA damage as well, even though normally PICH localizes to the cytoplasm in undamaged cells (Baumann et al., 2007). We induced DNA-damage by methyl-methan-sulfonate (MMS; induction of stalled replication forks) and mitomycin-c (MMC; induction of interstrand crosslinks) and analyzed the localization of PICH and Rif1 by immunofluorescence. Since in HeLaS3 cells p53 is inactivated (by the action of the HPV-encoded E6 oncoprotein) we analyzed the effect of MMS and MMC in both HeLaS3 and p53-positive U2OS cells. Both treatments induced a strong recruitment of Rif1

to DNA-damage foci in HeLaS3 as well as U2OS cells (Figure 45, A and B), confirming previous work (Xu and Blackburn, 2004). However, PICH was not recruited to these DNA-damage foci (Figure 45, A and B). Thus, PICH is not recruited to sites of stalled replication forks or interstrand crosslinks during interphase, suggesting that PICH does not to function in interphase DNA-damage repair.

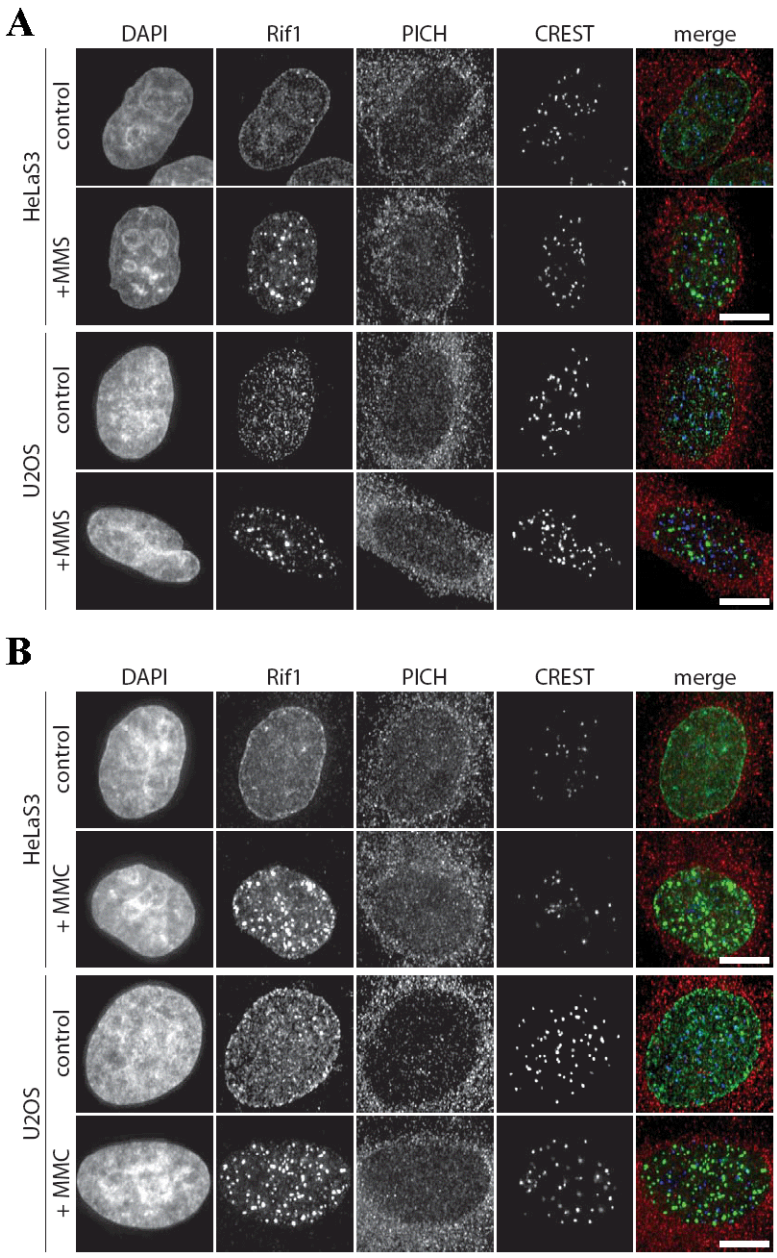

Figure 45: PICH does not localize to foci of DNA damage during interphase. A) Immunofluorescence of HeLaS3 and U2OS cells treated with 0.02% MMS for 1 hr. B) Immunofluorescence of HeLaS3 and U2OS cells treated with 120ng/µL MMC for 20hrs. A+B) PICH is not recruited to foci of DNA-damage. DNA stained with DAPI, Rif1 is shown in green, PICH in red and CREST in blue. Scale bars represent 10µm.

4.3.9 Summary

Both PICH and co-targeted Plk1 have been shown previously to function in prometaphase chromosome arm architecture and cohesion (Kurasawa and Yu-Lee, 2010; Leng et al., 2008). However, the siRNA duplexes used in both previous studies have recently been shown to also affect the SAC component Mad2, resulting in checkpoint failure (Hübner et al., 2009). In order to understand the mitotic function of PICH independently of off-target effects, we performed both antibody microinjection and siRNA transfections using siRNA duplexes that specifically target PICH, followed by time-lapse microscopy. We confirmed that PICH does not function in SAC signaling and showed instead that PICH deficiency results in the formation of chromatin bridges during anaphase. Additionally, we identified the ATPase activity of PICH as being essential to resolve chromatin bridges, which are likely to emerge from non-centromeric chromatin.

We have also shown that PICH interacts with and regulates the localization of the BTR complex, which has been shown to suppress chromosomal instability (Payne and Hickson, 2009). Furthermore, ATPase-inactive PICH recruits the BTR complex to chromatin bridges, suggesting a synergistic function at these structures. In addition, we identified the new PICH-binding protein Rif1, whose localization to centromeric UFBs depends on PICH. However, the function of PICH seems to be limited to mitosis, as PICH does not localize to sites of DNA damage during interphase that are positive for the BTR complex or Rif1. Thus, PICH, Rif1 and BLM may act in a complex to prevent chromatin bridge formation during mitosis, thereby suppressing chromosomal instability and maintain the integrity of the genome.

4.4 Tables, summarizing potential PICH binding partner and PICH phosphorylation sites

A summary of PICH-binding partners that have been identified by mass spectrometry in this study is listed below. In short, we identified members of the BTR complex, confirming independent results (Hutchins et al., 2010). In addition, we found several proteins know to function in DNA repair (e.g. KU70, KU86, RIF1 and CHK1) or DNA and RNA processing (e.g. RCC1, RCC2, FUBP2, DHX15, NONO). Interestingly, we also identified proteins with so far unknown functions (e.g. BEND3).

Table 5: Table, summarizing potential PICH binding partner found by mass spectrometry. Binding partners that have been known already are highlighted in bold letters. Binding partners of potential interest are highlighted in cursive letters. Members of the BTR complex and FA complex interact specifically with ATPase-dead PICH. Rif1 interacts with both PICH-WT and PICH-WAB.

No.	Name (Accession no.)	MW	(No. of unique peptides found)		
			PICH-WT	PICH-WAB	empty-myc
1	sp|Q2NKX8|ERC6L_HUMAN	141 kDa	186	403	
2	**sp|P53350|PLK1_HUMAN**	**68 kDa**	**40**	**51**	
3	*sp|Q5T5X7|BEND3_HUMAN*	*94 kDa*	*7*	*8*	0
4	*sp|Q5UIP0|RIF1_HUMAN*	*274 kDa*	*9*	*7*	*1*
5	sp|Q92945|FUBP2_HUMAN	73 kDa	4	5	1
6	sp|P26599|PTBP1_HUMAN	57 kDa	6	5	1
7	sp|P31689|DNJA1_HUMAN	45 kDa	3	5	1
8	sp|O14965|STK6_HUMAN	46 kDa	1	4	
9	sp|P14635|CCNB1_HUMAN	48 kDa		4	
10	sp|P26641|EF1G_HUMAN	50 kDa	3	4	2
11	sp|P23246|SFPQ_HUMAN	76 kDa	3	4	0
12	sp|P06493|CDC2_HUMAN	34 kDa		4	
13	**sp|P54132|BLM_HUMAN**	**159 kDa**		**4**	
14	sp|Q9Y230|RUVB2_HUMAN	51 kDa	1	3	
15	*sp|O14757|CHK1_HUMAN*	*54 kDa*		*3*	
16	*sp|Q9P258|RCC2_HUMAN*	*56 kDa*	*7*	*3*	*1*
17	sp|O43143|DHX15_HUMAN	91 kDa	6	3	
18	sp|Q9Y265|RUVB1_HUMAN	50 kDa	2	3	
19	sp|P63241|IF5A1_HUMAN	17 kDa	2	3	1
20	sp|P28482|MK01_HUMAN	41 kDa	1	3	
21	sp|P31040|DHSA_HUMAN	73 kDa	1	3	
22	sp|P06737|PYGL_HUMAN	97 kDa	3	3	1
23	sp|Q96QK1|VPS35_HUMAN	92 kDa	1	3	
24	sp|O75663|TIPRL_HUMAN	31 kDa	3	2	
25	*sp|P12956|KU70_HUMAN*	*70 kDa*	*3*	*2*	
26	*sp|P13010|KU86_HUMAN*	*83 kDa*	*5*	*1*	

27	sp|O43684|BUB3_HUMAN	37 kDa	4	2	
28	sp|Q15058|KIF14_HUMAN	186 kDa	1	2	
29	sp|Q15233|NONO_HUMAN	54 kDa	3	2	
30	sp|Q8WXX5|DNJC9_HUMAN	30 kDa	2	2	
31	sp|Q9HB71|CYBP_HUMAN	26 kDa	2	2	
32	sp|Q9BQG0|MBB1A_HUMAN	149 kDa	2	2	
33	sp|P55265|DSRAD_HUMAN	136 kDa	4	1	0
34	sp|P36873|PP1G_HUMAN	37 kDa	2	1	
35	sp|Q13148|TADBP_HUMAN	45 kDa	2	1	
36	sp|P63244|GBLP_HUMAN	35 kDa	4	1	
37	sp|P24534|EF1B_HUMAN	25 kDa	2	1	
38	*sp|P18754|RCC1_HUMAN*	*45 kDa*	*3*	*0*	
39	**sp|Q13472|TOP3A_HUMAN**	**112 kDa**		**1**	
40	*sp|O15287|FANCG_HUMAN*	*69 kDa*	*1*		

The next two tables summarize the phosphorylation sites of PICH that have been identified by mass spectrometry.

Table 6: Table, summarizing phosphorylation sites of PICH identified by mass spectrometry. The first section compares thymidine- (interphase) and nocodazole- (mitosis) arrested cells by SILAC. The second section compares PICH-WT to PICH-TA in nocodazole-arrested cells. The PICH-PBD is highlighted in red. Abbreviations: mouse (m), xenopus (x), C. elegans (c), drosophila (d) and zebrafish (z).

Site	Conservation	Found in		PICH-WT	PICH-TA
		Interphase	Mitosis		
T 763	m, x			1	
S 774	m, x		+	5	
S 790	m		+	1	1
T 797	m			1	1
T 798				1	
T 805			+	2	2
S 807				6	1
S 810			+	4	1
T 813				1	
S 820	m, x, c	+	+	4	5
S 829		+	+	1	
S 864	m, z			4	
S 946	c			1	
S 960	m, x, c			1	
S 968	m, c			1	1
S 969	m			2	
S 971	c, z			3	2
S 980	m, x, d			2	1
S 984				2	

S 995	m, c		+	1	
S 1000	m, x			1	
S 1028	m, x, c, z	+	+	5	7
S 1036	c			2	1
S 1042				1	
S 1062	m, c, z, d			1	
T 1063	m, x, c, z	+	+	6	
S 1069	x, c, d	+	+	6	3
S 1077	m, c		+	1	
S 1082	d			1	1
S 1098	m, x, c, d			1	
S 1118	m, x				1
Y 1126					1
S 1134				1	1
S 1135				1	1
S 1147	m, z			1	1
S 1152				1	
S 1188			+		
S 1242	m			+	

Table 7: Table, summarizing the phosphorylation sites of PICH identified by mass spectrometry. Phosphorylation sites found within PICH-WT and PICH-TA after arresting cells in mitosis (nocodazole). Abbreviations: mouse (m), xenopus (x), C. elegans (c), drosophila (d) and zebrafish (z).

Site	Conservation	(No. of unique peptides found; phos. / non-phos.)	
		PICH-WT	PICH-WAB
S 14	m	2/1	4/4
S 441		1/2	1/4
S 755	m, x, c	1/4	7/22
S 759			5/24
T 760	m, z, d		3/26
T 763	m, x	2/3	4/25
T 770	m, c, z		1/28
S 774	m, x	1/2	2/4
T 797	m	1/4	1/12
S 807		2/3	3/11
S 810			3/11
T 813	m		1/13
S 820	m, x, c	3/4	6/7
S 829		1/6	3/10
S 864	m, z	2/5	3/6
S 905			2/15
S 910	m, x	1/3	2/15
S 913	x, c, z	1/3	3/14

S 946	x, c	1/3	3/6
Y 949	m	-	1/8
S 971	c, z,	1/2	1/6
S 980	m, d	1/2	3/4
S 984			3/4
T 997			2/23
S 1000	m	4/7	5/20
S 1004	m, z, d	4/7	6/19
S 1028	m, x, c, z	3/3	9/10
S 1036	c		1/18
S 1042			1/17
S 1049	m, x, z		3/15
S 1069	x, c, d		1/3
S 1082	d		2/4
S 1092	m, x, c, z	1/4	2/6
S 1117	m, x, c, z	2/1	5/1
S 1118	m, x		1/5
S 1134		1/4	2/12
S 1135			1/13
S 1139	x, c, z		1/13
S 1147	m, z	1/3	1/11
T 1172	m, c		1/15
S 1173	m	2/6	3/13
S 1181	m, c, z		1/15
S 1188		3/5	8/8

5. DISCUSSION

The DNA-dependent ATPase PICH was identified as a protein that dynamically associates with different parts of the mitotic chromosomes during the course of mitosis (Baumann et al., 2007). Furthermore, it was originally described as the "tension-sensor" of the SAC (Baumann et al., 2007). However, this function of PICH as a component of the SAC has recently been attributed to an off-target effect of siRNA duplexes that do not only deplete PICH, but also Mad2 (Hübner et al., 2009). In the present study we have investigated the dynamic localization of PICH during the cell cycle in more detail. Furthermore, we have also re-examined the function of PICH and found it to be essential for the faithful resolution of chromatin bridges in late anaphase.

5.1 Regulation of the subcellular localization of PICH

In interphase PICH localizes to the cytoplasm and upon mitotic entry PICH gets relocalized to the centromere/KT region of chromosomes (Baumann et al., 2007). During anaphase it finally binds to ultra-fine DNA-bridges that connect separating sister chromatids and get resolved before mitotic exit. These striking changes in the subcellular localization of PICH are probably tightly regulated, but the underlying mechanisms have not previously been known.

First, we investigated which domains of PICH are essential for chromosomal localization. We found that a mutant of PICH (PICH-NC) that lacks both the N- and C-terminal TPR domains localizes to chromosome arms. TPR domains are known to mediate protein-protein interactions. The fact that only the deletion of both TPR domains impairs PICH localization implies that either of the TPR domains is sufficient on its own. Moreover, this result also raises the question of whether the TPR domains of PICH mediate the interaction to a regulator of the chromosome arm localization of PICH and, if so, what the identity of this regulator is.

Second, we tested the hypothesis that the ATPase activity of PICH might determine the localization of the protein. PICH has been predicted to be a DNA-dependent ATPase, which belongs to the family of SNF2/SWI helicases (Baumann et al., 2007). We initially proved this prediction by an *in vitro* ATPase assay. Indeed, we could demonstrate that PICH has ATPase activity *in vitro* that depends on the two classical ATPase-motifs Walker A and Walker B.

Interestingly, abolishing the ATPase activity of PICH *in vivo* recruits PICH all over the chromosome arms, arguing that the ATPase activity of PICH might be required for delocalizing PICH from the chromosome arms. Locking PICH in the chromosome arm-bound state by interference with its ATPase activity opens the question of whether PICH normally quickly turns over at chromosome arms in unperturbed cells and whether this turn-over has any functional significance. One could address the point whether turn-over occurs with photobleaching experiments. It is also possible that the inactivation of the ATPase activity might lock the protein in a functionally inactive state. The prolonged localization at chromosome arms could then simply be a result of the failure of PICH to fulfill its function at this location. Moreover, with regard to the role of the TPR domains of PICH in mediating chromosome arm localization, it would also be interesting to test whether the deletion of both TPR domains interferes with ATPase activity, and thereby leads to the localization of PICH to chromosome arms.

Previously, Plk1 has been shown to regulate the chromosome arm localization of PICH during mitosis, as the knockdown or chemical inhibition of Plk1 recruits PICH from the centromere/KT to the chromosome arms or keeps it at chromosome arms (Baumann et al., 2007; Santamaria et al., 2007). In line with this, we asked whether Plk1 regulates the ATPase activity of PICH *in vivo*. We performed rescue experiments and found that PICH-TA localizes only to the centromere/KT and not to the chromosome arms, as expected for a direct relationship between PICH and Plk1. However, upon inhibition of Plk1 PICH-TA was still recruited all over chromosome arms. This demonstrates that Plk1 does not need to bind to PICH in order to control its localization, implying that Plk1 kinase activity regulates the chromosome arm localization of PICH indirectly, presumably by phosphorylation of an as yet unknown substrate at chromosome arms.

It is known that during early mitosis, the kinase activity of Plk1 contributes to the removal of chromosome arm cohesin, an event which correlates with the delocalization of PICH (the prophase pathway) (Hauf et al., 2005; Sumara et al., 2002). But by rescue experiments we could rule out that the removal of chromosome arm cohesin by phosphorylation results in the delocalization of PICH from the arms. In line with this, also centromere/KT PICH is independent of centromere cohesin and cohesion, suggesting that the overall localization of PICH is independent of sister chromatid arm and centromere cohesin. However, the question to the substrate of Plk1 regulating PICH localization remains to be answered. As we have found that

the ATPase activity is required to remove PICH from chromosome arms, we further tested whether Plk1 regulates the ATPase activity of PICH *in vivo* and thereby influences the localization of PICH. However, the ATPase assays clearly show that PICH-TA is as active as wildtype PICH and the activity of wildtype PICH is unaffected even when Plk1 is chemically inhibited. Plk1, therefore, does not regulate the ATPase activity of PICH *in vivo*.

We further show that the ATPase activity of PICH is not regulated during the cell-cycle. Therefore, we hypothesize that the function of PICH is regulated by its cell-cycle stage dependent localization rather than by the modulation of its ATPase activity. This is also in agreement with the reported localization of PICH in interphase when it localizes to the cytoplasm (Baumann et al., 2007).

5.2 BEND3, a potential Plk1 substrate that regulates the localization of PICH and Plk1

In order to identify proteins that regulate the localization of PICH we performed immunoprecipitation experiments, followed by mass spectrometry. Among the proteins that were found to interact with PICH, we identified the so far uncharacterized protein BEND3 that belongs to the family of BEN domain containing proteins. BEN domains have been predicted to mediate protein-DNA and protein-protein interactions during chromatin organization and transcription (Abhiman et al., 2008). In addition, BEND3 has recently been identified as chromatin associated (Ohta et al., 2010) and, indeed, we could confirm that BEND3-myc localizes to mitotic chromatin. BEND3 depletion results in mitotic catastrophe, which suggested that BEND3 is required for cellular viability. If BEND3 was indeed a regulator of PICH localization, one could make two predictions for the effect of BEND3 depletion on PICH localization. First, if BEND3 was the Plk1 substrate that has to be phosphorylated in order to delocalize PICH from chromosome arms, then the depletion of BEND3 should mimic the depletion or chemical inhibition of Plk1 and should therefore result in the chromosome arm localization of PICH. Alternatively, if BEND3 was only initially required to localize PICH to chromosome arms, its depletion should result in a delocalization of PICH. Interestingly, we found PICH to be completely delocalized in cells depleted of BEND3, suggesting that BEND3

might be required for the initial localization of PICH at chromatin. In addition, we could show that Plk1 is delocalized as well when BEND3 is depleted, although the structure of the KT and the mitotic spindle is not affected. Interestingly, cells that are depleted for PICH are positive for Plk1 at the KT and vice versa (Santamaria et al., 2007), demonstrating the independency of PICH and Plk1 at the KT. Furthermore, BEND3 interacts with and is a potential substrate of Plk1 during mitosis, but this has to be tested further in the future.

5.3 Functional characterization of PICH

To circumvent the problem researchers faced in the past when depleting PICH by RNA interference we decided to use antibody microinjection to deplete PICH from living cells. To this end, we generated a monoclonal antibody against PICH. We show that neutralization of PICH does not affect SAC signaling, thereby confirming previous work which questioned the role of PICH in the SAC (Hübner et al., 2009). Surprisingly, we observed the occurrence of chromatin bridges and the formation of micronuclei as consequence of PICH depletion. Moreover, rescue experiments revealed that the ATPase activity of PICH is essential to prevent the formation of chromatin bridges.

We have also explored the mechanisms by which PICH prevents the formation of chromatin bridges and micronuclei. PICH is predicted to be a helicase of the SNF2/SWI family that interacts with components of the BTR complex (Baumann et al., 2007; Hutchins et al., 2010). In line with this, the RecQ helicase BLM (that is mutated in Bloom syndrome) has been shown to be required for the faithful segregation of chromosomes and its localization during mitosis has been linked to unreplicated fragile site loci (Chan et al., 2007; Chan et al., 2009a; German, 1993; Naim and Rosselli, 2009a).

Interestingly, we identified the protein Rif1 as a novel interaction partner of PICH. We also found that PICH regulates the localization of Rif1 to UFBs during mitosis. Rif1, initially characterized in humans to function downstream of ATM and 53BP1 in the S-phase checkpoint after DNA-damage (Silverman et al., 2004), has more recently been shown to contribute to cell survival after replication stress and to homology-directed DNA damage repair (Buonomo et al., 2009). In addition, Rif1 interacts with and provides a DNA-binding interface for the BTR

complex to restart stalled replication forks and maintain normal replication (Xu et al., 2010). Unfortunately, to date it is unclear what the mitotic phenotype of Rif1 depletion is. Due to its connection to PICH it is possible that it is required for PICH localization or that its depletion could induce chromatin bridges. Therefore, it will be of great interest to analyze the link between PICH, Rif1 and BTR complex during mitotic progression.

During interphase, both Rif1 and the BTR complex are recruited to sites of DNA damage (Silverman et al., 2004; Xu et al., 2010; Xu and Blackburn, 2004). However, PICH is not recruited to typical interphase DNA damage foci. Therefore, we speculate that PICH does not function in interphase, but plays a role in sister chromatid segregation during mitosis together with Rif1 and the BTR complex.

We have shown that PICH-deficiency induced chromatin bridges arise from non-centromeric chromatin. This raises the intriguingly question why non-centromeric but not centromeric chromatin led to chromatin bridges in PICH depleted cells? One possible explanation could be that PICH is simply not required for the resolution of centromeric chromatin. However, a perhaps more likely explanation is that centromeric chromatin comprises a distinct structure of DNA that is different from non-centromeric chromatin. Centromeric UFBs have previously been shown to be very prominent in dividing cells and can furthermore be induced by the inhibition of a type 2 topoisomerase, which suggests that they are likely to represent fully replicated but still catenated DNA strands (Baumann et al., 2007; Chan et al., 2007). Therefore, when the SAC is satisfied and centromeric cohesion is released by the action of separase, a type 2 topoisomerase can gain access to the two entangled centromeric DNA strands and resolve them independently of PICH (Hauf et al., 2001; Wang et al., 2008). This potential mechanism is in striking contrast to the resolution of non-centromeric chromatin. In prometa- and metaphase, when chromosome arm cohesion is already released, non-centromeric UFBs are flanked by the Fanconi anemia proteins FANCD2 and FANCI (Chan et al., 2009a). Non-centromeric UFBs are likely, therefore, to represent loci of Holliday junctions (HJ) at stalled replication forks that need further resolution before the initiation of anaphase (Figure 46) (Chan et al., 2009a; Naim and Rosselli, 2009a). Thus, we would like to emphasize that non-centromeric UFBs are probably no conventional substrate for type 2 topoisomerases and that their resolution most likely requires a type 1 topoisomerases (Figure 47), like TOP3A (for review see Wang, 2002). In line with this view, the

activity of type 1 topoisomerases has been implicated in the resolution of recombination intermediates before chromosome segregation and, more importantly, in a mechanistic way concluded to correlate with the degree of DNA negative supercoiling (Kirkegaard and Wang, 1985; Wang, 2002; Zhu et al., 2001). Therefore, a helicase that pulls the branches of the replication fork is ultimately required to maintain the negative supercoiling and thereby keeping the type 1 topoisomerase active. In support of this notion, PICH associates with TOP3A and was shown to colocalize with members of the BTR complex to UFBs, as they emerged at fragile site loci (Chan et al., 2007; Chan et al., 2009a; Hutchins et al., 2010; Naim and Rosselli, 2009a). Thus, it is tempting to speculate that PICH functions in branch migration of stalled replication folks to constantly maintain the negative supercoiling for their resolution before the onset of anaphase.

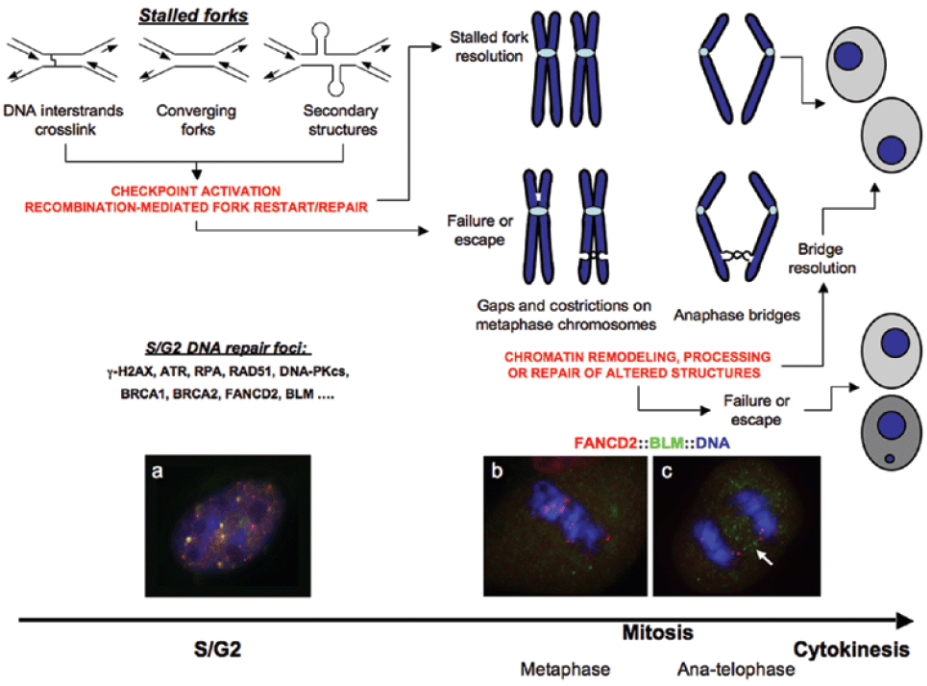

Figure 46: Proposed model for stalled replication fork recovery. When rescue mechanisms fail, daughter cells accumulate genomic anomalies like chromosome breakage or loss, represented by the appearance of micronuclei after cytokinesis. (a) An S/G2 nucleus stained by anti-FANCD2 (red) and anti-BLM (green) antibodies, showing partial colocalization of the foci formed by the two proteins (yellow dots). DNA (blue) was counterstained with DAPI. (b) A representative metaphase showing FANCD2 spots (red) on condensed chromosomes (blue). (c) A representative anaphase showing segregation of FANCD2 spots (red) and an ultrafine DNA bridge (white arrow) stained by BLM (green). Adapted from (Naim and Rosselli, 2009b).

A

Subfamily	Representative members
IA	Bacterial DNA topoisomerases I and III Yeast DNA topoisomerase III *Drosophila melanogaster* DNA topoisomerases IIIα and IIIβ Mammalian DNA topoisomerases IIIα and IIIβ
IB	Eukaryotic DNA topoisomerase I Mammalian mitochondrial DNA topoisomerase I Pox virus topoisomerase
IIA	Bacterial gyrase, DNA topoisomerase IV Phage T4 DNA topoisomerase Yeast DNA topoisomerase II *Drosophila* DNA topoisomerase II Mammalian DNA topoisomerases IIα and IIβ
IIB	*Sulfolobus shibatae* DNA topoisomerase VI (subunit A homologous to yeast Spo11)

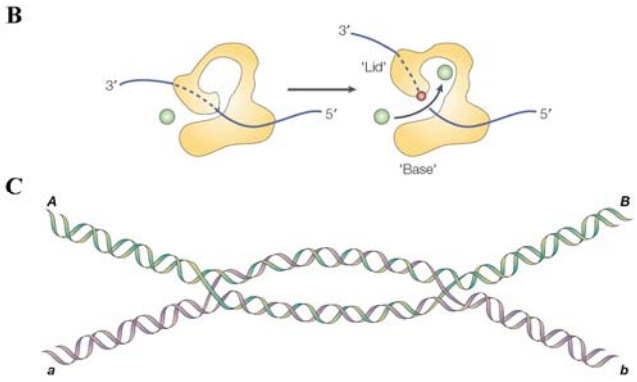

Figure 47: Topoisomerases and HJ resolution. A) Subfamilies of DNA topoisomerases. B) Mode of action of a type IA topoisomerase. On transient breakage of a DNA strand (blue line), the 5′ end of the broken DNA strand is covalently attached to the active-site tyrosyl group (red circle) in the 'lid' of the enzyme, and the 3′ end is noncovalently bound to the 'base' of the enzyme. Lifting the lid away from the base opens a gate in the DNA for the passage of another strand (green circle). Once the second strand has entered the central cavity of the enzyme, it must exit the cavity, after the rejoining of the broken strand, without passing through the rejoined DNA strand. C) By successive passage of an AB strand through an ab strand, or vice versa, these intermolecular intertwines can be completely resolved by a type IA enzyme, but not by either a type IB or a type II enzyme. A-C) Adapted from (Wang, 2002).

Although the different stages of mitosis have been intensively studied, DNA that connects the centromere/KTs of separating sister chromatids was only discovered through the localization of PICH, perhaps reflecting their inability to become visualized by conventional DNA dyes or fluorescently-tagged histones (Baumann et al., 2007). While PICH has become a robust marker for the detection of anaphase UFBs (Baumann et al., 2007; Chan et al., 2007; Chan et al., 2009a; Naim and Rosselli, 2009a), the question has remained of why anaphase UFBs have previously escaped detection. We tentatively provide two explanations, which are not mutually exclusive. The first and possibly the simplest explanation is that anaphase UFBs contain so little DNA that they simply cannot be visualized by conventional DNA dyes or fluorescently-tagged histones (Wang et al., 2008). Second, and more interesting from a mechanistic perspective, it has been shown *in vitro* that negative superhelical tension is released when DNA is wrapped around histones (Nakagawa et al., 2001; Pfaffle and Jackson, 1990). Assuming that PICH, together with a type 1 topoisomerase (Hutchins et al., 2010), removes negative superhelical tension, it would then be experimentally challenging to visualize anaphase UFBs with fluorescently-tagged histones when histone displacement correlates with the relaxation of negative superhelical tension.

5.4 Conclusions and Perspective

The DNA-dependent ATPase PICH localizes to the centromere/KT region of prometa- and metaphase chromosomes (Baumann et al., 2007). Upon the onset of anaphase, PICH localizes to centromeric UFBs that increase in length before they diminish (Baumann et al., 2007; Wang et al., 2008). In the first part of this thesis, we have identified the TPR-domains and the ATPase activity of PICH as two key parameters regulating the correct localization of PICH. In addition, we have explored why depletion or chemical inhibition of Plk1 results in the relocalization of PICH to the chromosome arms during prometaphase (Baumann et al., 2007; Santamaria et al., 2007), and asked through what mechanism Plk1 regulates the chromosome arm localization of PICH. Interestingly, the PICH-TA mutant (no Plk1 binding and thus no PICH phosphorylation on Plk1 sites) still localizes to chromosome arms when Plk1 is inhibited, revealing that Plk1 must regulate PICH localization through phosphorylation of another, as yet unidentified substrate. In line with this conclusion, we have identified the previously uncharacterized protein BEND3 as a binding partner of PICH. BEND3 has two potential bindings sites for the Plk1-PBD that could in principle mediate binding to and phosphorylation by Plk1. Depletion of BEND3 results in a misalignment of chromosomes at the metaphase plate and leads to the selective loss of PICH and Plk1 from the centromere/KT, although the spindle apparatus and KTs are unaffected.

Although we have identified mechanisms that regulate the dynamic localization of PICH, several questions remain unanswered.

1. How do the TPR-domains of PICH influence its chromosome arm localization?
2. Does PICH turn over at mitotic chromosomes? If so, is the ATPase activity of PICH required?
3. Is BEND3 the key Plk1 substrate that regulates the chromatin association of PICH?
4. What is the mechanism that underlies the severe phenotype of BEND3 depletion?

In the second part of this thesis, we have shown that PICH is important to prevent the formation of chromatin bridges during mitosis. Furthermore, we identified the new PICH-binding partner Rif1. Both PICH and Rif1 colocalize at centromeric UFBs and Rif1 has recently been shown to

provide a DNA-binding interface for the BTR complex (Xu et al., 2010). Interestingly, this complex is known to be required for the faithful segregation of chromosomes during mitosis (Chan et al., 2007). We could show that PICH mediates the localization of Rif1 to centromeric UFBs. Therefore, the delocalization of Rif1 could provide a plausible mechanism for how chromatin bridges arise in response to PICH depletion. Prompted by these findings, several interesting questions arise:

1. Do the chromatin bridges that are induced by PICH depletion arise at specific loci of DNA, e.g. at fragile site loci?

2. How does PICH mediate the localization of Rif1 to centromeric UFBs?

3. What is the mitotic phenotype of Rif1 depletion?

4. Does PICH influence the holiday junction (HR)-resolving activity of the BTR complex?

5. How do PICH, Rif1 and the BTR complex act together to prevent the formation of chromatin bridges during mitosis?

Hence, although PICH does not function as a central component of the spindle assembly checkpoint, this DNA-dependent ATPase clearly plays an important role in cell cycle progression. While the present study substantially advances our understanding of PICH, it is clear that a full understanding of the function and regulation of this intriguing protein will require further study.

6. MATERIALS AND METHODS

6.1 Antibody generation and antibodies used in this study

The PICH monoclonal antibody (clone no.: 124-26-3, IgG1) was generated against a truncated version (aa79-aa752) of the human (NCBI Reference Sequence: NP_060139.2) recombinant His-PICH protein expressed in *E. coli*. All mAbs were purified using HiTrap Protein G HP columns (GE Healthcare).

The following antibodies were used in this study: mouse PICH mAB (Injection - 1mg/ml, IF - 1mg/ml, WB - tissue culture supernatant in 1/10), rabbit PICH (Injection - 1mg/ml (Baumann et al., 2007)), mouse Mad2 mAB (Injection - 1mg/ml (Chan et al., 2009b)), mouse Myc mAB (Injection - 1mg/ml (Chan et al., 2009b)), mouse alpha-Tubulin (WB - 1/5000 (Sigma-Aldrich)), mouse Plk1 mAB (IF - 1mg/ml, WB - tissue culture supernatant in 1/10 (Hanisch et al., 2006)), human Crest autoimmune serum (IF - 1/2000 (Immunovision)), mouse GFP mAB (WB - tissue culture supernatant in 1/10), mouse CyclinB1 (WB - 1/1000 (Millipore)), rabbit IgG's (Abcam, ab37415-5), mouse Lamin A+B2 mAB (IF - tissue culture supernatant in 1/10). For immunofluorescence analysis, primary antibodies were detected using Cy2-, Cy3-, or Cy5-conjugated donkey anti–mouse, anti–rabbit, or anti–human IgGs (1/1000 (Dianova)). Secondary antibody used for western blot analysis was: goat anti-mouse (1/1000) obtained from Bio-Rad.

6.2 Antibody microinjection

Antibody microinjection was performed using the FemtoJet system equipped with Femtotips II purchased from Eppendorf (Hamburg, Germany) connected to an Axiovert S100 microscope from Zeiss (Jena, Germany). Antibody concentration was set to 1mg/ml in PBS including 1.66mg/ml TexasRed dextran (Invitrogen). Positive injection was achieved with injection times varying between 0.2 – 0.4sec, capillary pressure of 30 – 40hPa and injection pressure between 15-20hPa. Prior to the injection cells were seeded either on 35mm µ-Dishes with grid from Ibidi (Martinsried, Germany) for live-cell imaging or on coverslips for PTEMF fixation for indirect immunofluorescence.

6.3 Cloning procedures

For cloning of His-hPICH (aa79-aa752) a previously published plasmid coding for human PICH was used (Baumann et al., 2007) together with DNA oligonucleotides 5'-ACAGATGTGTGCAACTCTGGCTTG-3' and 5'-AGGCTGAGGCTGTGGTTTATTCAA-3' for in-frame cloning into a pET-28a(+) vector (Novagen). PICH-WT and PICH-TA (T1063 mutated to alanine) tagged N-terminally to GFP were previously published (Baumann et al., 2007). To generate PICH-WAB (mutated at K128 to alanine and E229 to glutamine) and PICH-WAB-TA a mixture of DNA oligonucleotides was used: K128A: 5'-GATGATATGGGATTAGGGGCGACTGTTCAAATCATTGCT-3', E229Q: 5'-TATGTCATCCTCGATCAAGCACATAAAATAAAA-3', T1063A: 5'-CAATTTGATGCTTCAGCTCCCAAAAATGACATC-3' using the QuickChange Site-Directed Mutagenesis kit (Stratagene). To generate plasmids refractory to PICH siRNA duplexes a series of seven silent point mutations were introduced using the DNA oigonucleotide 5'-GTTTTTCTGCTTACCACTCAGGTGGGAGGAGTGGGATTGACATTAACTGCAGCA-3' and it corresponding antisense. Underlined letters correspond to point mutations made.

6.4 Cell culture and synchronization

HeLa, U2OS, 293T and HeLa cells stably expressing H2B-GFP or H2B-mCherry were grown under standard conditions in DMEM (Invitrogen) supplemented with 10% FBS and penicillin and streptomycin (100 U/ml and 100 mg/ml, respectively) and cultured at 37°C, in a 5% CO2 atmosphere. Cell cycle synchronizations were performed by a single thymidine (2 mM) block 10-12 hrs post-transfection with siRNA duplexes. Nocodazole (100ng/ml), monastrol (150µM), puromycin (0.5µg/ml), and thymidine (2mM) were obtained from Sigma-Aldrich. MG132 (10µM) was obtained from EMD.

6.5 Cell extracts, immunoprecipitation and western blot analysis

Preparation of lysates and Western blotting analysis were performed as described previously (Sillje et al., 2006) using Tris lysis buffer (50mM Tris-HCl pH 7.5, 150mM NaCl, 1% IGEPAL CA-630) containing 20mM NaF, 20mM beta-glycerophosphate, 0.3mM Na-Vanadate, 20µg/ml

RNase A, 20µg/ml DNase supplemented fresh with 1mM Pefabloc SC (Roth) and 1/100 Phosphatase inhibitor cocktail 1+2 (Sigma-Aldrich). Immunoprecipitation against endogenouse PICH or overexpressed PICH was carried out using 0.5µg of corresponding antibody in addition to 20µL Affi-Prep protein A agarose beads (Bio-Rad) for 2 hours at 4°C followed by extensive washing with lysis buffer and PBS, supplemented to western blot analysis. Proteins were resolved by SDS-PAGE and transferred to Nitrocellulose or PVDF membranes (Millipore) and these were probed with primary antibodies overnight at 4°C. Membranes were washed with 0.5% Tween/PBS before incubation with secondary antibodies. Antibodies used are listed in the Appendix.

6.6 Enzyme-coupled ATPase assay

To analyze the ATPase activity of PICH a reaction-solution was prepared as follows: 25mM TEA pH 7.5, 13mM Mg-Acetate, 1.8mM DTT, 5mM ATP, 100µg/ml BSA, 3mM phosphoenolpyruvate, 20U/ml Pyruvate kinase, 20U/ml Lactic dehydrogenase purchased from Sigma-Aldrich. To measure the decrease of OD 340nm, following the conversion of NADH to NAD^+, the starting OD at 340nm of 2.5 - 3.0 was set by addition of NADH (20mg/ml) using a Ultrospec 3100 pro (GE Healthcare) in a total reaction volume of 125µl. Individual treated PICH was added as immunoprecipitate, linked to protein A agarose (Bio-Rad), and analyzed at OD 340nm in measurements at every 5 min in a total reaction time of 1 hour. To obtain optimal results, the reaction volume was mixed gently by pipetting up and down every 5 minutes. Graphical and statistical analysis was performed using SigmaPlot 11 (Systat Software Inc.).

6.7 Flow cytometry

Indicated cell lines were treated as mentioned, harvested by trypsinization and washed twice with 10mL PBS. Cells were fixed by addition of -20°C 70% ethanol in cold PBS and stored at 4°C. 1 hour prior to flow cytometry analysis cells were washed twice with ice-cold PBS and supplemented with 10 times the volume of the cell pellet of PBS plus 20mg/ml RNAse and 1/200 propidium iodide (1mg/ml, purchased from Sigma-Aldrich).

6.8 Immunofluorescence microscopy

Cells were grown on coverslips, fixed with PTEMF (immunostaining for kinetochore associated proteins) for 10 min at room temperature (Stucke et al., 2002) or -20°C methanol (immunostaining for phosphor-specific antibodies) for 10 min at -20°C, and incubated for 20 min at room temperature in 3% BSA/PBS. Antibody incubations were carried out for 1 h at room temperature, followed by three washes in 0.5% TritonX-100/PBS. DNA was stained with 1 µg/ml 4,6-diamidino-2-phenylindole (DAPI). Primary antibodies for immunostaining are listed in the Appendix. Primary antibodies were detected by Cy3-conjugated donkey antibodies (Dianova) and Alexa Fluor 647-conjugated goat antibodies (Invitrogen). Coverslips were mounted in phenylenediamine in 90% glycerol (v/v). Images were acquired using a DeltaVision Olympus IX71 microscope equipped with a 60x/1.42 oil objective. Collection and processing of acquired images was carried out using Softworx (Applied Precision, LLC). Samples were examined with optical sections acquired 0.4 µm apart in the z-axis, deconvolved for each focal plane and projected into a single plane image using the Softworx software (Applied Precision, LLC). Images were processed in Adobe Photoshop CS3 and figures were assembled using Adobe Illustrator CS4 (Adobe Systems).

6.9 Transient plasmid and siRNA transfection

Plasmid transfection was performed using TransIT-LT1 reagent (Mirus Bio Corporation) according to the manufacturer's instructions. siRNA duplexes were transfected using Oligofectamine (Invitrogen) as described previously (Elbashir et al., 2001). All used siRNA duplex sequences can be found in the Appendix. All plasmid and siRNA transfections were performed for 48hrs to 72hrs with cells synchronized for the last 24hrs in the presence of 2mM thymidine.

6.10 Time-laps microscopy

HeLaS3 cells stably expressing histone 2B-GFP (Sillje et al., 2006) or histone 2B-mCherry (Steigemann et al., 2009) were seeded in eight-well chambers from Ibidi (Martinsried, Germany), treated as indicated and imaged using a Nikon ECLIPSE Ti microscope equipped with a

CoolLED pE-1 excitation system and a 20x/0.75 air Plan Apo objective (Nikon). Images were acquired at multiple positions every 3 minutes. For antibody injection, GFP fluorescence and DIC images were acquired at each time point with 20msec and 2msec exposure times, respectively. TexasRed fluorescence was imaged every 5 time points with a 40msec exposure. For gene knockdown and rescue experiments, histone 2B-mCherry fluorescence was acquired at every time point with a 20msec exposure time. DIC images were collected as described above. To collect and process data MetaMorph 7.7 software (MDS Analytical Technologies) in combination with SigmaPlot 11 (Systat Software Inc.) was used.

7. APPENDIX

7.1 List of generated plasmids

name	gene	insert	tag	species	vector	comment
MK01	PICH	PICH (ATB binding mutant, GAT)	N-Gal4-AD	human	pAcT2	Yeast Two Hybrid
MK02	PICH	PICH (ATB binding mutant, GAT)	N-Gal4-BD	human	pFBT9	Yeast Two Hybrid
MK03	PICH	PICH (1-693)	N-Gal4-AD	human	pAcT2	Yeast Two Hybrid
MK04	PICH	PICH (1-693)	N-Gal4-BD	human	pFBT9	Yeast Two Hybrid
MK05	PICH	PICH (628-1250)	N-Gal4-AD	human	pAcT2	Yeast Two Hybrid
MK06	PICH	PICH (628-1250)	N-Gal4-BD	human	pFBT9	Yeast Two Hybrid
MK07	PICH	PICH (ATB binding mutant, GAT)	N-his	human	pvl1393	insect expression
MK08	PICH	PICH (1-892)	N-Gal4-BD	human	pFBT9	Yeast Two Hybrid
MK09	PICH	PICH (628-1250; T1063A mutant	N-Gal4-BD	human	pFBT9	Yeast Two Hybrid
MK10	PICH	PICH 1-580	flag	human	pcDNA3.1-flag	Mam. expression
MK11	PICH	PICH 1-693	flag	human	pcDNA3.1-flag	Mam. expression
MK12	PICH	PICH 1-892	flag	human	pcDNA3.1-flag	Mam. expression
MK13	PICH	PICH PFD		human	pFBT9	Y2H
MK14	PICH	PICH PFD-892		human	pFBT9	Y2H
MK15	PICH	PICH 689-1088		human	pFBT9	Y2H
MK16	PICH	PICH 1-1088	flag	human	pcDNA3.1-flag	Mam. expression
MK17	PICH	PICH T1063E	GFP	human	peGFPC2	Mam. expression
MK18	PICH	PICH T235A	GFP	human	peGFPC2	Mam. expression
MK19	PICH	PICH S338A	GFP	human	peGFPC2	Mam. expression
MK20	PICH	PICH T235A + S338A	GFP	human	peGFPC2	Mam. expression
MK21	PICH	PICH T303A	GFP	human	peGFPC2	Mam. expression
MK22	PICH	PICH T609A	GFP	human	peGFPC2	Mam. expression
MK23	PICH	PICH S459A	GFP	human	peGFPC2	Mam. expression
MK24	PICH	PICH T303E	GFP	human	peGFPC2	Mam. expression
MK25	PP2A	PP2A catalytic subunit	GFP	human	EX-C0306-M29	Mam. expression
MK26	PICH	PICH T303A	flag	human	pcDNA3.1-flag	Mam. expression
MK27	PICH	PICH S459A	flag	human	pcDNA3.1-flag	Mam. expression
MK28	Sgo1	Sgo1 1-176	flag	human	pcDNA3.1-flag	Mam. expression
MK29	PICH	PICH S790A	GFP	human	peGFPC2	Mam. expression
MK30	PICH	PICH S774A	GFP	human	peGFPC2	Mam. expression
MK31	PICH	PICH S945A	GFP	human	peGFPC2	Mam. expression
MK32	PICH	PICH S945A + T1063A	GFP	human	peGFPC2	Mam. expression
MK33	Sgo2	Sgo2 wt (resistent to oligo 3 from YenT. et al)	rfp	human	pcS2	Mam. expression O.Stemmann
MK34	Sgo2	Sgo2 Mad2 deficient binding, KLMR 150-153 to AAAA	rfp	human	pcS2	Mam. expression, gift from O.Stemmann
MK35	Sgo2	Sgo2 PP2A deficient binding, N58 to I58	rfp	human	pcS2	Mam. expression, gift from O.Stemmann
MK36	PICH	PICH T454A	GFP	human	peGFPC2	Mam. expression
MK37	PICH	PICH S683A	GFP	human	peGFPC2	Mam. expression
MK38	PICH	PICH 1-752, n-term his	his	human	pET28	bacterial expression
MK39	PICH	PICH 1-571, n-term his	his	human	pET28	bacterial expression
MK40	PICH	PICH 1-454, n-term his	his	human	pET28	bacterial expression
MK41	PICH	PICH 1-421, n-term his	his	human	pET28	bacterial expression
MK42	PICH	PICH 1-632, n-term his	his	human	pET28	bacterial expression
MK43	PICH	PICH 79-752, n-term his	his	human	pET28	bacterial expression
MK44	PICH	PICH 79-632, n-term his	his	human	pET28	bacterial expression
MK45	PICH	PICH 79-571, n-term his	his	human	pET28	bacterial expression
MK46	PICH	PICH 79-454, n-term his	his	human	pET28	bacterial expression
MK47	PICH	PICH 79-421, n-term his	his	human	pET28	bacterial expression
MK48	PICH	PICH 1-715aa	His (N)	human	pET28b	Bacterial expression
MK49	PICH	PICH S459A + S790A	GFP	human	pEGFP-C2	Mam. expression
MK50	PICH	PICH T797A	GFP	human	pEGFP-C2	Mam. expression
MK51	PICH	PICH S864A	GFP	human	pEGFP-C2	Mam. expression
MK52	PICH	PICH T1063D	GFP	human	peGFPC2	Mam. expression
MK53	PICH	PICH 459E+790E	GFP	human	peGFPC2	Mam. expression
MK54	PICH	PICH S143A	GFP	human	peGFPC2	Mam. expression
MK55	PICH	PICH T185A	GFP	human	peGFPC2	Mam. expression
MK56	PICH	PICH T509A	GFP	human	peGFPC2	Mam. expression
MK57	PICH	PICH 530A	GFP	human	peGFPC2	Mam. expression
MK58	PICH	PICH S557A	GFP	human	peGFPC2	Mam. expression
MK59	PICH	PICH minus N-TRP	GFP	human	peGFPC2	Mam. expression
MK60	PICH	PICH minus C-TRP	GFP	human	peGFPC2	Mam. expression
MK61	PICH	PICH minus NC-TPR	GFP	human	peGFPC2	Mam. expression
MK62	Wapl	wt	Myc	human	pcDNA3.1-myc	Mam. expression
MK63	PICH	PICH A28W	GFP	human	peGFPC2	Mam. expression
MK64	PICH	PICH G1207W	GFP	human	peGFPC2	Mam. expression
MK65	PICH	PICH A28+G1207W	GFP	human	peGFPC2	Mam. expression
MK66	PPP1gama	wt	Myc	human	pcDNA3.1-myc	Mam. expression
MK67	PICH	PICH T1063A	Flag	human	pcDNA3.1-flag	Mam. expression
MK68	PICH	PICH S807A	GFP	human	pEGFP-C2	Mam. expression
MK69	ILF3	wt	Flag	human	pcDNA3.1-flag	Mam. expression
MK70	PICH	PICH G1207W	Flag	human	pcDNA3.1-flag	Mam. expression
MK71	PICH	PICH A28W+G1207W	Flag	human	pcDNA3.1-flag	Mam. expression
MK72	PICH	wt	Flag	human	pcDNA3.1-flag	Mam. expression
MK73	PICH	wt	Myc	human	pcDNA3.1-myc	Mam. expression
MK74	PICH	774A,807A,810A,813A,864A	GFP	human	peGFPC2	Mam. expression

MK75	PICH	774A,807A,810A,813A,864A, 995A	GFP	human	peGFPC2	Mam. expression
MK76	PICH	PICH minus N-TPR	Flag	human	pcDNA3.1-flag	Mam. expression
MK77	PICH	PICH minus N-TPR	Myc	human	pcDNA3.1-myc	Mam. expression
MK78	PICH	PICH minus C-TPR	Flag	human	pcDNA3.1-flag	Mam. expression
MK79	PICH	PICH minus C-TPR	Myc	human	pcDNA3.1-myc	Mam. expression
MK80	PICH	PICH minus N+C-TPR	Flag	human	pcDNA3.1-flag	Mam. expression
MK81	PICH	PICH minus N+C-TPR	Myc	human	pcDNA3.1-myc	Mam. expression
MK82	PICH	PICH A28W+F44A	Flag	human	pcDNA3.1-flag	Mam. expression
MK83	PICH	PICH GAT+DQAH	GFP	human	peGFPC2	Mam. expression
MK84	PICH	774A,807A,810A,813A,864A, 995A	GFP	human	peGFPC2	Mam. expression
MK85	PICH	PICH S1028E	GFP	human	peGFPC2	Mam. expression
MK86	PICH	774A,807A,810A,813A,864A, 995A, 980, 1098	GFP	human	peGFPC2	Mam. expression
MK87	PICH	PICH 820A+1028A	GFP	human	peGFPC2	Mam. expression
MK88	PICH	PICH minus N-TPR (oligo 1 res.)	GFP	human	peGFPC2	Mam. expression
MK89	PICH	PICH minus C-TPR (oligo 1 res.)	GFP	human	peGFPC2	Mam. expression
MK90	PICH	PICH minus N+C-TPR (oligo 1 res.)	GFP	human	peGFPC2	Mam. expression
MK91	SA2	SA2 12xA	GFP	human	peGFPC2	Mam. Expression, gift from O. Stemmann
MK92	PICH	11xA (Cdk1 sites)	GFP	human	peGFPC2	Mam. expression
MK93	PICH	PICH GAT+DQAH	GFP	human	peGFPC2	Mam. expression
MK94	PICH	Wt (oligo3 res.)	GFP	human	peGFPC2	Mam. expression
MK95	PICH	T1063A (oligo3 res.)	GFP	human	peGFPC2	Mam. expression
MK96	PICH	GAT+DQAH (oligo3 res.)	GFP	human	peGFPC2	Mam. expression
MK97	PICH	T1063A + GAT+DQAH (oligo3 res.)	GFP	human	peGFPC2	Mam. expression
MK98	PICH	11xA (Cdk1 sites) (oligo3 res.)	GFP	human	peGFPC2	Mam. expression
MK99	BEND3	wt	Myc	human	pcDNA3.1-myc	Mam. expression
MK100	SA2	SA2-12xA	MYC	human	pcDNA3.1-myc	Mam. expression

7.2 List of DNA oligonucleotides

DNA Oligo no.:	Used for	Comment	Sequence
M3967	cloning	cloning-N-TPR Domain (XmaI) for pACT2	GCG CCCGGG C atggaggcatcccgaaggttt
M3968	cloning	cloning-C-TPR Domain (XmaI) for pACT2	GCG CCCGGG C gctacaaatgactatgagactcttg
M3969	cloning	cloning-Pich Family Domain (XmaI) for pACT2	GCG CCCGGG C tttacaatcgaggatcttcagaact
M3970	cloning	cloning-N-TPR Domain + stop codon (XhoI) for pACT2	GCG CTCGAG TTA GATTCTGCTCAGCACTTTTTCATTG
M3971	cloning	cloning-C-TPR Domain + stop codon (XhoI) for pACT2	GCG CTCGAG TCAATTGTTATTAAGTTGCTTATACAAAC
M3972	cloning	cloning-Pich Family Domain + stop codon (XhoI) for pACT2	GCG CTCGAG TTA TTCTTCTACCACATCAAGCTCTTC
M3973	cloning	cloning-HELICc Domain + stop codon (XhoI) for pACT2	GCG CTCGAG TTA CACAACATTCTCTTTTTGTCCAATTC
M3974	cloning	cloning-N-TPR Domain (SmaI) for pFBT9	GCG CCCGGG C atggaggcatcccgaaggttt
M3975	cloning	cloning-C-TPR Domain (SmaI) for pFBT9	GCG CCCGGG C gctacaaatgactatgagactcttg
M3976	cloning	cloning-Pich Family Domain (SmaI) for pFBT9	GCG CCCGGG C tttacaatcgaggatcttcagaact
M3977	cloning	cloning-N-TPR Domain + stop codon (SalI) for pFBT9	GCG GTCGAC TTA GATTCTGCTCAGCACTTTTTCATTG
M3978	cloning	cloning-C-TPR Domain + stop codon (SalI) for pFBT9	GCG GTCGAC TCA ATTGTTATTAAGTTGCTTATACAAAC
M3979	cloning	cloning-Pich Family Domain + stop codon (SalI) for pFBT9	GCG GTCGAC TTA TTCTTCTACCACATCAAGCTCTTC
M3980	cloning	cloning-HELICc Domain + stop codon (SalI) for pFBT9	GCG GTCGAC TTA CACAACATTCTCTTTTTGTCCAATTC
M4028	cloning	PICH (689 - C-term.) XmaI for pACT2	gcgcccggggcgatgtggtagaagaatctcactata
M4029	cloning	PICH (883 – C-term.) XmaI for pACT2	gcgcccgggccaactaaaggatgatgagattttacg
M4030	cloning	PICH (1080 – C-term.) XmaI for pACT2	gcgcccgggccccagtagtgtaaataagtctatga
M4031	cloning	PICH (N-term. - 892) XhoI for pACT2	gcgctcgagttaacgtaaaatctcatcatccttttagttg
M4032	cloning	PICH (N-term. - 1088) XhoI for pACT2	gcgctcgagttagttcatagacttatttacactactggg
M4033	cloning	PICH (N-term. - 892) SalI for pFBT9	gcggtcgacttaacgtaaaatctcatcatccttttagttg
M4034	cloning	PICH (N-term. - 1088) SalI for pFBT9	gcggtcgacttagttcatagacttatttacactactggg
M4291	Site-Direct Mut	PICH T235A f1	GCACATAAAATAAAAGCCTCATCTACTAAGT
M4292	Site-Direct Mut	PICH T235A r1	ACTTAGTAGATGAGGCTTTTATTTTATGTGC
M4293	Site-Direct Mut	PICH S338A f1	GTACAGAAGAAAAAGGCAAGCAACCCAGAGG
M4294	Site-Direct Mut	PICH S338A r1	CCTCTGGGTTGCTTGCCTTTTTCTTCTGTAC
M4328	cloning	PICH Xho1 for peGFP-C1	gcgCTCGAGGCatggaggcatcccgaaggttt
M4329	cloning	PICH (1-892) Xma1 for peGFP-C1	gcg CCCGGG A CGTAAAATCTCATCATCCTTTAGTTG
M4330	cloning	PICH (1-1088) Xma1 for peGFP-C1	gcgCCCGGGGTTCATAGACTTATTTACACTACTGGG
M4340	Site-Direct Mut	PICH-T1063E-f1	AATTTGATGCTTCAGAGCCCAAAAATGACAT
M4341	Site-Direct Mut	PICH-T1063E-r1	ATGTCATTTTTGGGCTCTGAAGCATCAAATT
M4342	cloning	FBX22-f1 KpnI for pcDNA3.1 C1	GCG GGTACC T ATGGAGCCGGTAGGCTGCTGCGG
M4343	cloning	FBX22-r1 XhoI for pcDNA3.1 C1	GCG CTCGAG TTATTTAGATGACCCCAGATGTATG
M4344	cloning	FBX22-f2 XhoI for peGFP C1	GCG CTCGAG CC ATGGAGCCGGTAGGCTGCTGCGG
M4345	cloning	FBX22-r2 SmaI/XmaI for peGFP C1	GCG CCCGGG TTATTTAGATGACCCCAGATGTATG
M4346	Nested PCR	nesFBX22-f1	GTTCCTCCGAGCCGCCGTAGGACT
M4347	Nested PCR	nesFBX22-r1	CAGAACCCAAAAGTTACATATTATG
M4379f	Site-Direct Mut	PICH-T303A f	GAGAGAAGGATGCTGCCCCAGGAGAAAAAGCC
M4379r	Site-Direct Mut	PICH-T303A r	GGCTTTTTCTCCTGGGGCAGCATCCTTCTCTC
M4380	Site-Direct Mut	PICH-T303E f	GAGAGAAGGATGCTGAGCCAGGAGAAAAAGCC
M4381	Site-Direct Mut	PICH-T303E r	GGCTTTTTCTCCTGGCTCAGCATCCTTCTCTC
M4391	Site-Direct Mut	PICH S459E f1	acattgatggaagaagagggaaaaatgatattc
M4392	Site-Direct Mut	PICH S459E r1	GAATATCATTTTTCCCTCTTCTTCCATCAATGT
M4393	Site-Direct Mut	PICH T609E f1	cattaataagacaaactgagggtgaaaaaaagaac
M4394	Site-Direct Mut	PICH T609E r1	GTTCTTTTTTTCACCCTCAGTTTGTCTTATTAATG
M4400	cloning	PP2AC-f1 pcDNA3.1-flag - Kpn1	GCGGGTACCGATGGACGAGAAGGTGTTCACCAAG
M4401	cloning	PP2AC-r1 pcDNA3.1-flag - Apa1	GCGGGGCCCTTACAGGAAGTAGTCTGGGGTACG
M4402	Site-Direct Mut	PP2AC PD -f1 D88A	ATGGGAGATTATGTTGCCAGAGGATATTATTCA
M4403	Site-Direct Mut	PP2AC PD -r1 D88A	TGAATAATATCCTCTGGCAACATAATCTCCCAT
M4404	cloning	Sgo1-f1 Kpn1 for pcDNA3.1 flag	GCGGGTACCTATGGCCAAGGAAAGATGCCTGAAA
M4405	cloning	Sgo1-r1 Xho1	GCGCTCGAGTCATTGTATTTGTTTCATACTTTT

M4406	cloning	Sgo1-r2 aa1-176 Xho1+Stopcodon	GCGCTCGAGTCAACCTGAATCAAAATCAACTCCCAG
M4407	cloning	Sgo1- for-nested Primer	GGAGGAAGATAGCTGTTGCAGAAG
M4408	cloning	Sgo1- rev-nested Primer	GCAACAGAAAGAGGTGTAGATTG
M4436	Site-Direct Mut	PICH T740A f	TTTCCTTCTTCAGCAAAGAAGAAATGCCCT
M4437	Site-Direct Mut	PICH T740A r	AGGGCATTTCTTCTTTGCTGAAGAAGGAAA
M4438	Site-Direct Mut	PICH S774A f	AGTTCCAAAATGGCAGCCGTAGTCATTGATGAT
M4439	Site-Direct Mut	PICH S774A r	ATCATCAATGACTACGGCTGCCATTTTGGAACT
M4440	Site-Direct Mut	PICH S790A f	GAGAAACAAGATCTCGCCAGTATAAAGGTGAAT
M4441	Site-Direct Mut	PICH S790A r	ATTCACCTTTATACTGGCGAGATCTTGTTTCTC
M4442	Site-Direct Mut	PICH S14A f	GAAGCCGAGGCCTTGGCCCCAGAGCAGGCTGCT
M4443	Site-Direct Mut	PICH S14A r	AGCAGCCTGCTCTGGGGCCAAGGCCTCGGCTTC
M4454	Site-Direct Mut	PICH S945A f	GAGGAACCTTCAGCAGCTTCACCACAGTATGCA
M4455	Site-Direct Mut	PICH S945A r	TGCATACTGTGGTGAAGCTGCTGAAGGTTCCTC
M4509	Site-Direct Mut	Plk1 K200A f	TTTGGACTGGCAACC GCA GTCGAATATGACGGG
M4510	Site-Direct Mut	Plk1 K200A r	CCCGTCATATTCGACTGCGGTTGCCAGTCCAAA
M4511	Site-Direct Mut	Plk1 K265A f	TACCTCCGGATCAAG GCG AATGAATACAGTATT
M4512	Site-Direct Mut	Plk1 K265A r	AATACTGTATTCATTCGCCTTGATCCGGAGGTA
M4513	Site-Direct Mut	Plk1 K358A f	GAGCGTCCCCGGGAA GCA GAAGAACCAGTGGTT
M4514	Site-Direct Mut	Plk1 K358A r	AACCACTGGTTCTTCTGCTTCCCGGGGACGCTC
M4558	Site-Direct Mut	PICH S790E f	GAGAAACAAGATCTC GAA AGTATAAAGGTGAAT
M4559	Site-Direct Mut	PICH S790E r	ATTCACCTTTATACTTTCGAGATCTTGTTTCTC
M4560	cloning	PICH 428 r (XhoI)	GCG CTCGAG TTA CCCAAGATTTAGCAAACAACAAG
M4561	cloning	PICH 99 r (XhoI)	GCG CTCGAG TTA GTGCTCAAAGAGTTGGTTGTGCAG
M4667	Nested PCR	PP2A A alpha f nes	CGTTTCAGCACAGCGCTGGCCGCAG
M4668	Nested PCR	PP2A A alpha r nes	GAGGGACTTGTGGGGGTTGGAGGG
M4669	cloning	PP2A A alpha f for pcDNA-flag kpn1	GCG GGTACC CC ATGGCGGCGGCCGACGGCGACGAC
M4670	cloning	PP2A A alpha r for pcDNA-flag xho1	GCG CTCGAG TTA TCAGGCGAGAGACAGAACAGTCAG
M4671	Nested PCR	PP2A A beta f nes	GGGGCCTGGGCGCGGGGCGGGAG
M4672	Nested PCR	PP2A A beta r nes	GACTAGAAATTTGTGACAAGAATC
M4673	cloning	PP2A A beta f for pcDNA-flag kpn1	GCG GGTACC CC ATGGCGGGCGCATCAGAGCTCGGG
M4674	cloning	PP2A A beta r for pcDNA-flag xho1	GCG CTCGAG TTA TGCCAATGCAAGAACACTTATAG
M4675	Nested PCR	PP2A C alpha f nes	GTGCGGGCGGCGGCGCGGGAGCAGC
M4676	Nested PCR	PP2A C alpha r nes	CCATTAGGTCGATATATGGTTC
M4685	cloning	PICH aa1 for (Nde1)	GCG CATATG ATGGAGGCATCCCGAAGGTTTCC
M4686	cloning	PICH aa79 for (Nde1)	GCG CATATG ACAGATGTGTGCAACTCTGGCTTG
M4687	cloning	PICH aa752 rev (Xho1)	GCG CTCGAG TTA AGGCTGAGGCTGTGGTTTATTCAA
M4688	cloning	PICH aa715 rev (Xho1)	GCG CTCGAG TTA TTTATTTTGAGACTCGAATTCAAC
M4689	cloning	PICH aa632 rev (Xho1)	GCG CTCGAG TTA ATCCTCGATTGTAAAGAGCTCTC
M4690	cloning	PICH aa571 rev (Xho1)	GCG CTCGAG TTA AACCACAACATTCTCTTTTTGTC
M4691	cloning	PICH aa454 rev (Xho1)	GCG CTCGAG TTA TGTGTCATCAGTTACTTGATCAAT
M4692	cloning	PICH aa421 rev (Xho1)	GCG CTCGAG TTA AGCCCGTGCAGACAGCAGCCTAG
M4721	cloning	PICHr for pcDNA3.1 flag + NLS + Stop (Xho1)	CTCGAG TCACACCTTGCGCTTCTTCTTCGGCGGCC CATTGTTATTAAGTTGCTTATAC
M4724	cloning	Sgo2-f1 for pcDNA3.1 flag	GCG GGTACC T ATGGAGTGCCCAGTGATGGAAAC
M4725	cloning	Sgo2-r1 for pcDNA3.1 flag	GCG CTCGAG TCATCTTCTCATCTTGTCTCTGAG
M4726	Nested PCR	nesSgo2-f	CTGAGCTGGGTGGGGGTGCCCC
M4727	Nested PCR	nesSgo2-r	GATTCCTTATGCTTTGAAAATTC
M4863	Site-Direct Mut	PICH T454A for	CAAGTAACTGATGAC GCA TTGATGGAAGAATCT
M4864	Site-Direct Mut	PICH S683A for	GTACACATGTGATCTG GCT GTTAAAGAAGAGCTT
M4902	Site-Direct Mut	PICH T454A rev	AGATTCTTCCATCAATGCGTCATCAGTTACTTG
M4903	Site-Direct Mut	PICH S683A rev	AAGCTCTTCT TTAACAGCCA GATCACATGT GTAC
M4936	sequencing	pp2aaa599down	CGTCAAGAGTGAGATCATCCC
M4937	sequencing	pp2aaa346up	CAGAGGGCGAGTGCTCGTGTG
M4951	sequencing	Sgo2 550down	CATTACCTGATATTCCCTCTTC
M4952	sequencing	Sgo2 1102down	CTGCTAGTGAAGTCAGCAAAATTG
M4953	sequencing	Sgo2 1648down	CAAACCAAAAGGATAAAGTAAC
M4954	sequencing	Sgo2 2200down	GTATAGAATACACAGTTAAAAG
M4955	sequencing	Sgo2 2752down	CTGAAATGAACCAGATATATG
M4956	sequencing	Sgo2 3300down	GACAGCGTTCAGGGAAAGTC
M5041	sequencing	Sgo2 680up	CTCTGGGAGGTACATCAACTATAG
M5119	Site-Direct Mut	PICH T1063D f	CAATTTGATGCTTCAGACCCCAAAAATGACATC
M5120	Site-Direct Mut	PICH T1063D r	GATGTCATTTTTGGGGTCTGAAGCATCAAATTG
M5121	Site-Direct Mut	PICH T797A f	ATAAAGGTGAATGTTGCCACCTTGCAAGATGGT
M5122	Site-Direct Mut	PICH T797A r	ACCATCTTGCAAGGTGGCAACATTCACCTTTAT
M5123	Site-Direct Mut	PICH S864A f	GAGGATCCTCTGGAAGCTTTTAATTATGTACTT
M5124	Site-Direct Mut	PICH S864A r	AAGTACATAATTAAAAGCTTCCAGAGGATCCTC
M5200	cloning	PICH aa1 for (Not1)	GCG GCGGCCGC A ATGGAGGCATCCCGAAGGTTTCC
M5201	cloning	PICH aa79 for (Not1)	GCG GCGGCCGG A ACAGATGTGTGCAACTCT GGCTTG
M5218	Site-Direct Mut	PICH T329A f	TTTCTCAGGAGGGCTAAAGAAGACGTA
M5219	Site-Direct Mut	PICH T329A r	TACGTCTTCTTTAGCCCTCCTGAGAAA
M5220	Site-Direct Mut	PICH S652A f	GCTCAGAGGAAAGCTGATATAAAACTA
M5221	Site-Direct Mut	PICH S652A r	TAGTTTTATATCAGCTTTCCTCTGAGC
M5222	Site-Direct Mut	PICH S1092A f	AACTCTAGAAGAGCTCTGGCTTCTAGG
M5223	Site-Direct Mut	PICH S1092A r	CCTAGAAGCCAGAGCTCTTCTAGAGTT
M5224	Site-Direct Mut	PICH S1098A f	GCTTCTAGGAGGGCTCTTATTAATATG
M5225	Site-Direct Mut	PICH S1098A r	CATATTAATAAGAGCCCTCCTAGAAGC
M5226	Site-Direct Mut	PICH S143A f	ATGTTTGATGCAGCACTTGTGAATCAT
M5227	Site-Direct Mut	PICH S143A r	ATGATTCACAAGTGCTGCATCAAACAT
M5228	Site-Direct Mut	PICH T185A f	AAGGATGAACGGGCCAGAAACCTCAAT
M5229	Site-Direct Mut	PICH T185A r	ATTGAGGTTTCTGGCCCGTTCATCCTT
M5230	Site-Direct Mut	PICH T509A f	CGAATCGATGGGGCAGTTACTCATCTT
M5231	Site-Direct Mut	PICH T509A r	AAGATGAGTAACTGCCCCATCGATTCG
M5232	Site-Direct Mut	PICH S530A f	AATAAAGATTACGCTGTTTTTCTGCTT
M5233	Site-Direct Mut	PICH S530A r	AAGCAGAAAAACAGCGTAATCTTTATT
M5234	Site-Direct Mut	PICH S557A f	ATTTTTGACCCTGCCTGGAATCCTGCA
M5235	Site-Direct Mut	PICH S557A r	TGCAGGATTCCAGGCAGGGTCAAAAAT

M5270	cloning	PICH 95 (Xho1) for peGFP down	gcgCTCGAG CG CAACTCTTTGAGCACCAGAAGG
M5271	cloning	PICH 1195 (Xma1) for peGFP up	gcgCCCGGG TTA CTCTGCCGCCTTATCCTGGGG
M5299	Site-Direct Mut	PICH S1134-5A f	GAAGGGGTGGAGGAAGCCGCCGGCGAAGCCTCCAAG
M5300	Site-Direct Mut	PICH S1134-5A r	CTTGGAGGCTTCGCCGGCGGCTTCCTCCACCCCTTC
M5301	Site-Direct Mut	PICH S1036A f	GAAGATGAAGATGAT GCT TTTAAAGATACCTCA
M5302	Site-Direct Mut	PICH S1036A r	TGAGGTATCTTTAAAAGCATCATCTTCATCTTC
M5330	Site-Direct Mut	CyclinB1 R42A f	CCCGGACTGAGGCCAGCAACAGCTCTTGGGGAC
M5331	Site-Direct Mut	CyclinB1 R42A r	GTCCCCAAGAGCTGTTGCTGGCCTCAGTCCGGG
M5342	cloning	Wapl Kpn1 down - for pcDNA3.1 myc/flag	gcgGGTACCCATGACATCCAGATTTGGGAAAACA
M5343	cloning	Wapl Xho1 up - for pcDNA3.1 myc/flag	gcgCTCGAG CTAGCAATGTTCCAAATATTCAAT
M5351	cloning	SA2 Kpn1 down - for pcDNA3.1 myc/flag	gcgGGTACCCatgatagcagctccagaaatacc
M5352	cloning	SA2 Xho1 up - for pcDNA3.1 myc/flag	gcgCTCGAGTTAAAACATTGACACTCCAAGAAC
M5395	Site-Direct Mut	PICH A28W f	AGATATGTGAAAGAG TGG AAAGAAGCAACTAAG
M5396	Site-Direct Mut	PICH A28W r	CTTAGTTGCTTCTTTCCACTCTTTCACATATCT
M5397	Site-Direct Mut	PICH G1207W f	ACTCTTGTAAAGCGT TGG AAAGAACTAAAAGAG
M5398	Site-Direct Mut	PICH G1207W r	CTCTTTTAGTTCTTTCCAACGCTTTACAAGAGT
M5417	cloning	PP1 gamma Kpn1 down- for pcDNA31. myc/flag	gcgGGTACCC ATGGCGGATTTAGATAAACTCA
M5418	cloning	PP1 gamma Xho1 up- for pcDNA31. myc/flag	gcgCTCGAG CTATTTCTTTGCTTGCTTTGTG
M5431	cloning	PCNA BamH1 down for pcDNA3.1 myc flag	gcgGGATCCATGTTCGAGGCGCGCCTGGTCCAG
M5432	cloning	PCNA Xho1 up for pcDNA3.1 myc flag	gcgCTCGAGCTAAGATCCTTCTTCATCCTCGATC
M5433	cloning	FEN1 Kpn1 down for pcDNA3.1 myc flag	gcgGGTACC C ATGGGAATTCAAGGCCTGGCCAAAC
M5434	cloning	FEN1 Xho1 up for pcDNA3.1 myc flag	gcgCTCGAGTTATTTTCCCCTTTTAAACTTCCC
M5441	Site-Direct Mut	PICH S807 f	GGTAAAGGTACAGGTGCTGCTGACTCTATAGCT
M5442	Site-Direct Mut	PICH S807 r	AGCTATAGAGTCAGCAGCACCTGTACCTTTACC
M5443	Site-Direct Mut	PICH S984 f	AATAGCTTGTGTGGCGCTGCACCTAATTCCAGA
M5444	Site-Direct Mut	PICH S984 r	TCTGGAATTAGGTGCAGCGCCACACAAGCTATT
M5445	Site-Direct Mut	PICH S980 f	GTTGAGAAAGAAAATGCCTTGTGTGGCTCTGCA
M5446	Site-Direct Mut	PICH S980 r	TGCAGAGCCACACAAGGCATTTTCTTTCTCAAC
M5447	Site-Direct Mut	PICH S807 + S810 + T813 f	GGTACAGGTGCTGCTGACGCTATAGCTGCTTTAC CAAAGGGG
M5448	Site-Direct Mut	PICH S807 + S810 + T813 r	CCCCTTTGGTAAAGCAGCTATAGCGTCAGCAGC ACCTGTACC
M5449	cloning	ILF3 nested f	CACCAAGGAACTCTATCACAATTTG
M5450	cloning	ILF3 nested r	GTTAACTGTGATGCATAAAACTCGATC
M5451	cloning	ILF3 Kpn-f	gcgGGTACCCATGCGTCCAATGCGAATTTTTGTG
M5452	cloning	ILF3 Not-r	gcgGCGGCCGCTTATCTGTACTGGTAGTTCATGCTG
M5493	Site-Direct Mut	PICH S774D f	AGTTCCAAAATGGCAGATGTAGTCATTGATGAT
M5494	Site-Direct Mut	PICH S774D r	ATCATCAATGACTACATCTGCCATTTTGGAACT
M5495	Site-Direct Mut	PICH S807D f	GGTAAAGGTACAGGTGATGCTGACTCTATAGCT
M5496	Site-Direct Mut	PICH S807D r	AGCTATAGAGTCAGCATCACCTGTACCTTTACC
M5497	Site-Direct Mut	PICH S810D f	ACAGGTAGTGCTGACGATATAGCTACTTTACCA
M5498	Site-Direct Mut	PICH S810D r	TGGTAAAGTAGCTATATCGTCAGCACTACCTGT
M5499	Site-Direct Mut	PICH S864D f	GAGGATCCTCTGGAAGATTTTAATTATGTACTT
M5500	Site-Direct Mut	PICH S864D r	AAGTACATAATTAAAATCTTCCAGAGGATCCTC
M5528	cloning	PICH TPR r1	CTCGAG TTAGATTCTGCTCAGCACTTTTTCATTG
M5529	cloning	PICH TPR f2	GGTACC C GCTACAAATGACTATGAGACTCTTG
M5530	cloning	PICH TPR f3	GGTACC C CAAAAAATACAGGAAGCCTTGGAG
M5531	cloning	PICH TPR r3	CTCGAG TTACTCTGCCGCCTTATCCTGGGGAGA
M5536	Site-Direct Mut	PICH F44A f	GAAGCATTTAAACTTGCCAATTTGGCAAAGGAC
M5537	Site-Direct Mut	PICH F44A r	GTCCTTTGCCAAATTGGCAAGTTTAAATGCTTC
M5538	Site-Direct Mut	PICH L1223A f	falsche sequence bestellt
M5539	Site-Direct Mut	PICH L1223A r	falsche sequence bestellt
M5557	Site-Direct Mut	PICH S995A f	GCAGGGTTTGTGCATGCAAAAACATGTCTCAGT
M5558	Site-Direct Mut	PICH S995A r	ACTGAGACATGTTTTTGCATGCACAAACCCTGC
M5560	Site-Direct Mut	PICH L1223A f2	falsche sequence bestellt
M5561	Site-Direct Mut	PICH L1223A r2	falsche sequence bestellt
M5567	Site-Direct Mut	PICH S1028A f	GCTAGAAGGATTGTTGCAGATGGCGAAGATGAA
M5568	Site-Direct Mut	PICH S1028A r	TTCATCTTCGCCATCTGCAACAATCCTTCTAGC
M5569	Site-Direct Mut	PICH S1028E f	GCTAGAAGGATTGTTGAAGATGGCGAAGATGAA
M5570	Site-Direct Mut	PICH S1028E r	TTCATCTTCGCCATCTTCAACAATCCTTCTAGC
M5571	cloning	PICH-Splice2 f	gcgCTCGAG CG ATGGGATTAGGGAAGACTGTTCAAA
M5658	Site-Direct Mut	PICH L1223A f3	GAG GCC CTA AAC TGC GCA GTT AAA GCG CTT GAC
M5659	Site-Direct Mut	PICH L1223A r3	GTCAAGCGCT TTAACTGCGC AGTTTAGGGC CTC
M5675	Site-Direct Mut	PICH S820A f	CCAAAGGGGTTTGGAGCTGTAGAAGAACTTTGT
M5676	Site-Direct Mut	PICH S820A r	ACAAAGTTCTTCTACAGCTCCAAACCCCTTTGG
M5677	Site-Direct Mut	PICH S960A f	CTTTTCTTGGAAGACGCAGCAGACAACAGACAA
M5678	Site-Direct Mut	PICH S960A r	TTGTCTGTTGTCTGCTGCGTCTTCCAAGAAAAG
M5679	Site-Direct Mut	PICH S968A f	AACAGACAAAACTTTGCCAGTCAGTCTTTAGAG
M5680	Site-Direct Mut	PICH S968A r	CTCTAAAGACTGACTGGCAAAGTTTTGTCTGTT
M5681	cloning	NudC f1 kpn1	gcg GGTACC C ATGGGCGGAGAGCAGGAGGAGGAG
M5682	cloning	NudC r1 xho1	gcg CTCGAG CTAGTTGAATTTAGCCTTGGAAAAA
M5683	cloning	NudC f1 nest	GGAGCGTAGAGAGCGCGGGACTAG
M5684	cloning	NudC r1 nest	GTGGGAAAGAAAGTTGGGTGGTTGC
M5707	Site-Direct Mut	PICH KEN-1 f	AGAGTTTACCGAATTGGACAA GCA GCG GCT GTTGT GGTTTATAGGCTAATC
M5708	Site-Direct Mut	PICH KEN-1 r	GATTAGCCTATAAACCACAACAGCCGCTGCTTGTCC AATTCGGTAAACTCT
M5709	Site-Direct Mut	PICH KEN-2 f	CAGTCTTTAGAGCATGTTGAG GCA GCA GCT AGCT TGTGTGGCTCTGCACCT
M5710	Site-Direct Mut	PICH KEN-2 r	AGGTGCAGAGCCACACAAGCTAGCTGCTGCCTCAA CATGCTCTAAAGACTG
M5691	cloning	PICH TPR f4 for peGFP Xho	gcg CTCGA GCT CAAAAAATACAGGAAGCCTTGGAG
M5692	cloning	PICH TPR r4 rev peGFP Kpn	gcg GGTACC TTACTCTGCCGCCTTATCCTGGGGAGA
M5693	Site-Direct Mut	repair T375A f	cctaggctgctgtctgcacgggcttgttgtttg
M5694	Site-Direct Mut	repair T375A r	CAAACAACAAGCCCGTGCAGACAGCAGCCTAGG
M5696	cloning	PHB2 nest f	GCGGGGTAGAGGCGGGCCGGCACC
M5697	cloning	PHB2 nest r	CCTCAAAAACTGGAGAAGCAGATC

M5698	cloning	PHB2 Kpn f	gcg GGTACC T ATGGCCCAGAACTTGAAGGACTTGG
M5699	cloning	PHB2 Xho r	gcg CTCGAG TCATTTCTTACCCTTGATGAGGCTG
M5713	cloning	CamK2D f Kpn1	gcgGGTACC T ATGGCTTCGACCACAACCTGCACC
M5714	cloning	CamK2D r Xho1	gcgCTCGAG TTACTTGATGGGTACTGTTGGTGAC
M5715	cloning	CamK2D f nest	CGCGCGTCTGCTCGCTTCTGGTC
M5716	cloning	CamK2D r nest	GAATAAGTAGAAGGAGCTGACC
M5738	Site-Direct Mut	CaMK2d D136A f	GGCATAGTTCACAGGGCCCTGAAGCCTGAGAATTTG
M5739	Site-Direct Mut	CaMK2d D136A f	CAAATTCTCAGGCTTCAGGGCCCTGTGAACTATGCC
M5961	Site-Direct Mut	PICH S1076A f	CCAGGAAGGTTCTTTGCATCTCAAATACCCAGT
M5962	Site-Direct Mut	PICH S1076A r	ACTGGGTATTTGAGATGCAAAGAACCTTCCTGG
M5964	cloning	Plk1- f1 -Plk1 for C-term mCherry	gcgGTTTAAACATGAGTGCTGCAGTGACTGCAGGG
M5965	cloning	Plk1- r1 -Plk1 for C-term mCherry	gcgAAGCTTGGAGGCCTTGAGACGGTTGCTGGC
M5966	cloning	PICH- f1 -PICH for C-term gfp	gcg CTCGAG CT atggaggcatcccgaaggtttcc
M5967	cloning	PICH- r1 -PICH for C-term gfp	gcg GGTACC ATTGTTATTAAGTTGCTTATACA
M6015	Site-Direct Mut	PICH T168A-f	GAATTCATCAAGTGGGCTCCAGGAATGAGAGTC
M6016	Site-Direct Mut	PICH T258A-f	CTCCTCCTCACAGGAGCCCCAATCCAGAATAAT
M6017	Site-Direct Mut	PICH S-399A-f	CTAATGGAGACGCGCGCACCTTTGGCTGAGCTA
M6018	Site-Direct Mut	PICH S1069A-f	CCCAAAAATGACATCGCTCCACCAGGAAGGTTC
M6029	cloning	Plk1- r2 -for C-term mCherry (kpn1)	gcg GGTACC GGAGGCCTTGAGACGGTTGCTGGC
M6051	cloning	CFP-f1 Xho1	gcg CTCGAG TC ATGGTGAGCAAGGGCGAGGAGCTG
M6052	cloning	CFP-r1 Apa1 mit stop	gcg GGGCCC TTACTTGTATAGCTCGTCCATGCC
M6053	cloning	PICH kpn1	gcg GGTACC t atggaggcatcccgaaggtttccg
M6054	cloning	PICH-oSTOP Xho1 reverse primer	gcg CTCGAG ATTGTTATTAAGTTGCTTATACAAA
M6055	cloning	RFP-f1 Xho1	gcg CTCGAG TC ATGAGCTAGCTGATTANGGAGAAC
M6056	cloning	RFP-r1 Apa1	gcg GGGCCC TCACTTGTGCCCCAGTTTGCTAGGG
M6057	cloning	Plk1 Kpn1	gcg GGTACC t ATGAGTGCTGCAGTGACTGCAGGG
M6058	cloning	Plk1-oSTOP Xho1 reverse primer	gcg CTCGAG GGAGGCCTTGAGACGGTTGCTGGC
M6059	Site-Direct Mut	PICH S14A	GAAGCCGAGGCCTTGGCCCCAGAGCAGGCTGCTC
M6060	Site-Direct Mut	PICH S441A	GAAATGAGGGGGAAGATGCCCCAGATGTGGACC
M6061	Site-Direct Mut	PICH S755A	CCACAGCCTCAGCCTGCACCTCTTCTAAGTACTC
M6062	Site-Direct Mut	PICH S946A	GGAACCTTCAGCATCTGCACCACAGTATGCATGTG
M6063	Site-Direct Mut	PICH S1188A	GAACAGTTGGTTGGTGCTCCCCAGGATAAGGCGG
M6064	cloning	PICH-NLSr xho1	CTCGAG TCACACCTTGCGCTTCTTCTTCGGCGG ATTGTTATTAAGTTGCTTATACAAACTTAAAG
M6065	cloning	PICH-NLSr Kpn1	GGTACC TCACACCTTGCGCTTCTTCTTCGGCGG ATTGTTATTAAGTTGCTTATACAAACTTAAAG
M6118	Site-Direct Mut	S14rev	GAGCAGCCTGCTCTGGGGCCAAGGCCTCGGCTTC
M6119	Site-Direct Mut	S441rev	GGTCCACATCTGGGGCATCTTCCCCCTCATTTC
M6120	Site-Direct Mut	S755rev	GAGTACTTAGAAGAGGTGCAGGCTGAGGCTGTGG
M6121	Site-Direct Mut	S946rev	CACATGCATACTGTGGTGCAGATGCTGAAGGTTCC
M6122	Site-Direct Mut	S1069rev	GAACCTTCCTGGTGGAGCGATGTCATTTTTGGG
M6123	Site-Direct Mut	S1188rev	CCGCCTTATCCTGGGGAGCACCAACCAACTGTTC
M6124	Site-Direct Mut	T258rev	ATTATTCTGGATTGGGGCTCCTGTGAGGAGGAG
M6155	Site-Direct Mut	oligo-3mut-f	GTTTTTCTGCTTACCACTCAGGTGGGAGGAGTGGG ATTGACATTAACTGCAGCA
M6156	Site-Direct Mut	oligo-3mut-r	TGCTGCAGTTAATGTCAATCCCACTCCTCCCACCTG AGTGGTAAGCAGAAAAAC
M6229	cloning	~~PP1A-human Kpn1-f~~	gcg GGTACC ATGTCCGACAGCGAGAAGCTCAACC
M6230	cloning	PP1A-human Xho1-r	gcg CTCGAG CTATTTCTTGGCTTTGGCGGAATTG
M6231	cloning	nest PP1A-f	GGAGGCAGGAGCGGGCCAGG
M6232	cloning	nest PP1A-r	GATTTCTGTACAATCAATCC
M6236	Site-Direct Mut	PP1A-T320A-f	GGAGGCCGACCCATC GCC CCACCCCGCAATTCC
M6237	Site-Direct Mut	PP1A-T320A-r	GGAATTGCGGGGTGGGGCGATGGGTCGGCCTCC
M6256	cloning	~~PPP1R1A-f Kpn1~~	gcg GGTACC ATGGAGCAAGACAACAGCCCCCGAAAG
M6257	cloning	PPP1R1A-r Xho1	gcg CTCGAG TCAGACCGAGTTGGCTCCCTTGGAATC
M6258	cloning	~~PPP1R2A-f Kpn1~~	gcg GGTACC ATGGCGGCCTCGACGGCCTCGCAC
M6259	cloning	PPP1R2A-r Xho1	gcg CTCGAG CTATGAACTTCGTAATTTGTTTTGC
M6294	cloning	PP1A-human Kpn1-f	gcg GGTACC C ATGTCCGACAGCGAGAAGCTCAACC
M6295	cloning	PPP1R1A-f Kpn1	gcg GGTACC C ATGGAGCAAGACAACAGCCCCCGAAAG
M6296	cloning	PPP1R2A-f Kpn1	gcg GGTACC C ATGGCGGCCTCGACGGCCTCGCAC
M6313	Site-Direct Mut	B56delta S566A f	GAGTTCCTAACTGCC gcc CAGGAGGCTCTCTGA
M6314	Site-Direct Mut	B56delta S566A r	TCAGAGAGCCTCCTGGGCGGCAGTTAGGAACTC
M6322	cloning	B56delta-f Kpn1	gcg GGTACC C ATGCCCTATAAACTGAAAAAGGAG
M6323	cloning	B56delta-r Xba1	gcg TCTAGA TCAGAGAGCCTCCTGGCTGGCAGTTAG
M6355	cloning	PP2B-420-480-f (autoinhibitory peptide) Kpn1	gcg GGTACC C GTGCTGACGCTGAAAGGCTTGACC
M6355	cloning	PP2B-420-480-r (autoinhibitory peptide + STOP) Xho1	gcg CTCGAG TCAATTAATTCGGTCTAAGCCCTTG
M6357	cloning	Hec1 Kpn1-f	gcg GGTACC C ATGAAGCGCAGTTCAGTTTCCAGCG
M6358	cloning	Hec1 Xho1-r	gcg CTCGAG TCATTCTTCAGAAGACTTAATTAG
M6364	Site-Direct Mut	PICH RRQVF-AAQAA f	CTGTAGAGGAAAAAATATAC GCA GCA CAG GCT GCC AAGGACTCATTAATAAGACAAAC
M6365	Site-Direct Mut	PICH RRQVF-AAQAA r	GTTTGTCTTATTAATGAGTCCTTGGCAGCCTGTGC TGCGTATATTTTTTCCTCTACAG
M6369	Site-Direct Mut	PICH FLRRTK-ALRATA f	CTTAATGGCAATCATAAAACCCTAT GCT CTC AGG GCG ACT GCA GAAGACGTACAGAAGAAAAAGTCAAG
M6370	Site-Direct Mut	PICH FLRRTK-ALRATA r	CTTGACTTTTTCTTCTGTACGTCTTCTGCAGTCGCC CTGAGAGCATAGGGTTTTATGATTGCCATTAAG
M6371	Site-Direct Mut	PICH RVVIF-AVAIA f	CGGTTTAACATTAACTGCAGCAACT GCA GTG GCC ATT GCT GACCCTAGCTGGAATCCTGCAACTG
M6372	Site-Direct Mut	PICH RVVIF-AVAIA r	CAGTTGCAGGATTCCAGCTAGGGTCAGCAATGGCC ACTGCAGTTGCTGCAGTTAATGTTAAACCG
M6375	Site-Direct Mut	I1-T35E-f	CGGAGGCGCCGCCCC GAG CCTGCCACCCTCGTGC
M6376	Site-Direct Mut	I1-T35E-r	GCACGAGGGTGGCAGGCTCGGGGCGGCGCCTCCG
M6377	Site-Direct Mut	I1-T35D-f	CGGAGGCGCCGCCCC GAC CCTGCCACCCTCGTGC
M6378	Site-Direct Mut	I1-T35D-r	GCACGAGGGTGGCAGGGTCGGGGCGGCGCCTCCG
B1	Site-Direct Mut	PP1gT311A-f	GCCACGAGACCTGTAACCCCTCCAAGGGGTATG
B2	Site-Direct Mut	PP1gT311A-r	CATACCCCTTGGAGGGGTTACAGGTCTCGTGGC
B15	cloning	PP1a-Xho1-f	gcg CTCGAG CT ATGTCCGACAGCGAGAAGCTCAACC
B16	cloning	PP1a-Kpn-r	gcg GGTACC CTATTTCTTGGCTTTGGCGGAATTGC

B17	cloning	PP1b-Xho1-f	gcg CTCGAG CT ATGGCGGACGGGGAGCTGAACGTGG
B18	cloning	PP1b-Kpn-r	gcg GGTACC TCACCTTTTCTTCGGCGGATTAGC
B19	cloning	PP1g-Xho1-f	gcg CTCGAG CT ATGGCGGATTTAGATAAACTCAAC
B20	cloning	PP1g-Kpn-r	gcg GGTACC CTATTTCTTTGCTTGCTTTGTGATC
B21	Site-Direct Mut	PP1aH124A-f	CTGCTCCGTGGGAAC GCC GAGTGTGCCAGCATC
B22	Site-Direct Mut	PP1aH124A-r	GATGCTGGCACACTCGGCGTTCCCACGGAGCAG
B23	Site-Direct Mut	PP1bH124A-f	CTCTTAAGAGGAAAC GCT GAGTGTGCTAGCATC
B24	Site-Direct Mut	PP1bH124A-r	GATGCTAGCACACTCAGCGTTTCCTCTTAAGAG
B25	Site-Direct Mut	PP1gH125A-f	CTTCTCAGAGGGAAC GCT GAATGTGCCAGCATC
B26	Site-Direct Mut	PP1gH125A-r	GATGCTGGCACATTCAGCGTTCCCTCTGAGAAG
B27	cloning	PP1b-Kpn-f	gcg G GAT CC C ATGGCGGACGGGGAGCTGAACGTGG
B28	cloning	PP1b-Xho1-r	gcg CTCGAG TCACCTTTTCTTCGGCGGATTAGCTG
B29	Site-Direct Mut	PP1b-T316A-f	TCTGGACGTCCTGTC GCT CCACCTCGAACAGCT
B30	Site-Direct Mut	PP1b-T316A-r	AGCTGTTCGAGGTGGAGCGACAGGACGTCCAGA
B41	cloning	PP1a-pET28-f Nde1	gcg CATATG ATGTCCGACAGCGAGAAGCTCAACC
B42	cloning	PP1a-pET28-r Xho1 no stop	gcg CTCGAG TTTCTTGGCTTTGGCGGAATTGCGG
B43	cloning	PP1b-pET28-f Nde1	gcg CATATG ATGGCGGACGGGGAGCTGAACGTGG
B44	cloning	PP1b-pET28-r Xho1 no stop	gcg CTCGAG CCTTTTCTTCGGCGGATTAGCTGTTC
B45	cloning	PP1g-pET28-f Nde1	gcg CATATG ATGGCGGATTTAGATAAACTCAAC
B46	cloning	PP1g-pET28-r Xho1 no stop	gcg CTCGAG TTTCTTTGCTTGCTTTGTGATCATAC
B74	sequencing	SA2-1 451down	GAATTCGATGAGGATAGTGGAG
B75	sequencing	SA2-1 900down	GATAGCTGAAATTCGAGCTATTTG
B76	sequencing	SA2-1 1352down	GAGGAAGACAAGGTCCAAATGCC
B77	sequencing	SA2-1 1791down	GGAAATATATACCACTGGACG
B78	sequencing	SA2-1 2241down	GATAACTGAAAGCAGCTCTAC
B79	sequencing	SA2-1 2763down	CAGTCTGCAACAGCTTTTTAATG
B80	sequencing	SA2-1 3233down	CTACAGGAAAACGGAAAGTGG
B97	cloning	PICH Kpn1 rev for peGFP-C1	gcg GGTACC TCAATTGTTATTAAGTTGCTTATAC
B178	cloning	BEND3 for pcDNA3.1 f Kpn1	gcg G GTA CCC ATGAACTCAACTGAATTCACCGAAG
B179	cloning	BEND3 for pcDNA3.1 r Xba1	gcg TCT AGA TCACTTCTCCACTTTCTTTGCTTTC
B182	cloning	Bend3-nes-f	CTGTAGCAGAGAAGTTCCTTG
B183	cloning	Bend3-nes-r	GTATTGCTCAGTCCCAAGGG
B189	sequencing	Bend3-seq1	CACTGACAACGACCCCAACATC
B190	sequencing	Bend3-seq2	CCTCACTGAGTTCCTGGACG
B191	sequencing	Bend3-seq3	CTGTTCCCCGAGCTCTTCAC
B192	sequencing	Bend3-seq4	CGGTGCCTTCTCCCTACCTG

7.3 List of siRNA duplexes

Target gene	Sequence	Source
Gl2	Acc. No. X65324, 153 - 173 relative to the first nucleotide of the start codon	(Elbashir et al., 2001)
Wapl2	AAGGTTAAGTGTTCCTCTTAT	(Kueng et al., 2006)
Wapl1	AACGGACTACCCTTAGCACAA	(Kueng et al., 2006)
PICH (corresponds to PICH-3)	AGUAGGUGGUGUCGGUUUA	(Hübner et al., 2009)
Sgo1	CAGUAGAACCUGCUCAGAA	(McGuinness et al., 2005)
Sgo2	TCGGAAGTGTAATTTCTTATT	Yen T., 2007
5'UTR PICH	AACTGGAACCCAATCCGAGGG	
3'UTR PICH	AACTTCTGCCCTGCAACGCCC	
SA2-3UTR-1	AACTGAAGAAAGTGTAGGATA	
SA2-3UTR-2	AATCTAAGTGGAAGAGGAAAT	
Smc2-1	TGCTATCACTGGCTTAAATTT	Ono T, Cell, 2003
Smc2-2	CATATTGGACTCCATCTGCTT	Ono T, Cell, 2003
Hbo1	AAGAAATGCGCCTTCTTCTGA	Liu X, PNAS, 2008
PHB2-1	GAAUCGUAUCUAUCUCACA	K Fukui, CurrBiol, 2007
PHB2-2	CUGAACCCCUCUUGGAUUAAG	K Fukui, CurrBiol, 2008
BEND3-1	AACCTCAAGAAAGCAAAGAAA	
BEND3-2	AACCGAAGATGTAGAAGAAGT	

7.4 List of antibodies

7.4.1 Immunofluorescence

Goat anti-BLM (Santa Cruz B.)
CREST (Immunovision)
mouse anti-Cyclin B1 (in-house production)
mouse anti-GFP (in-house production)
mouse anti-Hec1 (GeneTex)
mouse anti-Lamin A+B2 (in-house production)
mouse anti-Mad1 (Sigma)
rabbit anti-Mad2 (Bethyl)
mouse anti-myc (9E10, in-house production)
rat anti-PICH (Baumann et al., 2007)
mouse anti-PICH (in-house production)
mouse anti-Plk1 (in-house production)
rabbit anti-Plk1 (Abcam)
mouse anti-Sgo1 (Abnova)
rabbit anti-Sgo2 (Bethyl)
mouse anti-alpha-tubulin (Sigma)
rabbit anit-Rif1 (gift from Dr. Weidong Wang)

7.4.2 Western blotting

mouse anti-Aurora B (AIM1, BD Transduction)
rabbit anti-Cdc27 (BD Biosciecne)
mouse anti-Blinkin (Kiyomitsu et al., 2007)
rabbit anti-Borealin (Klein et al., 2006)
mouse anti-Bub1 (in-house production)
mouse anti-Bub3 (BD Transduction)
mouse anti-BubR1 (in-house production)
mouse anti-Cdc20 (Chemicon)
mouse anti-Cdc27 (BD Transduction)
mouse anti-Cyclin B1 (Upstate)
mouse anti-Flag (Sigma)
mouse anti-GFP (in-house production)
mouse anti-Hec1 (GeneTex)
rabbit anti-histone H3-phospho-serine 10 (Upstate)
mouse anti-Mad1 (Sigma)
rabbit anti-Mad2 (Bethyl)
monoclonal anti-Mps1 (Stucke et al., 2002)
mouse anti-myc (9E10, in-house production)
rabbit anti-PICH (Baumann et al., 2007)
mouse anti-PICH (in-house production)
mouse anti-Plk1 (in-house production)
goat anti-SA2 (Bethyl)
mouse anti-Sgo1 (Abnova)
rabbit anti-Sgo2 (Bethyl)

rabbit anti-SMC1 (Abcam)
rabbit anti-SMC3 (Bethyl)
rabbit anti-Survivin (Biozol)
rabbit anti-Tao1 (Bethyl)
monoclonal anti-alpha-tubulin (DM1A, Sigma)
rabbit anti-Wapl (Abcam)
rabbit-IgG (Invitrogen)
mouse-IgG (Invitrogen)

7.5 Abbreviations

All units are abbreviated according to the International Unit System.

aa: amino acid
AB: antibody (pAB: polyclonal, mAB: monoclonal)
APC/C: anaphase-promoting complex/cyclosome
ATP: adenosine-triphosphate
A.U.: arbitrary units
BEN: BEN domain (after BANP, E5R and NAC1)
BSA: bovine serum albumin
Blinkin: Bub-linking kinetochore protein
BLM: Bloom syndrome helicase
Bub: budding inhinhibited by benzimidazole
BTR/BTB: the BTR complex (composed of BLM, TOP3A, RMI1)
CAK: Cdk activating kinase
Cdc: cell division cycle
Cdk: cyclin-dependent kinase
CENP: centromeric protein
CIP: calf intestine phosphatase
CKI: Cyclin-dependen kinase inhibitor
CREST: Calcinosis cutis, Raynaud-Syndrom, Esophageale Dysfunktion, Sklerodaktylie, Teleangiektasia
CPC: chromosomal passenger complex
C-terminus: carboxy-terminus
DAPI: 4´,6-diamidino-2-phenylindole
DIC: differential interference contrast microscopy
DMSO: dimethyl sulfoxide
DNA/dsDNA: deoxyribonucleic acid (double stranded DNA)
DSB: double-strand break
EMSA: electrophoretic mobility shift assay
FA: Fanconi anemia
FACS: fluorescent activated cell sorting
FBS: fetal bovine serum
GFP: green fluorescent protein
GST: glutathione S-transferase
hrs: hour(s)
Hec1: highly expressed in cancer protein 1
H2B: histone H2B
HJ: Holiday Junction

ICL: intra/inter-strand crosslink
IgG: immunoglobulin G
INCENP: inner centromere protein
INO80: inositol requiring 80
IPTG: isopropyl-beta-D-thiogalactopyranoside
kDa: kilodalton
KT: kinetochore
Mad: mitotic arrest deficient
MAP: mitogen-activated protein
MARKK: microtubule affinity-regulation kinase kinase
MBP: maltose binding protein
MCAK: mitotic centromere-associated kinesin
MCC: mitotic checkpoint complex
MCS: multiple cloning site
min: minute(s)
MMS: methyl methan sulfonate
MMC: mitomycin-c
Mps1: multipolar spindle-1
mRNA: messenger ribonucleic acid
MT: microtubule
MTOC: microtubule organizing center
NEBD: nuclear envelope breakdown
NLS: nuclear localization signal
N-terminus: amino-terminus
PBD: polo-box binding domain
PBS: phosphate-buffered saline
PCR: polymerase chain reaction
PFD: PICH family domain
PICH: Plk1-interacting checkpoint helicase
Plk: polo-like kinase
Rif1: RAP1-interacting factor
qRT-PCR: quantitative real-time polymerase chain reaction
RNA/siRNA: ribonucleic acid (small interfering RNA)
RNAi: RNA interference
rpm: rounds per minute
SAC: spindle assembly checkpoint
SDS-PAGE: sodium dodecylsulfate polyacrylamid gelelectrophoresis
SF: superfamily
shRNA: short hairpin ribonucleic acid
siRNA: small interference ribonucleic acid
SNF: sucrose non-fermeting
ssDNA: single stranded deoxyribonucleic acid
SWI: mating-type switching
TAL: ZK-Thiazolidinone
Tao1: Thousand and one amino acid protein 1, also known as MARKK
TOP3A: topoisomerase 3 alpha
TPR: tetratrichopeptide repeats
UFB: ultra-fine DNA-bridge
UTR: untranslated region
WT: wildtype

8. REFERENCES

Abdel-Monem, M., H. Durwald, and H. Hoffmann-Berling. 1976. Enzymic unwinding of DNA. 2. Chain separation by an ATP-dependent DNA unwinding enzyme. *Eur J Biochem*. 65:441-449.

Abdel-Monem, M., and H. Hoffmann-Berling. 1976. Enzymic unwinding of DNA. 1. Purification and characterization of a DNA-dependent ATPase from Escherichia coli. *Eur J Biochem*. 65:431-440.

Abhiman, S., L.M. Iyer, and L. Aravind. 2008. BEN: a novel domain in chromatin factors and DNA viral proteins. *Bioinformatics*. 24:458-461.

Abrieu, A., L. Magnaghi-Jaulin, J.A. Kahana, M. Peter, A. Castro, S. Vigneron, T. Lorca, D.W. Cleveland, and J.C. Labbe. 2001. Mps1 is a kinetochore-associated kinase essential for the vertebrate mitotic checkpoint. *Cell*. 106:83-93.

Ahonen, L.J., M.J. Kallio, J.R. Daum, M. Bolton, I.A. Manke, M.B. Yaffe, P.T. Stukenberg, and G.J. Gorbsky. 2005. Polo-like kinase 1 creates the tension-sensing 3F3/2 phosphoepitope and modulates the association of spindle-checkpoint proteins at kinetochores. *Curr Biol*. 15:1078-1089.

Andrews, P.D., Y. Ovechkina, N. Morrice, M. Wagenbach, K. Duncan, L. Wordeman, and J.R. Swedlow. 2004. Aurora B regulates MCAK at the mitotic centromere. *Dev Cell*. 6:253-268.

Archambault, V., and D.M. Glover. 2009. Polo-like kinases: conservation and divergence in their functions and regulation. *Nat Rev Mol Cell Biol*. 10:265-275.

Awad, S., D. Ryan, P. Prochasson, T. Owen-Hughes, and A.H. Hassan. 2010. The Snf2-homolog Fun30 acts as a homodimeric ATP-dependent chromatin-remodeling enzyme. *J Biol Chem*.

Bardwell, V.J., and R. Treisman. 1994. The POZ domain: a conserved protein-protein interaction motif. *Genes Dev*. 8:1664-1677.

Barr, F.A., H.H. Sillje, and E.A. Nigg. 2004. Polo-like kinases and the orchestration of cell division. *Nat Rev Mol Cell Biol*. 5:429-440.

Baumann, C., R. Korner, K. Hofmann, and E.A. Nigg. 2007. PICH, a centromere-associated SNF2 family ATPase, is regulated by Plk1 and required for the spindle checkpoint. *Cell*. 128:101-114.

Becker, P.B., and W. Horz. 2002. ATP-dependent nucleosome remodeling. *Annu Rev Biochem*. 71:247-273.

Beerens, N., J.H. Hoeijmakers, R. Kanaar, W. Vermeulen, and C. Wyman. 2005. The CSB protein actively wraps DNA. *J Biol Chem*. 280:4722-4729.

Bharadwaj, R., and H. Yu. 2004. The spindle checkpoint, aneuploidy, and cancer. *Oncogene*. 23:2016-2027.

Biggins, S., and A.W. Murray. 2001. The budding yeast protein kinase Ipl1/Aurora allows the absence of tension to activate the spindle checkpoint. *Genes Dev*. 15:3118-3129.

Birot, A., L. Duret, L. Bartholin, B. Santalucia, I. Tigaud, J. Magaud, and J. Rouault. 2000. Identification and molecular analysis of BANP. *Gene*. 253:189-196.

Blangy, A., H.A. Lane, P. d'Herin, M. Harper, M. Kress, and E.A. Nigg. 1995. Phosphorylation by p34cdc2 regulates spindle association of human Eg5, a kinesin-related motor essential for bipolar spindle formation in vivo. *Cell*. 83:1159-1169.

Boehmer, P.E., M.S. Dodson, and I.R. Lehman. 1993. The herpes simplex virus type-1 origin binding protein. DNA helicase activity. *J Biol Chem*. 268:1220-1225.

Brennan, I.M., U. Peters, T.M. Kapoor, and A.F. Straight. 2007. Polo-like kinase controls vertebrate spindle elongation and cytokinesis. *PLoS One*. 2:e409.

Buonomo, S.B., Y. Wu, D. Ferguson, and T. de Lange. 2009. Mammalian Rif1 contributes to replication stress survival and homology-directed repair. *J Cell Biol*. 187:385-398.

Burkard, M.E., C.L. Randall, S. Larochelle, C. Zhang, K.M. Shokat, R.P. Fisher, and P.V. Jallepalli. 2007. Chemical genetics reveals the requirement for Polo-like kinase 1 activity in positioning RhoA and triggering cytokinesis in human cells. *Proc Natl Acad Sci U S A*. 104:4383-4388.

Carlson, M., and B.C. Laurent. 1994. The SNF/SWI family of global transcriptional activators. *Curr Opin Cell Biol*. 6:396-402.

Carmena, M., M.G. Riparbelli, G. Minestrini, A.M. Tavares, R. Adams, G. Callaini, and D.M. Glover. 1998. Drosophila polo kinase is required for cytokinesis. *J Cell Biol*. 143:659-671.

Chan, K.L., P.S. North, and I.D. Hickson. 2007. BLM is required for faithful chromosome segregation and its localization defines a class of ultrafine anaphase bridges. *EMBO J*. 26:3397-3409.

Chan, K.L., T. Palmai-Pallag, S. Ying, and I.D. Hickson. 2009a. Replication stress induces sister-chromatid bridging at fragile site loci in mitosis. *Nat Cell Biol*. 11:753-760.

Chan, Y.W., L.L. Fava, A. Uldschmid, M.H. Schmitz, D.W. Gerlich, E.A. Nigg, and A. Santamaria. 2009b. Mitotic control of kinetochore-associated dynein and spindle orientation by human Spindly. *J Cell Biol*. 185:859-874.

Chen, R.H., J.C. Waters, E.D. Salmon, and A.W. Murray. 1996. Association of spindle assembly checkpoint component XMAD2 with unattached kinetochores. *Science*. 274:242-246.

Cleveland, D.W., Y. Mao, and K.F. Sullivan. 2003. Centromeres and kinetochores: from epigenetics to mitotic checkpoint signaling. *Cell*. 112:407-421.

Cote, J., J. Quinn, J.L. Workman, and C.L. Peterson. 1994. Stimulation of GAL4 derivative binding to nucleosomal DNA by the yeast SWI/SNF complex. *Science*. 265:53-60.

D'Avino, P.P., V. Archambault, M.R. Przewloka, W. Zhang, K.S. Lilley, E. Laue, and D.M. Glover. 2007. Recruitment of Polo kinase to the spindle midzone during cytokinesis requires the Feo/Klp3A complex. *PLoS One*. 2:e572.

Ditchfield, C., V.L. Johnson, A. Tighe, R. Ellston, C. Haworth, T. Johnson, A. Mortlock, N. Keen, and S.S. Taylor. 2003. Aurora B couples chromosome alignment with anaphase by targeting BubR1, Mad2, and Cenp-E to kinetochores. *J Cell Biol*. 161:267-280.

Doree, M., and T. Hunt. 2002. From Cdc2 to Cdk1: when did the cell cycle kinase join its cyclin partner? *J Cell Sci*. 115:2461-2464.

Durr, H., A. Flaus, T. Owen-Hughes, and K.P. Hopfner. 2006. Snf2 family ATPases and DExx box helicases: differences and unifying concepts from high-resolution crystal structures. *Nucleic Acids Res*. 34:4160-4167.

Eisen, J.A., K.S. Sweder, and P.C. Hanawalt. 1995. Evolution of the SNF2 family of proteins: subfamilies with distinct sequences and functions. *Nucleic Acids Res*. 23:2715-2723.

Elbashir, S.M., J. Harborth, W. Lendeckel, A. Yalcin, K. Weber, and T. Tuschl. 2001. Duplexes of 21-nucleotide RNAs mediate RNA interference in cultured mammalian cells. *Nature*. 411:494-498.

Elia, A.E., L.C. Cantley, and M.B. Yaffe. 2003a. Proteomic screen finds pSer/pThr-binding domain localizing Plk1 to mitotic substrates. *Science*. 299:1228-1231.

Elia, A.E., P. Rellos, L.F. Haire, J.W. Chao, F.J. Ivins, K. Hoepker, D. Mohammad, L.C. Cantley, S.J. Smerdon, and M.B. Yaffe. 2003b. The molecular basis for phosphodependent substrate targeting and regulation of Plks by the Polo-box domain. *Cell*. 115:83-95.

Elowe, S., S. Hummer, A. Uldschmid, X. Li, and E.A. Nigg. 2007. Tension-sensitive Plk1 phosphorylation on BubR1 regulates the stability of kinetochore microtubule interactions. *Genes Dev*. 21:2205-2219.

Fabbro, M., B.B. Zhou, M. Takahashi, B. Sarcevic, P. Lal, M.E. Graham, B.G. Gabrielli, P.J. Robinson, E.A. Nigg, Y. Ono, and K.K. Khanna. 2005. Cdk1/Erk2- and Plk1-dependent phosphorylation of a centrosome protein, Cep55, is required for its recruitment to midbody and cytokinesis. *Dev Cell*. 9:477-488.

Ferrari, S. 2006. Protein kinases controlling the onset of mitosis. *Cell Mol Life Sci*. 63:781-795.

Flaus, A., D.M. Martin, G.J. Barton, and T. Owen-Hughes. 2006. Identification of multiple distinct Snf2 subfamilies with conserved structural motifs. *Nucleic Acids Res*. 34:2887-2905.

Gandhi, R., P.J. Gillespie, and T. Hirano. 2006. Human Wapl is a cohesin-binding protein that promotes sister-chromatid resolution in mitotic prophase. *Curr Biol*. 16:2406-2417.

German, J. 1993. Bloom syndrome: a mendelian prototype of somatic mutational disease. *Medicine (Baltimore)*. 72:393-406.

Giet, R., C. Petretti, and C. Prigent. 2005. Aurora kinases, aneuploidy and cancer, a coincidence or a real link? *Trends Cell Biol*. 15:241-250.

Gimenez-Abian, J.F., I. Sumara, T. Hirota, S. Hauf, D. Gerlich, C. de la Torre, J. Ellenberg, and J.M. Peters. 2004. Regulation of sister chromatid cohesion between chromosome arms. *Curr Biol*. 14:1187-1193.

Glover, D.M., I.M. Hagan, and A.A. Tavares. 1998. Polo-like kinases: a team that plays throughout mitosis. *Genes Dev*. 12:3777-3787.

Gorbalenya, A.E., and E.V. Koonin. 1988. One more conserved sequence motif in helicases. *Nucleic Acids Res*. 16:7734.

Gorbalenya, A.E., and E.V. Koonin. 1993. Helicases: amino acid sequence comparisons and structure-function relationships. *Current Opinion in Structural Biology*. 3:419-429.

Gorbalenya, A.E., E.V. Koonin, A.P. Donchenko, and V.M. Blinov. 1988a. A conserved NTP-motif in putative helicases. *Nature*. 333:22.

Gorbalenya, A.E., E.V. Koonin, A.P. Donchenko, and V.M. Blinov. 1988b. A novel superfamily of nucleoside triphosphate-binding motif containing proteins which are probably involved in duplex unwinding in DNA and RNA replication and recombination. *FEBS Lett*. 235:16-24.

Goto, H., T. Kiyono, Y. Tomono, A. Kawajiri, T. Urano, K. Furukawa, E.A. Nigg, and M. Inagaki. 2006. Complex formation of Plk1 and INCENP required for metaphase-anaphase transition. *Nat Cell Biol*. 8:180-187.

Hagting, A., N. Den Elzen, H.C. Vodermaier, I.C. Waizenegger, J.M. Peters, and J. Pines. 2002. Human securin proteolysis is controlled by the spindle checkpoint and reveals when the APC/C switches from activation by Cdc20 to Cdh1. *J Cell Biol*. 157:1125-1137.

Hanisch, A., A. Wehner, E.A. Nigg, and H.H. Sillje. 2006. Different Plk1 functions show distinct dependencies on Polo-Box domain-mediated targeting. *Mol Biol Cell*. 17:448-459.

Hardwick, K.G., R.C. Johnston, D.L. Smith, and A.W. Murray. 2000. MAD3 encodes a novel component of the spindle checkpoint which interacts with Bub3p, Cdc20p, and Mad2p. *J Cell Biol*. 148:871-882.

Hardy, C.F., L. Sussel, and D. Shore. 1992. A RAP1-interacting protein involved in transcriptional silencing and telomere length regulation. *Genes Dev*. 6:801-814.

Hartwell, L.H., and D. Smith. 1985. Altered fidelity of mitotic chromosome transmission in cell cycle mutants of S. cerevisiae. *Genetics*. 110:381-395.

Hauf, S., R.W. Cole, S. LaTerra, C. Zimmer, G. Schnapp, R. Walter, A. Heckel, J. van Meel, C.L. Rieder, and J.M. Peters. 2003. The small molecule Hesperadin reveals a role for Aurora B in correcting kinetochore-microtubule attachment and in maintaining the spindle assembly checkpoint. *J Cell Biol*. 161:281-294.

Hauf, S., E. Roitinger, B. Koch, C.M. Dittrich, K. Mechtler, and J.M. Peters. 2005. Dissociation of cohesin from chromosome arms and loss of arm cohesion during early mitosis depends on phosphorylation of SA2. *PLoS Biol*. 3:e69.

Hauf, S., I.C. Waizenegger, and J.M. Peters. 2001. Cohesin cleavage by separase required for anaphase and cytokinesis in human cells. *Science*. 293:1320-1323.

Havas, K., I. Whitehouse, and T. Owen-Hughes. 2001. ATP-dependent chromatin remodeling activities. *Cell Mol Life Sci*. 58:673-682.

Herzog, F., I. Primorac, P. Dube, P. Lenart, B. Sander, K. Mechtler, H. Stark, and J.M. Peters. 2009. Structure of the anaphase-promoting complex/cyclosome interacting with a mitotic checkpoint complex. *Science*. 323:1477-1481.

Hoffelder, D.R., L. Luo, N.A. Burke, S.C. Watkins, S.M. Gollin, and W.S. Saunders. 2004. Resolution of anaphase bridges in cancer cells. *Chromosoma*. 112:389-397.

Hoffmann, I., P.R. Clarke, M.J. Marcote, E. Karsenti, and G. Draetta. 1993. Phosphorylation and activation of human cdc25-C by cdc2--cyclin B and its involvement in the self-amplification of MPF at mitosis. *EMBO J*. 12:53-63.

Howell, B.J., B.F. McEwen, J.C. Canman, D.B. Hoffman, E.M. Farrar, C.L. Rieder, and E.D. Salmon. 2001. Cytoplasmic dynein/dynactin drives kinetochore protein transport to the

spindle poles and has a role in mitotic spindle checkpoint inactivation. *J Cell Biol*. 155:1159-1172.

Hoyt, M.A., L. Totis, and B.T. Roberts. 1991. S. cerevisiae genes required for cell cycle arrest in response to loss of microtubule function. *Cell*. 66:507-517.

Huang, H., J. Feng, J. Famulski, J.B. Rattner, S.T. Liu, G.D. Kao, R. Muschel, G.K. Chan, and T.J. Yen. 2007. Tripin/hSgo2 recruits MCAK to the inner centromere to correct defective kinetochore attachments. *J Cell Biol*. 177:413-424.

Hübner, N.C., L.H. Wang, M. Kaulich, P. Descombes, I. Poser, and E.A. Nigg. 2009. Re-examination of siRNA specificity questions role of PICH and Tao1 in the spindle checkpoint and identifies Mad2 as a sensitive target for small RNAs. *Chromosoma*.

Hutchins, J.R., Y. Toyoda, B. Hegemann, I. Poser, J.K. Heriche, M.M. Sykora, M. Augsburg, O. Hudecz, B.A. Buschhorn, J. Bulkescher, C. Conrad, D. Comartin, A. Schleiffer, M. Sarov, A. Pozniakovsky, M.M. Slabicki, S. Schloissnig, I. Steinmacher, M. Leuschner, A. Ssykor, S. Lawo, L. Pelletier, H. Stark, K. Nasmyth, J. Ellenberg, R. Durbin, F. Buchholz, K. Mechtler, A.A. Hyman, and J.M. Peters. 2010. Systematic analysis of human protein complexes identifies chromosome segregation proteins. *Science*. 328:593-599.

Ito, T., M. Bulger, M.J. Pazin, R. Kobayashi, and J.T. Kadonaga. 1997. ACF, an ISWI-containing and ATP-utilizing chromatin assembly and remodeling factor. *Cell*. 90:145-155.

Izumi, T., and J.L. Maller. 1993. Elimination of cdc2 phosphorylation sites in the cdc25 phosphatase blocks initiation of M-phase. *Mol Biol Cell*. 4:1337-1350.

Jang, Y.J., C.Y. Lin, S. Ma, and R.L. Erikson. 2002. Functional studies on the role of the C-terminal domain of mammalian polo-like kinase. *Proc Natl Acad Sci U S A*. 99:1984-1989.

Kang, Y.H., J.E. Park, L.R. Yu, N.K. Soung, S.M. Yun, J.K. Bang, Y.S. Seong, H. Yu, S. Garfield, T.D. Veenstra, and K.S. Lee. 2006. Self-regulated Plk1 recruitment to kinetochores by the Plk1-PBIP1 interaction is critical for proper chromosome segregation. *Mol Cell*. 24:409-422.

Kaul, R., S. Mukherjee, F. Ahmed, M.K. Bhat, R. Chhipa, S. Galande, and S. Chattopadhyay. 2003. Direct interaction with and activation of p53 by SMAR1 retards cell-cycle progression at G2/M phase and delays tumor growth in mice. *Int J Cancer*. 103:606-615.

Kimura, K., M. Hirano, R. Kobayashi, and T. Hirano. 1998. Phosphorylation and activation of 13S condensin by Cdc2 in vitro. *Science*. 282:487-490.

Kirkegaard, K., and J.C. Wang. 1985. Bacterial DNA topoisomerase I can relax positively supercoiled DNA containing a single-stranded loop. *J Mol Biol*. 185:625-637.

Kitajima, T.S., S.A. Kawashima, and Y. Watanabe. 2004. The conserved kinetochore protein shugoshin protects centromeric cohesion during meiosis. *Nature*. 427:510-517.

Kitajima, T.S., T. Sakuno, K. Ishiguro, S. Iemura, T. Natsume, S.A. Kawashima, and Y. Watanabe. 2006. Shugoshin collaborates with protein phosphatase 2A to protect cohesin. *Nature*. 441:46-52.

Knipscheer, P., M. Raschle, A. Smogorzewska, M. Enoiu, T.V. Ho, O.D. Scharer, S.J. Elledge, and J.C. Walter. 2009. The Fanconi anemia pathway promotes replication-dependent DNA interstrand cross-link repair. *Science*. 326:1698-1701.

Krek, W., and E.A. Nigg. 1991. Differential phosphorylation of vertebrate p34cdc2 kinase at the G1/S and G2/M transitions of the cell cycle: identification of major phosphorylation sites. *EMBO J*. 10:305-316.

Kueng, S., B. Hegemann, B.H. Peters, J.J. Lipp, A. Schleiffer, K. Mechtler, and J.M. Peters. 2006. Wapl controls the dynamic association of cohesin with chromatin. *Cell*. 127:955-967.

Kumagai, A., and W.G. Dunphy. 1996. Purification and molecular cloning of Plx1, a Cdc25-regulatory kinase from Xenopus egg extracts. *Science*. 273:1377-1380.

Kurasawa, Y., and L.Y. Yu-Lee. 2010. PICH and Co-targeted Plk1 Coordinately Maintain Prometaphase Chromosome Arm Architecture. *Mol Biol Cell*.

Lamb, J.R., S. Tugendreich, and P. Hieter. 1995. Tetratrico peptide repeat interactions: to TPR or not to TPR? *Trends Biochem Sci*. 20:257-259.

Lane, H.A., and E.A. Nigg. 1996. Antibody microinjection reveals an essential role for human polo-like kinase 1 (Plk1) in the functional maturation of mitotic centrosomes. *J Cell Biol*. 135:1701-1713.

Leng, M., D. Bessuso, S.Y. Jung, Y. Wang, and J. Qin. 2008. Targeting Plk1 to chromosome arms and regulating chromosome compaction by the PICH ATPase. *Cell Cycle*. 7:1480-1489.

Leung, G.C., J.W. Hudson, A. Kozarova, A. Davidson, J.W. Dennis, and F. Sicheri. 2002. The Sak polo-box comprises a structural domain sufficient for mitotic subcellular localization. *Nat Struct Biol*. 9:719-724.

Li, R., and A.W. Murray. 1991. Feedback control of mitosis in budding yeast. *Cell*. 66:519-531.

Lia, G., E. Praly, H. Ferreira, C. Stockdale, Y.C. Tse-Dinh, D. Dunlap, V. Croquette, D. Bensimon, and T. Owen-Hughes. 2006. Direct observation of DNA distortion by the RSC complex. *Mol Cell*. 21:417-425.

Liu, R., H. Liu, X. Chen, M. Kirby, P.O. Brown, and K. Zhao. 2001. Regulation of CSF1 promoter by the SWI/SNF-like BAF complex. *Cell*. 106:309-318.

Lowery, D.M., D. Lim, and M.B. Yaffe. 2005. Structure and function of Polo-like kinases. *Oncogene*. 24:248-259.

Macurek, L., A. Lindqvist, D. Lim, M.A. Lampson, R. Klompmaker, R. Freire, C. Clouin, S.S. Taylor, M.B. Yaffe, and R.H. Medema. 2008. Polo-like kinase-1 is activated by aurora A to promote checkpoint recovery. *Nature*. 455:119-123.

Maiato, H., J. DeLuca, E.D. Salmon, and W.C. Earnshaw. 2004. The dynamic kinetochore-microtubule interface. *J Cell Sci*. 117:5461-5477.

Mapelli, M., L. Massimiliano, S. Santaguida, and A. Musacchio. 2007. The Mad2 conformational dimer: structure and implications for the spindle assembly checkpoint. *Cell*. 131:730-743.

McGuinness, B.E., T. Hirota, N.R. Kudo, J.M. Peters, and K. Nasmyth. 2005. Shugoshin prevents dissociation of cohesin from centromeres during mitosis in vertebrate cells. *PLoS Biol*. 3:e86.

Meetei, A.R., S. Sechi, M. Wallisch, D. Yang, M.K. Young, H. Joenje, M.E. Hoatlin, and W. Wang. 2003. A multiprotein nuclear complex connects Fanconi anemia and Bloom syndrome. *Mol Cell Biol*. 23:3417-3426.

Monahan, B.J., J. Villen, S. Marguerat, J. Bahler, S.P. Gygi, and F. Winston. 2008. Fission yeast SWI/SNF and RSC complexes show compositional and functional differences from budding yeast. *Nat Struct Mol Biol*. 15:873-880.

Morgan, D.O. 2007. The cell cycle : principles of control. New Science Press ; Sinauer Associates, London Sunderland, MA. xxvii, 297 p. pp.

Morrow, C.J., A. Tighe, V.L. Johnson, M.I. Scott, C. Ditchfield, and S.S. Taylor. 2005. Bub1 and aurora B cooperate to maintain BubR1-mediated inhibition of APC/CCdc20. *J Cell Sci*. 118:3639-3652.

Mundt, K.E., R.M. Golsteyn, H.A. Lane, and E.A. Nigg. 1997. On the regulation and function of human polo-like kinase 1 (PLK1): effects of overexpression on cell cycle progression. *Biochem Biophys Res Commun*. 239:377-385.

Musacchio, A., and K.G. Hardwick. 2002. The spindle checkpoint: structural insights into dynamic signalling. *Nat Rev Mol Cell Biol*. 3:731-741.

Musacchio, A., and E.D. Salmon. 2007. The spindle-assembly checkpoint in space and time. *Nat Rev Mol Cell Biol*. 8:379-393.

Naim, V., and F. Rosselli. 2009a. The FANC pathway and BLM collaborate during mitosis to prevent micro-nucleation and chromosome abnormalities. *Nat Cell Biol*. 11:761-768.

Naim, V., and F. Rosselli. 2009b. The FANC pathway and mitosis: a replication legacy. *Cell Cycle*. 8:2907-2911.

Nakagawa, T., M. Bulger, M. Muramatsu, and T. Ito. 2001. Multistep chromatin assembly on supercoiled plasmid DNA by nucleosome assembly protein-1 and ATP-utilizing chromatin assembly and remodeling factor. *J Biol Chem*. 276:27384-27391.

Nasmyth, K., and D. Shore. 1987. Transcriptional regulation in the yeast life cycle. *Science*. 237:1162-1170.

Neef, R., U. Gruneberg, R. Kopajtich, X. Li, E.A. Nigg, H. Sillje, and F.A. Barr. 2007. Choice of Plk1 docking partners during mitosis and cytokinesis is controlled by the activation state of Cdk1. *Nat Cell Biol*. 9:436-444.

Neef, R., C. Preisinger, J. Sutcliffe, R. Kopajtich, E.A. Nigg, T.U. Mayer, and F.A. Barr. 2003. Phosphorylation of mitotic kinesin-like protein 2 by polo-like kinase 1 is required for cytokinesis. *J Cell Biol*. 162:863-875.

Neigeborn, L., and M. Carlson. 1987. Mutations causing constitutive invertase synthesis in yeast: genetic interactions with snf mutations. *Genetics*. 115:247-253.

Nicklas, R.B., S.C. Ward, and G.J. Gorbsky. 1995. Kinetochore chemistry is sensitive to tension and may link mitotic forces to a cell cycle checkpoint. *J Cell Biol*. 130:929-939.

Nicklas, R.B., J.C. Waters, E.D. Salmon, and S.C. Ward. 2001. Checkpoint signals in grasshopper meiosis are sensitive to microtubule attachment, but tension is still essential. *J Cell Sci*. 114:4173-4183.

Nigg, E.A. 2001. Mitotic kinases as regulators of cell division and its checkpoints. *Nat Rev Mol Cell Biol*. 2:21-32.

Nilsson, J., M. Yekezare, J. Minshull, and J. Pines. 2008. The APC/C maintains the spindle assembly checkpoint by targeting Cdc20 for destruction. *Nat Cell Biol*. 10:1411-1420.

Nurse, P. 1990. Universal control mechanism regulating onset of M-phase. *Nature*. 344:503-508.

Nurse, P., and P. Thuriaux. 1980. Regulatory genes controlling mitosis in the fission yeast Schizosaccharomyces pombe. *Genetics*. 96:627-637.

Obaya, A.J., and J.M. Sedivy. 2002. Regulation of cyclin-Cdk activity in mammalian cells. *Cell Mol Life Sci*. 59:126-142.

Ohta, S., J.-C. Bukowski-Wills, L. Sanchez-Pulido, F.d.L. Alves, L. Wood, Z.A. Chen, M. Platani, L. Fischer, D.F. Hudson, C.P. Ponting, T. Fukagawa, W.C. Earnshaw, and J. Rappsilber. 2010. The Protein Composition of Mitotic Chromosomes Determined Using Multiclassifier Combinatorial Proteomics. *Cell*. 142:810-821.

Payne, M., and I.D. Hickson. 2009. Genomic instability and cancer: lessons from analysis of Bloom's syndrome. *Biochem Soc Trans*. 37:553-559.

Peter, M., E. Heitlinger, M. Haner, U. Aebi, and E.A. Nigg. 1991. Disassembly of in vitro formed lamin head-to-tail polymers by CDC2 kinase. *EMBO J*. 10:1535-1544.

Peters, J.M. 2002. The anaphase-promoting complex: proteolysis in mitosis and beyond. *Mol Cell*. 9:931-943.

Peters, J.M. 2006. The anaphase promoting complex/cyclosome: a machine designed to destroy. *Nat Rev Mol Cell Biol*. 7:644-656.

Petronczki, M., M. Glotzer, N. Kraut, and J.M. Peters. 2007. Polo-like kinase 1 triggers the initiation of cytokinesis in human cells by promoting recruitment of the RhoGEF Ect2 to the central spindle. *Dev Cell*. 12:713-725.

Petronczki, M., P. Lenart, and J.M. Peters. 2008. Polo on the Rise-from Mitotic Entry to Cytokinesis with Plk1. *Dev Cell*. 14:646-659.

Pfaffle, P., and V. Jackson. 1990. Studies on rates of nucleosome formation with DNA under stress. *J Biol Chem*. 265:16821-16829.

Pichierri, P., A. Franchitto, and F. Rosselli. 2004. BLM and the FANC proteins collaborate in a common pathway in response to stalled replication forks. *EMBO J*. 23:3154-3163.

Pines, J. 2006. Mitosis: a matter of getting rid of the right protein at the right time. *Trends Cell Biol*. 16:55-63.

Pinsky, B.A., and S. Biggins. 2005. The spindle checkpoint: tension versus attachment. *Trends Cell Biol*. 15:486-493.

Qi, W., Z. Tang, and H. Yu. 2006. Phosphorylation- and polo-box-dependent binding of Plk1 to Bub1 is required for the kinetochore localization of Plk1. *Mol Biol Cell*. 17:3705-3716.

Rauh, N.R., A. Schmidt, J. Bormann, E.A. Nigg, and T.U. Mayer. 2005. Calcium triggers exit from meiosis II by targeting the APC/C inhibitor XErp1 for degradation. *Nature*. 437:1048-1052.

Reynolds, N., and H. Ohkura. 2003. Polo boxes form a single functional domain that mediates interactions with multiple proteins in fission yeast polo kinase. *J Cell Sci*. 116:1377-1387.

Rieder, C.L., R.W. Cole, A. Khodjakov, and G. Sluder. 1995. The checkpoint delaying anaphase in response to chromosome monoorientation is mediated by an inhibitory signal produced by unattached kinetochores. *J Cell Biol*. 130:941-948.

Rieder, C.L., A. Schultz, R. Cole, and G. Sluder. 1994. Anaphase onset in vertebrate somatic cells is controlled by a checkpoint that monitors sister kinetochore attachment to the spindle. *J Cell Biol*. 127:1301-1310.

Rosin, M.P., and J. German. 1985. Evidence for chromosome instability in vivo in Bloom syndrome: increased numbers of micronuclei in exfoliated cells. *Hum Genet*. 71:187-191.

Rudolph, B., R. Saffrich, J. Zwicker, B. Henglein, R. Muller, W. Ansorge, and M. Eilers. 1996. Activation of cyclin-dependent kinases by Myc mediates induction of cyclin A, but not apoptosis. *EMBO J*. 15:3065-3076.

Russell, P., and P. Nurse. 1986. cdc25+ functions as an inducer in the mitotic control of fission yeast. *Cell*. 45:145-153.

Russell, P., and P. Nurse. 1987. Negative regulation of mitosis by wee1+, a gene encoding a protein kinase homolog. *Cell*. 49:559-567.

Saha, A., J. Wittmeyer, and B.R. Cairns. 2002. Chromatin remodeling by RSC involves ATP-dependent DNA translocation. *Genes Dev*. 16:2120-2134.

Santamaria, A., R. Neef, U. Eberspacher, K. Eis, M. Husemann, D. Mumberg, S. Prechtl, V. Schulze, G. Siemeister, L. Wortmann, F.A. Barr, and E.A. Nigg. 2007. Use of the novel Plk1 inhibitor ZK-thiazolidinone to elucidate functions of Plk1 in early and late stages of mitosis. *Mol Biol Cell*. 18:4024-4036.

Sczaniecka, M.M., and K.G. Hardwick. 2008. The spindle checkpoint: how do cells delay anaphase onset? *SEB Exp Biol Ser*. 59:243-256.

Seki, A., J.A. Coppinger, C.Y. Jang, J.R. Yates, and G. Fang. 2008. Bora and the kinase Aurora a cooperatively activate the kinase Plk1 and control mitotic entry. *Science*. 320:1655-1658.

Shen, X., G. Mizuguchi, A. Hamiche, and C. Wu. 2000. A chromatin remodelling complex involved in transcription and DNA processing. *Nature*. 406:541-544.

Sillje, H.H., S. Nagel, R. Korner, and E.A. Nigg. 2006. HURP is a Ran-importin beta-regulated protein that stabilizes kinetochore microtubules in the vicinity of chromosomes. *Curr Biol*. 16:731-742.

Silverman, J., H. Takai, S.B. Buonomo, F. Eisenhaber, and T. de Lange. 2004. Human Rif1, ortholog of a yeast telomeric protein, is regulated by ATM and 53BP1 and functions in the S-phase checkpoint. *Genes Dev*. 18:2108-2119.

Steigemann, P., C. Wurzenberger, M.H. Schmitz, M. Held, J. Guizetti, S. Maar, and D.W. Gerlich. 2009. Aurora B-mediated abscission checkpoint protects against tetraploidization. *Cell*. 136:473-484.

Stern, B.M., and A.W. Murray. 2001. Lack of tension at kinetochores activates the spindle checkpoint in budding yeast. *Curr Biol*. 11:1462-1467.

Stern, M., R. Jensen, and I. Herskowitz. 1984. Five SWI genes are required for expression of the HO gene in yeast. *J Mol Biol*. 178:853-868.

Strausfeld, U., A. Fernandez, J.P. Capony, F. Girard, N. Lautredou, J. Derancourt, J.C. Labbe, and N.J. Lamb. 1994. Activation of p34cdc2 protein kinase by microinjection of human cdc25C into mammalian cells. Requirement for prior phosphorylation of cdc25C by p34cdc2 on sites phosphorylated at mitosis. *J Biol Chem*. 269:5989-6000.

Strebhardt, K., and A. Ullrich. 2006. Targeting polo-like kinase 1 for cancer therapy. *Nat Rev Cancer*. 6:321-330.

Stucke, V.M., H.H. Sillje, L. Arnaud, and E.A. Nigg. 2002. Human Mps1 kinase is required for the spindle assembly checkpoint but not for centrosome duplication. *EMBO J*. 21:1723-1732.

Subramanya, H.S., L.E. Bird, J.A. Brannigan, and D.B. Wigley. 1996. Crystal structure of a DExx box DNA helicase. *Nature*. 384:379-383.

Sudakin, V., G.K. Chan, and T.J. Yen. 2001. Checkpoint inhibition of the APC/C in HeLa cells is mediated by a complex of BUBR1, BUB3, CDC20, and MAD2. *J Cell Biol*. 154:925-936.

Sudakin, V., D. Ganoth, A. Dahan, H. Heller, J. Hershko, F.C. Luca, J.V. Ruderman, and A. Hershko. 1995. The cyclosome, a large complex containing cyclin-selective ubiquitin ligase activity, targets cyclins for destruction at the end of mitosis. *Mol Biol Cell*. 6:185-197.

Sumara, I., J.F. Gimenez-Abian, D. Gerlich, T. Hirota, C. Kraft, C. de la Torre, J. Ellenberg, and J.M. Peters. 2004. Roles of polo-like kinase 1 in the assembly of functional mitotic spindles. *Curr Biol*. 14:1712-1722.

Sumara, I., E. Vorlaufer, P.T. Stukenberg, O. Kelm, N. Redemann, E.A. Nigg, and J.M. Peters. 2002. The dissociation of cohesin from chromosomes in prophase is regulated by Polo-like kinase. *Mol Cell*. 9:515-525.

Sunkel, C.E., and D.M. Glover. 1988. polo, a mitotic mutant of Drosophila displaying abnormal spindle poles. *J Cell Sci*. 89 (Pt 1):25-38.

Svejstrup, J.Q. 2003. Rescue of arrested RNA polymerase II complexes. *J Cell Sci*. 116:447-451.

Tanaka, T.U., N. Rachidi, C. Janke, G. Pereira, M. Galova, E. Schiebel, M.J. Stark, and K. Nasmyth. 2002. Evidence that the Ipl1-Sli15 (Aurora kinase-INCENP) complex promotes chromosome bi-orientation by altering kinetochore-spindle pole connections. *Cell*. 108:317-329.

Taylor, S.S., and F. McKeon. 1997. Kinetochore localization of murine Bub1 is required for normal mitotic timing and checkpoint response to spindle damage. *Cell*. 89:727-735.

Toyoshima-Morimoto, F., E. Taniguchi, and E. Nishida. 2002. Plk1 promotes nuclear translocation of human Cdc25C during prophase. *EMBO Rep*. 3:341-348.

Toyoshima-Morimoto, F., E. Taniguchi, N. Shinya, A. Iwamatsu, and E. Nishida. 2001. Polo-like kinase 1 phosphorylates cyclin B1 and targets it to the nucleus during prophase. *Nature*. 410:215-220.

Utani, K., Y. Kohno, A. Okamoto, and N. Shimizu. 2010. Emergence of micronuclei and their effects on the fate of cells under replication stress. *PLoS One*. 5:e10089.

van Attikum, H., and S.M. Gasser. 2005. The histone code at DNA breaks: a guide to repair? *Nat Rev Mol Cell Biol*. 6:757-765.

van Vugt, M.A., and R.H. Medema. 2004. Checkpoint adaptation and recovery: back with Polo after the break. *Cell Cycle*. 3:1383-1386.

Wang, J.C. 2002. Cellular roles of DNA topoisomerases: a molecular perspective. *Nat Rev Mol Cell Biol*. 3:430-440.

Wang, L.H., B. Mayer, O. Stemmann, and E.A. Nigg. 2010. Centromere DNA decatenation depends on cohesin removal and is required for mammalian cell division. *J Cell Sci*. 123:806-813.

Wang, L.H., T. Schwarzbraun, M.R. Speicher, and E.A. Nigg. 2008. Persistence of DNA threads in human anaphase cells suggests late completion of sister chromatid decatenation. *Chromosoma*. 117:123-135.

Watanabe, N., H. Arai, J. Iwasaki, M. Shiina, K. Ogata, T. Hunter, and H. Osada. 2005. Cyclin-dependent kinase (CDK) phosphorylation destabilizes somatic Wee1 via multiple pathways. *Proc Natl Acad Sci U S A*. 102:11663-11668.

Watanabe, N., H. Arai, Y. Nishihara, M. Taniguchi, T. Hunter, and H. Osada. 2004. M-phase kinases induce phospho-dependent ubiquitination of somatic Wee1 by SCFbeta-TrCP. *Proc Natl Acad Sci U S A*. 101:4419-4424.

Wojcik, E., R. Basto, M. Serr, F. Scaerou, R. Karess, and T. Hays. 2001. Kinetochore dynein: its dynamics and role in the transport of the Rough deal checkpoint protein. *Nat Cell Biol*. 3:1001-1007.

Wong, O.K., and G. Fang. 2006. Loading of the 3F3/2 antigen onto kinetochores is dependent on the ordered assembly of the spindle checkpoint proteins. *Mol Biol Cell*. 17:4390-4399.

Wu, L., and I.D. Hickson. 2003. The Bloom's syndrome helicase suppresses crossing over during homologous recombination. *Nature*. 426:870-874.

Xu, D., P. Muniandy, E. Leo, J. Yin, S. Thangavel, X. Shen, M. Ii, K. Agama, R. Guo, D. Fox, 3rd, A.R. Meetei, L. Wilson, H. Nguyen, N.P. Weng, S.J. Brill, L. Li, A. Vindigni, Y. Pommier, M. Seidman, and W. Wang. 2010. Rif1 provides a new DNA-binding interface for the Bloom syndrome complex to maintain normal replication. *EMBO J*. 29:3140-3155.

Xu, L., and E.H. Blackburn. 2004. Human Rif1 protein binds aberrant telomeres and aligns along anaphase midzone microtubules. *J Cell Biol*. 167:819-830.

Yanagida, M. 2009. Clearing the way for mitosis: is cohesin a target? *Nat Rev Mol Cell Biol*. 10:489-496.

Yu, H. 2006. Structural activation of Mad2 in the mitotic spindle checkpoint: the two-state Mad2 model versus the Mad2 template model. *J Cell Biol*. 173:153-157.

Yu, H. 2007. Cdc20: a WD40 activator for a cell cycle degradation machine. *Mol Cell*. 27:3-16.

Zachariae, W., M. Schwab, K. Nasmyth, and W. Seufert. 1998. Control of cyclin ubiquitination by CDK-regulated binding of Hct1 to the anaphase promoting complex. *Science*. 282:1721-1724.

Zhu, Q., P. Pongpech, and R.J. DiGate. 2001. Type I topoisomerase activity is required for proper chromosomal segregation in Escherichia coli. *Proc Natl Acad Sci U S A*. 98:9766-9771.

Zraly, C.B., F.A. Middleton, and A.K. Dingwall. 2006. Hormone-response genes are direct in vivo regulatory targets of Brahma (SWI/SNF) complex function. *J Biol Chem*. 281:35305-35315.

9. ACKNOWLEDGMENTS

First and foremost I would like to thank Prof. Dr. Erich A. Nigg for giving me the opportunity of working in his lab and for invaluable advice and guidance during my time.

I would like to thank Prof. Dr. Markus Affolter and Dr. Kevin Hardwick for their contributions to this project as members of my PhD Advisory Committee in Basel and Prof. Dr. Markus Affolter for reviewing this manuscript. Furthermore, I am thankful to Prof. Dr. Markus Affolter and Prof. Dr. Josef Jiricny for being member of my thesis-defense committee.

I am grateful to all past and present lab members who helped me in performing experiments, discussing ideas or anything else I have needed. My thanks go to Elisabeth and Alicja for their continuous help in generating our PICH monoclonal antibody, Alison and Zdenka for their administrative support and Klaus and Roland for their technical support.

My thanks go to Dr. Olaf Stemmann for helpful discussions and plasmids. Thanks go to Dr. Weidong Wang for Rif1 antibody. I am thankful to Alex Schmidt and Manuel Bauer for helping me with mass spectrometry.

Special thanks go to my colleagues that have become friends: Nadja Hübner, Luca Fava, Gary Chan, Gernot Guderian, Katharina Mayer, Christian Arquint, Lily Wang and Anna Santamaria.

Zu guter Letzt möchte ich denjenigen danken, die mir am nächsten liegen:

Zu tiefster Dankbarkeit verpflichtet bin ich Dir, denn ohne Deine aufopferungsvolle Unterstützung wäre das nicht möglich gewesen. Danke, Mama.

Mein ganz besonderer Dank gilt meinem Onkel und seiner Familie. Danke, „Onkel“ Matthias und „Tante“ Corinna.

Ich danke meiner fantastische Schwester und Ihrem Ehemann, sowie meinen Großeltern.

I am very grateful to my beautiful girlfriend Claire for sharing her life and patience with me.

10. CURRICULUM VITAE

Personal data

name:	Manuel Kaulich	
address:	Strassburgerallee 99	
	4055, Basel, Switzerland	
email:	Manuel.Kaulich@unibas.ch	
date of birth:	22.09.1980	
family status:	single	
nationality:	German	
parents:	Mother:	Marlies Kaulich
	Father:	Axel Kaulich

Schooling

1987 – 1993	Basic primary school am Bürgerpark, Berlin
1993 – 1995	Geschwister-Scholl-Grammar school, Berlin
1995 – 1997	Schiller-Secondary modern school, Brandenburg
1997 – 2000	1. Comprehensive secondary school-Strausberg, Brandenburg

German Federal Armed Forces

2000 – 2001	142.Artillerieregiment, Mecklenburg-Vorpommern-Eggesin, Germany

University

2001 – 2004	Bachelor of Science, Molecular Biotechnology, University of Luebeck, Germany
April 2004 – July 2004	Bachelor Thesis, Department of Biochemistry, University of Luebeck, Germany Supervisor: Rolf Hilgenfeld Title: „Cloning, expression, and purification of the „macrophage infectivity potentiator“ from *Chlamydia trachomatis* in *Escherichia coli*”
2004 – 2006	Master of Science, Molecular Life Science, University of Luebeck, Germany

October 2005 - July 2006	Master Thesis, Department of Pathology, University of Luebeck, Germany Supervisor: Hartmut Merz Title: "Overexpression of Cyclooxygenase 2 and the consequences for tumor growth *in vivo*."
April 2007 – September 2009	Graduate student at the Ludwig-Maximilians University, Munich, Germany
September 2009 - today	Graduate student at the University of Basel, Basel, Switzerland

Practical experience

August 2002 – September 2002	Practical course in the Department of Human Genetics, University of Luebeck, Germany
April 2003 - November 2003	Practical course in the Department of Biochemistry, University of Luebeck, Germany
August 2004 – October 2004	Internship in the Laboratoire d'Ingénierie des Systèmes Macromoléculaires (LISM), Centre National de la Recherche Scientifique (CNRS), Marseille, France
August 2005 – October 2005	Internship in the Department of Anatomy and Cell Biology and Faculty of Dentistry, McGill University, 3640 University Street, Room 1/14, Montreal, Quebec H3A 2B2, Canada DAAD Fellowship for foreign internships.

PhD

August 2006 – September 2009	Graduate student at the Max Planck Institute of Biochemistry, Department of Cell Biology, Am Klopferspitz 18, D-82152 Martinsried
September 2009 – Today Switzerland	Graduate student at the Biocenter Basel, Department Growth and Development, Klingelbergstrasse 50/70, CH-4056 Basel,
January 2007- January 2008	Departmental speaker of the Department of Cell Biology, Am Klopferspitz 18, D-82152 Martinsried, Germany

Sideline job

2002 – 2006	Medical assistant in the ENT-station 26b of the University of Luebeck, Germany
2004 – 2006	Scientific assistant in the Department of Pathology, University of Luebeck, Germany

Publications

Hellenbroich Y, Kaulich M, Opitz S, Schwinger E, Zuhlke C.:
No association of the SCA1 $(CAG)_{31}$ allele with Huntington's disease, myotonic dystrophy type 1 and spinocerebellar ataxia type 3., Psychiatr Genet., 2004

Hübner NC, Wang LH, Kaulich M, Descombes P, Poser I, Nigg EA.: Re-examination of siRNA specificity questions role of PICH and Tao1 in the spindle checkpoint and identifies Mad2 as a sensitive target for small RNAs., Chromosoma, 2009

Advanced Training

August 2007	EMBO Advanced Lecture Series in Signal Transduction, Spetses, Greece
April 2008 – September 2009	Advanced Oxford English course, Martinsried, Germany

Language skills

German	- native language
English	- excellent in reading and writing
French	- good in reading and writing